Stochastic Assessment of Climate-induced Risk for Water Resources Systems in a Bottom-Up Framework

By

Abdullah Alodah

A Ph.D. thesis submitted under the supervision of

Prof. Ousmane Seidou

Presented to the University of Ottawa in Partial Fulfillment of the Requirements for Ph.D. in Civil Engineering

Under the auspices of the Ottawa-Carleton Institute for Civil Engineering (OCICE)

uOttawa

University of Ottawa

Ottawa, Ontario, Canada

Abstract.

Significant challenges in water resources management arise because of the ever-increasing pressure on the world's heavily exploited and limited water resources. These stressors include demographic growth, intensification of agriculture, climate variability, and climate change. These challenges to water resources are usually tackled using a top-down approach, which suffers from many limitations including the use of a limited set of climate change scenarios, the lack of methodology to rank these scenarios, and the lack of credibility, particularly on extremes. The bottom-up approach, the recently introduced approach, reverses the process by assessing vulnerabilities of water resources systems to variations in future climates and determining the prospects of such a wide range of changes. While it solves some issues of the top-down approach, several issues remain unaddressed. The current project seeks to provide end-users and the research community with an improved version of the bottom-up framework for streamlining climate variability into water resources management decisions. The improvement issues that are tackled are a) the generation of a sufficient number of climate projections that provide better coverage of the risk space; b) a methodology to quantitatively estimate the plausibility of a future desired or undesired outcome and c) the optimization of the size of the projections pool to achieve the desired precision with the minimum time and computing resources. The results will hopefully help to cope with the present-day and future challenges induced mainly by climate.

In the first part of the study, the adequacy of stochastically generated climate time series for water resources systems risk and performance assessment is investigated. A number of stochastic weather generators (SWGs) are first used to generate a large number of realizations (i.e. an ensemble of climate outputs) of precipitation and temperature time series. Each realization of the generated climate time series is then used individually as an input to a hydrological model to obtain streamflow time series. The usefulness of weather generators is evaluated by assessing how the statistical properties of simulated precipitation, temperatures, and streamflow deviate from those of observations. This is achieved by plotting a large ensemble of (1) synthetic precipitation and temperature time series in a Climate Statistics Space (CSS), and (2) hydrological indices using simulated streamflow data in a Risk and Performance Indicators Space (RPIS). The performance of the weather generator is assessed using visual inspection and the Mahalanobis distance

between statistics derived from observations and simulations. A case study was carried out using five different weather generators: two versions of WeaGETS, two versions of MulGETS and the *k*-nearest neighbor weather generator (*k*nn).

In the second part of the thesis, the impacts of climate change, on the other hand, was evaluated by generating a large number of representative climate projections. Large ensembles of future series are created by perturbing downscaled regional climate models' outputs with a stochastic weather generator, then used as inputs to a hydrological model that was calibrated using observed data. Risk indices calculated with the simulated streamflow data are converted into probability distributions using Kernel Density Estimations. The results are dimensional joint probability distributions of risk-relevant indices that provide estimates of the likelihood of unwanted events under a given watershed configuration and management policy. The proposed approach offers a more complete vision of the impacts of climate change and opens the door to a more objective assessment of adaptation strategies.

The third part of the thesis deals with the estimation of the optimal size of SWG realizations needed to calculate risk and performance indices. The number of realizations required to reach is investigated utilizing Relative Root Mean Square Error and Relative Error. While results indicate that a single realization is not enough to adequately represent a given stochastic weather generator, results generally indicate that there is no major benefit of generating more than 100 realizations as they are not notably different from results obtained using 1000 realizations. Adopting a smaller but carefully chosen number of realizations can significantly reduce the computational time and resources and therefore benefit a larger audience particularly where high-performance machines are not easily accessible. The application was done in one pilot watershed, the South Nation Watershed in Eastern Ontario, yet the methodology will be of interest for Canada and beyond.

Overall, the results contribute to making the bottom-up more objective and less computationally intensive, hence more attractive to practitioners and researchers.

Keywords: *water resources management, risk assessment, hydrometeorology, climate change impacts, stochastic hydrological modelling, uncertainty analysis, climate sensitivity*

Acknowledgments

All Praises and Thanks are due to Allah; the Creator and the Lord of the Heavens and the Earth. "Indeed! He has power over all things."

It has been a privilege to work closely with my supervisor Professor Ousmane Seidou, whom I have thoroughly enjoyed knowing and learning from. I have gained much from all the knowledge, wisdom, and perspective that Prof. Seidou has imparted to me. I would like also to thank the committee members of my Ph.D. defence, Prof. Ioan Nistor, Prof. Fateh Chebana, Prof. Majid Mohammadian and Prof. Duminda Perera, for their constructive input and guidance. I am also gratefully indebted to Prof. Kaz Adamowski for his valuable comments on the thesis proposal.

Ruba, my lovely wife, is the friend, philosopher, and guide, who is always with me in all my ups and downs. To state the least, I must mention her dedication, sacrifices, and love without which everything is meaningless. To my children Khallad and Sulaiman, thank you for your laughter, and the limitless supply of hugs. You always remind me of what's most important and teach me what life is all about. Also, I wouldn't have accomplished this, and many others, without the guidance, boundless support, and continuous encouragement from my wonderful parents, Sulaiman and Sharifah. I owe them a profound debt of gratitude. I will do my best to make them proud and try hard to meet their high expectations. Many thanks go to my brothers and sisters for their boundless support, encouragement and prayers.

I am also grateful for my friends, Abdullah Aljanah, Hasan Alfaifi, Fahad Alzahrani, Abdulhakim Mohammad, Gado Djibo Abdouramane and many others, near and far, for their endless support throughout my journey.

Finally, I am very grateful to the Saudi Arabian Cultural Bureau in Canada, Qassim University, and the Ministry of Education in Saudi Arabia for the appreciated help and for sponsoring my educational journey.

Abdullah

Table of Contents

List of Figures

List of Tables

List of Abbreviations

Abbreviation	*Meaning*
7Q*x*	The annual 7-day minimum flow with an *x*-year return period
AM	The annual maximum flow
CDF	Cumulative Distribution Functions
CF	Change Factors downscaling
CMIP5	The fifth phase of the Coupled Model Intercomparison Project
cms	Cubic meters per second
CSS	Climate Statistics Space
GCM	General Climate Model
GEV	Generalized Extreme Value distribution function
GHG	Greenhouse Gas emission
HRU	hydrologic Response Unit
IPCC	The Intergovernmental Panel on Climate Change
KDE	Kernel Density Estimations
KNN	k-Nearest Neighbor weather generator
MD	Mahalanobis distance
ME	MulGETS using Exponential distribution for precipitation amounts
MG	MulGETS using Gamma distribution for precipitation amounts
ML	Maximum likelihood estimators
MulGETS	Multi-site Weather Generator of École de Technologie Supérieure
NA-CORDEX	The North American domain of Coordinated Regional Climate Downscaling Experiment
NS (NSE)	The Nash–Sutcliffe efficiency coefficient
PBIAS	The percentage of bias
PCP	Precipitation
PDF	Probability Density Function

ppm	Parts per million
QQ	Quantile-Quantile transformation
RCM	Regional Climate Model
RCP	Representative Concentration Pathways
RE	Relative Error
RMSE	The Root Mean Squared Error
RMSEr	The Relative Root Mean Squared Error
RPIS	Risk and Performance Indicators Space
RSR	The RMSE-observations standard deviation ratio
SFOD (SFOC)	Simulated Flow using Observed Data (Simulated Flow using Observed Climate)
SFSD (SFSC)	Simulated Flow using Synthetic Data (Simulated Flow using Synthetic Climate)
SNW	South Nation Watershed
SUFI-2	Sequential Uncertainty Fitting algorithm ver. 2
SWAT	The Soil and Water Assessment Tool
SWAT-CUP	SWAT-Calibration and Uncertainty Program
SWG	Stochastic Weather Generator
Tmax	Maximum Temperature
Tmin	Minimum Temperature
WBL	Weibull distribution function
WE	WeaGETS using Exponential distribution for precipitation amounts
WeaGETS	Uni-site Weather Generator of École de Technologie Supérieure
WG	WeaGETS using Gamma distribution for precipitation amounts

List of Symbols

Symbol	*Definition*
$\mathcal{V}_T$	Subset of climate statistics describing a time series X_t
X_t	Time series representing a climate or hydrological state
T	Length in years of all climatic and hydrological time series
°C	Degree Celsius
λ	Exponential distribution parameter (1/mean)
μ	Mean
σ	Standard deviation
Q_t^{obs}	Observed discharge
$SFOC_t$	Simulated flow using observed climate for time t
α	Shape parameter or significance level
β	Scale parameter
O	Observed values
P	Predicted values
$\overline{O}$	Mean of the observed values
α_3	Skewness coefficient
α_4	Kurtosis coefficient
Φ	Eigenvectors
Σ	The covariance vector
Λ	The eigenvalues
ϱ	Correlation coefficient
$\grave{x}$	The x principal axes
$\grave{y}$	The y principal axes
χ^2	Chi-square distribution
df	Degree of freedom
SE_ρ	Standard error
CI	Confidence interval

PCP_t^{RCM}	Perturbed RCM precipitation output
PCP_t^{RCM}	Original RCM precipitation output
PCP_t^{OBS}	Observed precipitation data
TMP_t^{RCM}	Perturbed RCM temperature output
TMP_t^{RCM}	Original RCM temperature output
TMP_t^{OBS}	Observed temperature climate
X_{CORR}	Corrected RCM simulations
X_{RCM}	Climate variable extracted from raw RCM data
ξ	Shape parameter
K	Non-negative kernel smoothing function
h	Non-negative bandwidth of the kernel density estimator
S	Number of stations
$\hat{\rho}_h$	Lag-h correlation
$\mathbb{R}$	Real space

“We know increasingly well

that we do *not* know enough.”

***Kundzewicz* (*2011*)**

CHAPTER 1. *Introduction*

1.1 Background

Significant challenges in water resources management arise because of the ever-increasing pressure on the world's heavily exploited and limited water resources. These stressors include demographic growth, intensification of agriculture, climate variability, and climate change. To make things more complicated, the way these stressors will evolve in the future is highly uncertain, leading to a lot of uncertainty of how water resources systems will perform in the future, and on the impact of decisions taken today. Water resource managers and policymakers are increasingly challenged by the need to take immediate decisions that will have direct impacts on the performance of the systems under their responsibility both in the short-term and -by extension- the long-term. Climate change has forced the research community to revisit the assumptions and theory behind water resources systems design and management. For instance, the assumption of stationarity in the hydrological cycle, when planning and managing water resource systems, has been extensively questioned with many underlying uncertainties including, among others, climate-induced variability (Milly *et al.*, 2008). Yet, this assumption may no longer be valid alongside the growing number of catastrophic flooding disasters, mainly due to a changing precipitation regime, and such nonstationary extreme events must be reflected in hydrological risk studies to ultimately minimize profound adverse impacts on the environment and human wellbeing (Salas *et al.*, 2018). Researchers and practitioners are therefore persuaded to develop methodologies and innovative approaches that can be streamlined into adaptation decisions with the available data resources.

There is abundant literature on the dependence between hydrological processes and the climate regime (e.g., Gleick, 1989; Chahine, 1992; Whitfield & Cannon, 2000; Arora & Boer, 2001; Frich *et al*., 2002; Bierkens *et al*., 2008). It is well established that the linkage between hydrologic and climatic systems are not fully captured by deterministic models. Rather, there is inherent uncertainty in climate and flow variables due to their stochastic nature and because of the lack of information about the current station of hydrologic and climatic systems, which lead researchers to use statistical methods to describe the behavior of water systems and try to manage them effectively. Hence, probabilistic or stochastic models can serve the purposes of generating long hydrometeorological time series (from rainfall and ultimately to streamflow ensembles), as random variables whose values can change over time and cannot be predicted with certainty. The use of synthetic weather generation techniques, rather than deterministic climate scenarios, to force hydrological models is common in water-related studies, particularly in water resources vulnerability-driven studies (e.g., Caron *et al*., 2008; Bastola *et al*., 2012; Harris *et al*., 2014; Glenis *et al*., 2016; Herman *et al*., 2016; Borgomeo *et al*., 2018). The characterization of uncertainty in simulated discharge is rendered difficult by the fact that only a limited number of realizations is usually generated (Goovaerts, 1999). Stochastic models are attractive in concept because they can provide an endless number of outputs in the desired length.

The notion of risk in the water resource systems planning and management fields is vital for safe and sustainable exploitation of water resources systems. Hydrological risk of receiving immoderate or highly fluctuating amounts of flow rates has direct and indirect effects on human livelihood. One example is the energy generation by a hydropower project which would be threatened by having rapid fluctuations or deficiency in water

supply from the source (river or reservoir), and in contrast flooding. There are also noticeably increasing efforts to study risks imposed upon aquatic habitat and to regulate minimum environmental flow requirements to sustain water quantity and quality across Canada and internationally and prevent any further deterioration of freshwater ecosystems, which are very vulnerable to climate change (e.g., Tharme, 2003; Arthington *et al*., 2006; Linnansaari *et al*., 2012; Pastor *et al*., 2014). The possible hazard of such deterioration sometimes does not have immediate effects, but rather some time-lagged consequences. Therefore, the analysis herein will also focus on the risks associated with low probability hydrological flow rates, or disastrous extreme events.

The assessment of risks associated with climate variability usually comprises the analysis of water resource systems vulnerabilities to changes in climate variability and low probability extreme events (Salas *et al*., 2018). Climate-induced risk, and its impact on the hydroclimatic regime, in particular, has been a center topic of several previous studies (e.g., Fowler *et al*., 2007; Salas *et al*., 2018). In risk and uncertainty analysis, short or incomplete historical climate records, either in their length or spatial coverage, have always been a problematic challenge. Such a shortage can limit hydrological analyses and consequently make water-engineering designs more difficult (Loucks *et al*., 1981). Therefore, weather generators have been intensively used to generate long synthetic time series that are expected to have the same variability as the historical time series. A weather generator is a computer model used to simulate synthetic time series of weather data for a particular location by replication the statistical attributes of a local variable (such as the mean, variance, and autocorrelation) (IPCC, 2007), and several different algorithms with different

characteristics have been developed. The impact of the choice of a given weather generator on the estimated risk is still an open problem.

For climate change risk assessment, on the other hand, time and resources constraints may force many authors to limit the number of scenarios to simulate to a manageable number, often only a pessimistic and an optimistic scenario. While some studies use raw outputs of future climate models without bias correction (e.g., Chen *et al*., 2011), there are concerns about climate change models of mismatching location-specific information. While Global Circulation Models or General Climate Models, (GCMs) can provide a glimpse of what the future climate would be, the tools, called downscaling, are used to enclose this gap and refine their large-scale outputs to more precise projections for local application. While the reduction of large-scale errors is a significant step. Two different downscaling techniques can yield very different risk and performance indicators, but there has been no consensus in the scientific community on a definitive technique to compare these downscaling methods. The need to reexamine such methods in the light of risk perspective is therefore obvious.

A key change in perspective to deal with the aforementioned issues has been put forward by so-called *bottom-up* approaches. In contrast to "predict, then directly act" in the top-down approach, the bottom-up approach, also referred to as climate sensitivity analysis, is an effective risk-based, decision-making technique that has recently emerged in hydroclimatic modelling aiming at overcoming many limitations encountered by traditional approaches used for water resources planning and project design (Brown *et al.,* 2012; Bouwer 2013; Weaver *et al.,* 2013; García *et al.,* 2014; Smid and Costa, 2018).

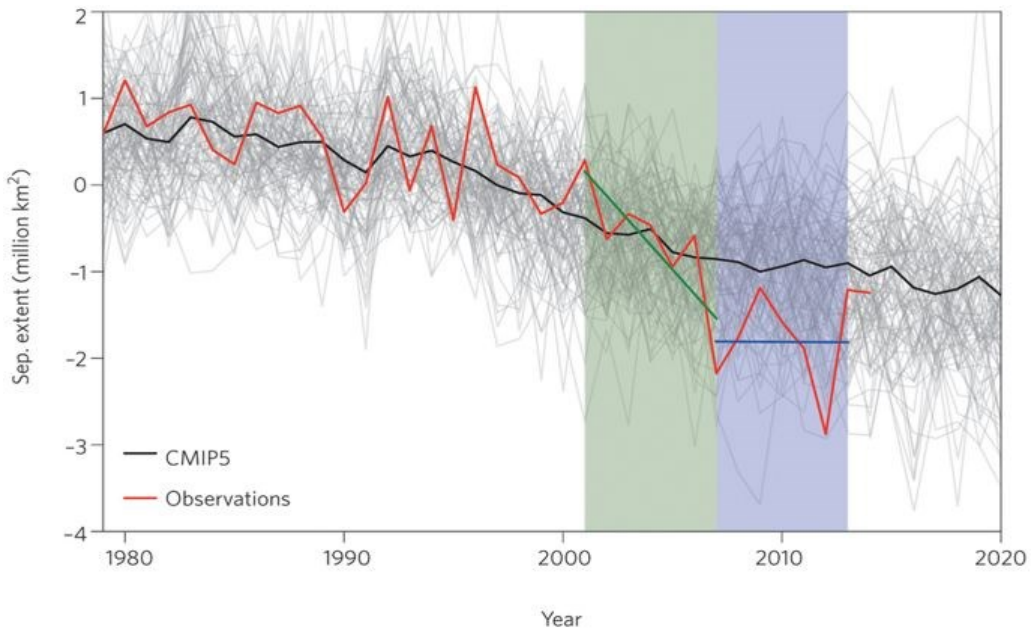

Figure 1.1 Arctic September sea-ice extent anomalies (Swart *et al*., 2015).

While both are important parts of the climate system, it is not always easy, especially for the public, to distinguish between internal climate variability and climate changes in response to external forcing (either natural or anthropogenic) and considerable efforts have been taken to provide a better explanation for the differences (e.g., Santer *et al*., 2008; Huber *et al*., 2010; Holland, 2012; Frankcombe *et al*., 2015; Swart *et al*., 2015). For instance, Arctic September sea-ice extent showed slowness (a pause with near-zero trend) between 2007–2013, which in turn can be misleading about longer-term changes as illustrated in Figure 1.1. The key difference to note is time, as illustrated in Figure 1.2. Internal climate variability describes changes that occur at smaller timeframes (e.g., a season or a year). Known examples of internal climate variability include the El Niño/Southern Oscillation (ENSO), the Pacific Decadal Oscillation (PDO), the North Atlantic Oscillation (NAO), and the Atlantic Multidecadal Oscillation (AMO). Climate change, on the other hand, refers to "statistically significant variation in either the mean state of the climate or in its variability, persisting for an extended period (typically decades

or longer)" according to the Intergovernmental Panel on Climate Change (IPCC, 2014). In modelling internal climate variability (or *noise*) and climate change (or *signal*), climatologists and hydrologists may resort to averaging many synthetic realizations of the climate (e.g., the use of stochastic weather generators) to reduce noise levels and improves estimates of the true signal (Santer *et al.*, 2008; Huber *et al.*, 2010).

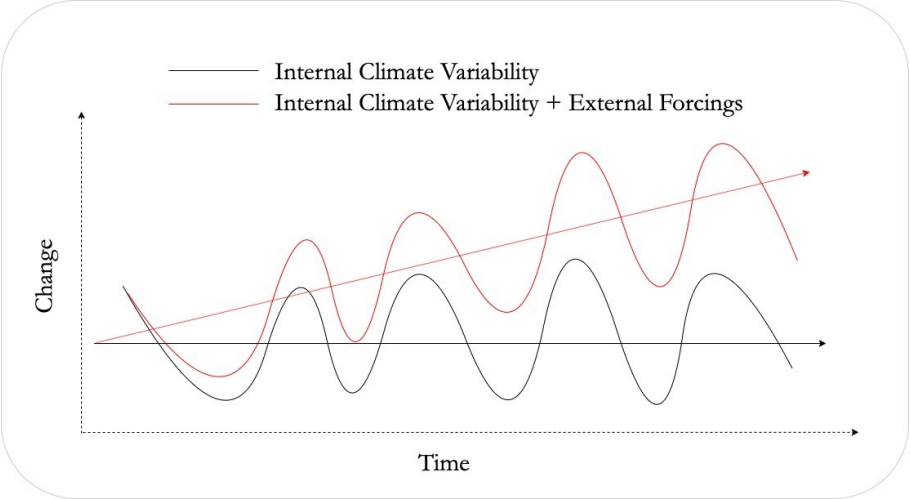

Figure 1.2 An illustration of internal climate variability and external forcing

The first part of the current work presents a new avenue to build a framework for assessing readily available stochastic weather generators by comparing the mapping between observed and generated climate states and describing statistics that are relevant to the problem at hand. Since a quantitative assessment of the likelihood of possible future states is lacking in both the traditional top-down and the alternative bottom-up approaches to climate change impacts assessment, the second part tackled this issue by generating a large number of representative climate projections using weather generators calibrated with the outputs of regional climate models. In both parts, a climate state, represented by a time series X_t, is summarized by a subset of climate statistics, $\mathcal{V}_T$ that are relevant to the problem under investigation (e.g., the mean, and the standard variation of precipitation and temperature), calculated for a period, T as introduced by Brown *et al.* (2012). $\mathcal{V}_T$ is

calculated for the observed time series and stochastically generated time series. A climate state will yield a level of risk and performance that can be measured through a set of indicators obtained by feeding an impact model with time series X_t. This was accomplished by using five stochastic weather generators to create plausible daily data series of precipitation and temperatures. Each one of the generated time series (i.e., realization of climate data) was then used as an input to a rainfall-runoff model to explore their realism in risk and performance indicators for an explicit accounting of streamflow. Further analysis is made in the third part to discuss the impact of the number of realizations in hydrological modeling.

1.2 Research objectives

Considering the aforementioned issues, the current project seeks to provide end-users and the research community with an improved version of the bottom-up framework for streamlining climate variability into water resources management decisions to cope with the present-day and future challenges induced mainly by climate. Improvement will come from contribution to issues that are yet to be adequately addressed in the bottom-up framework. The main research question of this work is how climate variability and change are reflected in a hydrological sense for risk discovery.

1.2.1 General objective

The core research focus of this work is to improve adaptation to climate variability and climate change through a better assessment of uncertainty in climate change projections. We will specifically examine the uncertainty in weather generators outputs, and the uncertainty in climate change projections, as they are the main drivers of the risk and performance of water resources systems.

1.2.2 Specific objectives

The **specific objectives** are:

- The development of a new avenue to generate a wide range of climate scenarios that combine climate model outputs and weather generators to capture as much as possible of the uncertainty in the future,
- The demonstration that the performance of weather generators are application-specific as each application has it own indices, and the development of a method for assessing the adequacy of a given stochastic weather generator for a particular application,
- The use of diagnostic tools to investigate the impact of the number of SWGs realizations on the accuracy of specific risk and performance indicators, and the development of a method to limit the computational burden of the bottom-up approach, and
- A showcase in the South Nation Watershed to identify potential impacts of climate change and climate variability and demonstrate the benefits of the proposed methodology.

1.3 Novelty

1.3.1 The proposition of a better way to assess SWG's performance for a particular problem (Alodah and Seidou, 2019a)

Stochastic weather generators are designed to produce synthetic time series that are commonly used for risk discovery, as they would contain rare events that can lead to potentially catastrophic impacts on the environment or even human lives. These time series are sometimes used as inputs to rainfall-runoff models to simulate the hydrological impacts of these rare events. This paper presents a method that evaluates the usefulness of weather generators by assessing how the statistical properties of simulated precipitation, temperatures, and streamflow deviate from those of observations. This is achieved by plotting a large ensemble of (1) synthetic precipitation and temperature time series in a Climate Statistics Space (CSS), and (2) hydrological indices using simulated streamflow data in a Risk and Performance Indicators Space (RPIS). The performance of the weather generator is assessed using

visual inspection and the Mahalanobis distance between statistics derived from observations and simulations.

1.3.2 Development of an improved version of the bottom-up approach (Alodah and Seidou, 2019b)

A quantitative assessment of the likelihood of possible future states is lacking in both the traditional top-down and the alternative bottom-up approaches to climate change impacts assessment. The issue is tackled herein by generating a large number of representative climate projections using weather generators calibrated with the outputs of regional climate models. The raw projections of Regional Climate Models (RCMs) are corrected using downscaling techniques. Large ensembles of future series are created by perturbing downscaled data with a stochastic weather generator, then used as inputs to a hydrological model that was calibrated using observed data. Risk indices calculated with the simulated streamflow data are converted into probability distributions using Kernel Density Estimations (KDE). The results are dimensional joint probability distributions of risk-relevant indices that provide estimates of the likelihood of unwanted events under a given watershed configuration and management policy. The proposed approach offers a more complete vision of the impacts of climate change and opens the door to a more objective assessment of adaptation strategies.

1.3.3 Determination of the minimum number of realizations of an SWG to estimate a given risk statistics with a predefined accuracy (Alodah and Seidou, 2019c)

While Stochastic Weather Generators (SWGs) are used intensively in climate and hydrological applications to simulate hydroclimatic time series and estimate risks and performance measures linked to climate variability, there have been few investigations into how many realizations are required for a robust estimation of these measures. Given the computational cost and time necessary to force climate-sensitive systems with multiple realizations, the estimation of the optimal number of synthetic time series to generate with a particular SWG for a predefined accuracy when estimating a particular risk or performance measure is particularly important. In this paper, the required number of

realizations of five SWGs coupled with a SWAT model (the Soil and Water Assessment Tool) in order to achieve a predefined Relative Root Mean Square Error is investigated.

1.4 Thesis organization

Apart from this introductory (*Chapter 1*), the thesis is broadly organized into seven chapters, as illustrated in Figure 1.3. A list of published works is provided at the end of this chapter. *Chapter 2* provides a quick glance at some backgrounds and past literature. As this thesis consists of a series of articles in *Chapters* 3, 4, and 5, each of these chapters (i.e., papers) comprises an introduction, materials and methodology, results and discussion, a conclusion, and the related references. *Chapter 3* presents a thorough discussion of the methodologies applied to examine the adequacy of weather generators for risk discovery. The following *Chapter 4* presents a new avenue to combine weather generator outputs and downscaled climate models' outputs to generate more scenarios driven from global circulation models. Subsequent *Chapter 5* presents the use of diagnostic tools to investigate impact of number of stochastic realizations for hydrologic applications. *Chapter 6* aims to demonstrate the added value of the methodology developed by comparing the information that a decision-maker can get from traditional approaches and the proposed approach. Lastly, *Chapter 7* provides a synthesis and a global conclusion that integrates the main points addressed in the articles and identifies areas for suggested further research.

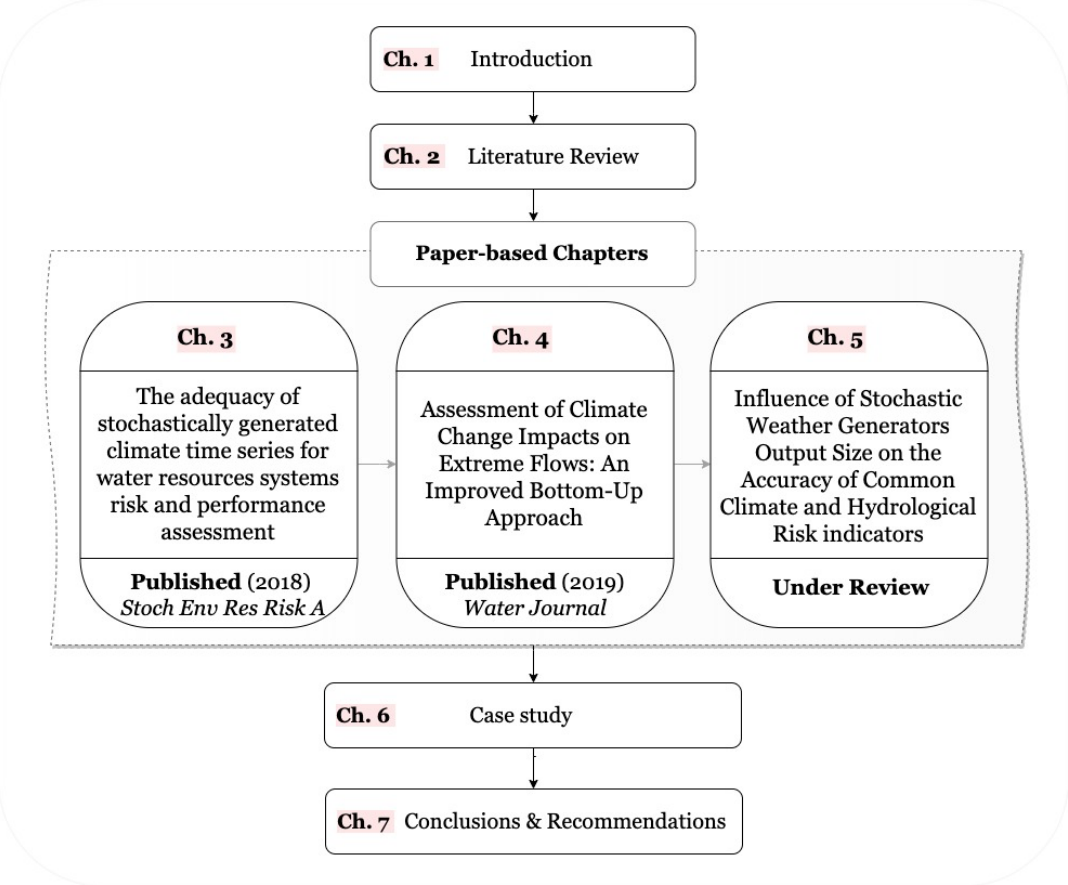

Figure 1.3 Major components of the thesis.

1.5 Peer-reviewed Publications

The following is a list of works prepared by the author during the course of the doctorate:

- **Alodah, A.,** & Seidou, O. (*2017*). The realism of stochastic weather generators in risk discovery. *WIT Transactions on Ecology and the Environment*, *220*, 239-249.

- Seidou, O., & **Alodah, A.** (*2018*). From top-down to bottom-up approaches to risk discovery: a paradigm shift in climate change impacts and adaptation studies related to the water sector. In *Proceedings of the Annual Conference of the Canadian Society for Civil Engineering (CSCE2018), Fredericton, NB, Canada* (pp. 13-16).

- **Alodah, A.,** & Seidou, O. (*2019a*). The adequacy of stochastically generated climate time series for water resources systems risk and performance assessment. *Stochastic environmental research and risk assessment*, *33*(1), 253-269.

- **Alodah, A.,** & Seidou, O. (*2019b*). Assessment of Climate Change Impacts on Extreme High and Low Flows: An Improved Bottom-Up Approach. *Water*, *11*(6), 1236.

- **Alodah, A.,** & Seidou, O. (2019c, *under review*). Influence of the Output Size of Stochastic Weather Generators on the Accuracy of Common Climate and Hydrologic Statistical Indices.

1.6 References

Arora, V. K., & Boer, G. J. (2001). Effects of simulated climate change on the hydrology of major river basins. *Journal of Geophysical Research: Atmospheres*, 106(D4), 3335-3348.

Arthington, A. H., Bunn, S. E., Poff, N. L., & Naiman, R. J. (2006). The challenge of providing environmental flow rules to sustain river ecosystems. *Ecological applications*, 16(4), 1311-1318.

Bastola, S., Murphy, C., & Fealy, R. (2012). Generating probabilistic estimates of hydrological response for Irish catchments using a weather generator and probabilistic climate change scenarios. *Hydrological processes*, 26(15), 2307-2321.

Bierkens, M. F., Dolman, A. J., & Troch, P. A. (Eds.). (2008). Climate and the hydrological cycle (Vol. 8). *International Association of Hydrological Sciences*.

Borgomeo, E., Mortazavi-Naeini, M., Hall, J. W., & Guillod, B. P. (2018). Risk, robustness and water resources planning under uncertainty. *Earth's Future*, 6(3), 468–487.

Bouwer, L.M. (2013). Projections of Future Extreme Weather Losses Under Changes in Climate and Exposure. *Risk Analysis* 33 (5): 915–30. doi:10.1111/j.1539-6924.2012.01880.x.

Brown C, Ghile Y, Laverty M, Li K (2012). Decision scaling: linking bottom up vulnerability analysis with climate projections in the water sector. *Water Resour Res* 48(9):9537

Caron, A., Leconte, R., & Brissette, F. (2008). An improved stochastic weather generator for hydrological impact studies. *Canadian Water Resources Journal*, 33(3), 233-256.

Chahine, M. T. (1992). The hydrological cycle and its influence on climate. *Nature*, 359(6394), 373.

Chen, J., F. P. Brissette, and R. Leconte (2011), Uncertainty of downscaling method in quantifying the impact of climate change on hydrology, *J. Hydrol*., 401, 190–202.

Fowler HJ, Blenkinsop S, Tebaldi C (2007). Linking climate change modelling to impacts studies: recent advances in downscaling techniques for hydrological modelling. *Int J Climatol.,* 27:1547–1578

Frankcombe, L. M., England, M. H., Mann, M. E., & Steinman, B. A. (2015). Separating internal variability from the externally forced climate response. *Journal of climate*, 28(20), 8184-8202.

Frich P, Alexander LV, Della-Marta PM, Gleason B, Haylock M, Tank AK, Peterson T (2002). Observed coherent changes in climatic extremes during the second half of the twentieth century. *Clim Res*, 19(3):193–212

García, L. E., Matthews, J. H., Rodriguez, D. J., Wijnen, M., DiFrancesco, K. N., & Ray, P. (2014). Beyond downscaling: a bottom-up approach to climate adaptation for water resources management. AGWA Report 01. Washington, DC: World Bank Group.

Gleick, P. H. (1989). Climate change, hydrology, and water resources. *Reviews of Geophysics*, 27(3), 329-344.

Glenis, V., Pinamonti, V., Hall, J. W., & Kilsby, C. G. (2015). A transient stochastic weather generator incorporating climate model uncertainty. *Advances in Water Resources*, 85, 14–26. https://doi.org/10.1016/j.advwatres.2015.08.002

Goovaerts, P. (1999). Geostatistics in soil science: state-of-the-art and perspectives. *Geoderma*, 89(1-2), 1-45.

Harris, C. N. P., Quinn, A. D., & Bridgeman, J. (2014). The use of probabilistic weather generator information for climate change adaptation in the UK water sector. *Meteorological Applications*, 21(2), 129-140.

Herman, J. D., Zeff, H. B., Lamontagne, J. R., Reed, P. M., & Characklis, G. W. (2016). Synthetic drought scenario generation to support bottom-up water supply vulnerability assessments. *Journal of Water Resources Planning and Management,* 142(11), 04016050.

Holland, M. (2012). The great sea-ice dwindle. *Nature Geoscience*, 6(1), 10.

Huber, M., Beyerle, U., & Knutti, R. (2014). Estimating climate sensitivity and future temperature in the presence of natural climate variability. *Geophysical Research Letters*, 41(6), 2086-2092.

IPCC, 2007: Climate Change 2007: The Physical Science Basis. Contribution of Working Group I to the Fourth Assessment Report of the Intergovernmental Panel on Climate Change [Solomon, S., D. Qin, M. Manning, Z. Chen, M. Marquis, K.B. Averyt, M. Tignor and H.L. Miller (eds.)]. Cambridge University Press, Cambridge, United Kingdom and New York, NY, USA.

PCC, 2014: Climate Change 2014: Synthesis Report. Contribution of Working Groups I, II and III to the Fifth Assessment Report of the Intergovernmental Panel on Climate Change [Core Writing Team, R.K. Pachauri and L.A. Meyer (eds.)]. IPCC, Geneva, Switzerland, 151 pp.

Kundzewicz ZW (2011). Comparative assessment: fact or fiction, workshop: including long term climate change in hydrologic design. World Bank, Washington, DC, 21c Nov 2011.

Linnansaari, T., Monk, W. A., Baird, D. J., & Curry, R. A. (2012). Review of approaches and methods to assess Environmental Flows across Canada and internationally. DFO Canadian Science Advisory Secretariat, Research Document, 39, 1-74.

Loucks D, Stedinger J, Haith D (1981). Water resource systems planning and analysis. Prentice-Hall, Englewood Cliffs, NJ

Milly, P. C. D., Betancourt, J., Falkenmark, M., Hirsch, R. M., Kundzewicz, Z. W., Lettenmaier, D. P., & Stouffer, R. J. (2008). Stationarity is dead: Whither water management?. *Science*, 319(5863), 573-574.

Pastor, A. V., Ludwig, F., Biemans, H., Hoff, H., & Kabat, P. (2014). Accounting for environmental flow requirements in global water assessments. *Hydrology and Earth System Sciences*, 18(12), 5041-5059.

Salas, J. D., Obeysekera, J., & Vogel, R. M. (2018). Techniques for assessing water infrastructure for nonstationary extreme events: a review. *Hydrological Sciences Journal*, 63(3), 325-352.

Santer, B. D., Thorne, P. W., Haimberger, L., Taylor, K. E., Wigley, T. M. L., Lanzante, J. R., ... & Karl, T. R. (2008). Consistency of modelled and observed temperature trends in the tropical troposphere. *International Journal of Climatology*: A Journal of the Royal Meteorological Society, 28(13), 1703-1722.

Smid, M., & Costa, A. C. (2018). Climate projections and downscaling techniques: a discussion for impact studies in urban systems. *International Journal of Urban Sciences*, 22(3), 277-307.

Swart, N. C., Fyfe, J. C., Hawkins, E., Kay, J. E., & Jahn, A. (2015). Influence of internal variability on Arctic sea-ice trends. *Nature Climate Change*, 5(2), 86.

Tharme, R. E. (2003). A global perspective on environmental flow assessment: emerging trends in the development and application of environmental flow methodologies for rivers. *River research and applications*, 19(5-6), 397-441.

Weaver, C.P., R.J. Lempert, C. Brown, J.A. Hall, D. Revell, and D. Sarewitz. (2013). Improving the Contribution of Climate Model Information to Decision-Making: The Value and Demands of Robust Decision Frameworks. *Wiley Interdisciplinary Reviews: Climate Change,* 4 (1): 39–60. doi:10.1002/wcc.202.

Whitfield, P. H., & Cannon, A. J. (2000). Recent variations in climate and hydrology in Canada. *Canadian Water Resources Journal*, 25(1), 19-65.

CHAPTER 2. *Literature Review*

2.1 Stochastic climate generation

A large number of environmental and hydrological applications, where hydro-ecological variables are simulated to evaluate alternative designs and policies especially for long-term, climate-sensitive water infrastructures (Brocca *et al*., 2013), cannot be satisfactorily carried out with sufficient observed hydro-climatic records. Instead, modellers resort to stochastic weather generators to generate long and gap-free time series of atmospheric variables using available historical climate data. To overcome a fundamental limitation of dealing with complex dynamics and thermodynamics of the atmospheric variables using physical models, weather generators are appealing approaches that are less demanding in terms of computational requirements (Peleg *et al*., 2017). The synthetically generated outputs ideally have the same characteristics as observations (e.g., mean or variance) and used to assess the impacts of climate variability (Ailliot *et al*., 2015; Guo *et al*., 2017). The implications of using such outputs as inputs to a hydrological model are investigated in this work.

Despite the excessive use of different weather generators to address water resources issues, their performance, however, has been repeatedly criticized (Fowler *et al*., 2007; Wilby & Fowler, 2011; Kim *et al*., 2013). Their drawbacks include their poor performance when modelling inter-annual variability of monthly means, although some recent rainfall generation models (e.g., Kim *et al*., 2013) were presumably able to overcome this issue by incorporating more information about the observed precipitation. They also suffer notoriously from their strictly site-specific nature (Fowler *et al*., 2007), which limits the usefulness of their results and makes them difficult to transferable to other locations and climates. Nevertheless, weather generators are practical for some

applications, such as reproducing the number of wet spells and estimating monthly precipitation levels for hydrological applications in developing countries (Wilby & Fowler, 2011). *In the face of the recent advances in weather generators, the accuracy of generated weather data has not always been adequately justified.* Precise meteorological data cannot be expected from weather generators considering the stochastic uncertainties involved, making any decision for or against the use of a certain weather generator in a decision or design framework particularly challenging. Therefore, the credibility of a given weather generator should be deliberated by quantifying their suitability for a specific field or climate zone.

With the multitude of numerous available approaches, this work focuses on three weather generators that apply different methodologies and techniques, namely: WeaGETS, MulGETS, and *k*-nn. The WeaGETS model (Chen *et al*., 2012) is an extension to the WGEN model (Richardson and Wright, 1984). Unlike WGEN, however, WeaGETS provides a spectral correction approach for a better estimation of low-frequency component and consequently improved simulation of monthly and interannual variability. Yet, WeaGETS is rather more suited to small watersheds wherein a single station can be used to represent the entire watershed (Chen *et al*., 2012), and is thus of limited use for modelling multi-site watersheds within large basins (Mehrotra *et al*., 2006). The selection of weather generators in this study is not exhaustive but since the objective is to present a framework to evaluate weather generators, the choice is made to work on a small ensemble of models.

The so-called Multi-site weather Generator (MulGETS) has been introduced by Chen *et al.,* (2014) to provide a weather generator with the capability to account for the spatial attributes of climate data. For generation of precipitation amounts, the best-fit probability distribution function of precipitation amounts is well documented in the scientific literature. The gamma distribution

function has been traditionally the most preferred to wet-day daily precipitation (e.g., Thom, 1951; Buishand, 1978; Geng *et al.,* 1986; Şen and Eljadid, 1999). Moreover, other distributions have been recommended such as exponential (e.g., Woolhiser and Roldan, 1982; Wilks, 1998; Burgueño *et al*., 2005), Weibull (e.g. Burgueño*et al*., 2005). Hanson and Vogel (2008) recommended the Pearson Type-III (P3) distribution to be applied to the full record of daily precipitation data. Beside WeaGETS and MulGETS, the *K*-nearest neighbor scheme (k-nn) is used for precipitation sequences applying the model by Goyal *et al.* (2012) while the method by Sharif and Burn (2007) was implemented for the generation of temperature sequences. k-nn is a broadly used non-parametric procedure to simulate daily weather variables with no assumptions of the probability distributions. Its principal concept is to stochastically reshuffle the values from the observed records by looking for a similar pattern to the day of interest (Yates *et al*., 2003).

2.2 Dealing with a nonstationary environment

Hydrological systems are mainly climate-driven and changes in climate patterns are significantly altering global water resources. It is of primary importance to inspect the unavoidable challenges in the future that are likely to occur in water resources systems attributed to the accumulated greenhouse gas emission (GHG), mainly long-lived CO_2 emissions (the dominant anthropologically-generated GHGs) (Stocker *et al*., 2013; Salas *et al.*, 2018). There is incredibly large published literature across dispensaries on how significant changes are in future temperature and precipitation, especially for the North Hemisphere, and their hydrological impacts. Changes in mean temperature of the North Hemisphere (Figure 2.1), for instance, are affecting the timing of the thaw period as well as evapotranspiration patterns contributing to abnormally high heavy precipitation and consequently enhance hydrological cycle (Frich *et al.,* 2002). Alfieri *et al.,* (2016) implied a strong correlation between the increase in atmospheric temperature and future

flood risk at a global scale. For the particular case of Europe (Alfieri *et al.,* 2016), flood is predicted to occur more frequently under a changing climate. Recent variations in climate and hydrology across North American river basins have been heavily investigated (e.g., Whitfield and Cannon, 2000; Adamowski & Bocci, 2001; Frich *et al.,* 2002*;* Widmann *et al*., 2003; Brown *et al.,* 2011; Seidou *et al*., 2012; Chen *et al*., 2013).

However, the extent of potential climate change projected by GCMs hinges heavily on the choice of GHG emission scenario and consequently the radiative forcing (or climate forcing). GCMs play a critical role by linking the effect of GHGs on current and future climate regime at global and regional scales. Climate scenarios are approximation means used to serve the purposes of estimating changes in the climate patterns of the 21st century and beyond defined by underlying key metrics and assumptions (including socio-economic, demographic and technological changes) to obtain future GHG emissions in the atmosphere (Goosse *et al*., 2010). The latest set of scenarios, adopted by IPCC AR5 (2014), is known as Representative Concentration Pathways (RCPs), depending on estimated radiative forcing levels of 8.5, 6.0, 4.5, and 2.6 W/m² by the end of 21st century for RCP8.5, RCP6, RCP4.5 and RCP2.6, respectively.

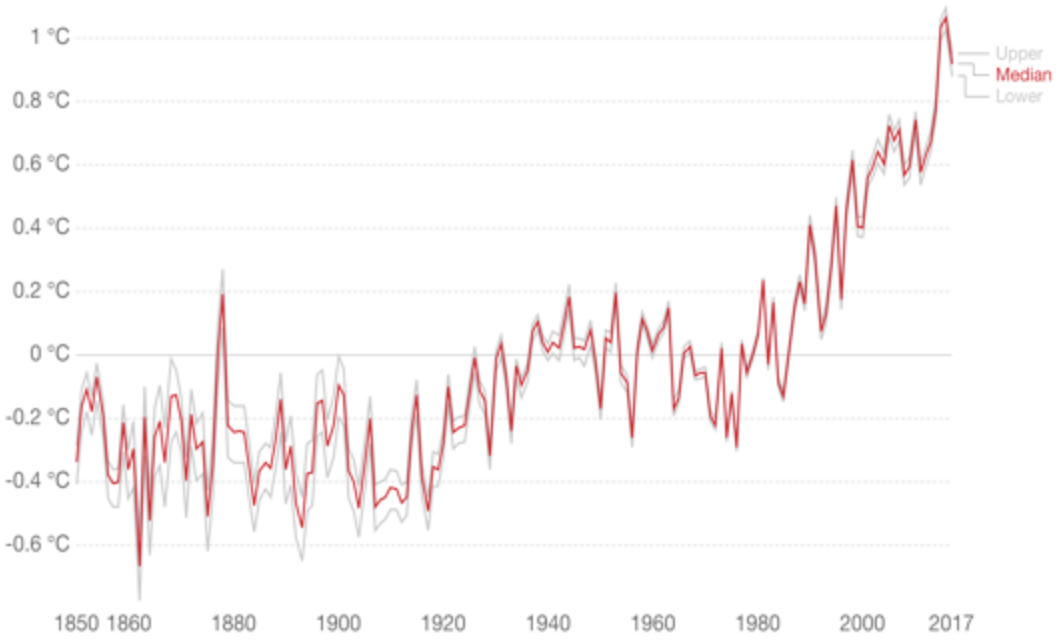

Figure 2.1 The median temperature anomalies in the North Hemisphere relative to 1961-1990 based on HadCRUT4 dataset (Ritchie and Roser, 2017).

There is an increasing agreement to consider the role of these projected changes in water management decisions. However, an example of a challenge in hydroclimatic modelling of climate change is estimating the magnitude of Earth's response to the projected increase in GHGs in this century, which is still uncertain. Representative concentration pathways, the state-of-art scenarios, are estimated based on climate sensitivity (which is another source of uncertainty) to radiative forcing. Climate sensitivity is an indication, frequently used in climate change studies, of how sensitive the climate system is to a given forcing perturbation either by natural cause (e.g., volcanic eruptions, or solar output) or by anthropologically generated GHGs. Simply put, it is a key measure of how much warming (ΔT) resulted from a certain increase (usually doubling CO_2 from pre-industrial levels of 280 ppm) in atmospheric carbon dioxide, or in a unit change in radiative forcing.

Amongst some objective estimates of climate sensitivity range (Figure 2.2), there are no consensus approximations of climate response to a doubling of atmospheric carbon dioxide (to a concentration of 560 ppm) although initially proposed estimation by National Academy of Sciences (1979) to be in the range of 1.5-4.5 °C still adopted by IPCC recent reports (2007, 2014). Nevertheless, Annan and Hargreaves (2006) rule out exaggerated climate sensitivity exceeding 6°C and IPCC (2014) considers it very unlikely to be less than 1.5 °C. However, a recent comprehensive work by Andrews *et al.* (2018) suggested that response in global temperature might be greater and more uncertain than previously estimated bounds, specifically at the upper end. Therefore, it is obvious given these estimates how difficult to quantify possible impacts of projected future climate change considering these underlying processes.

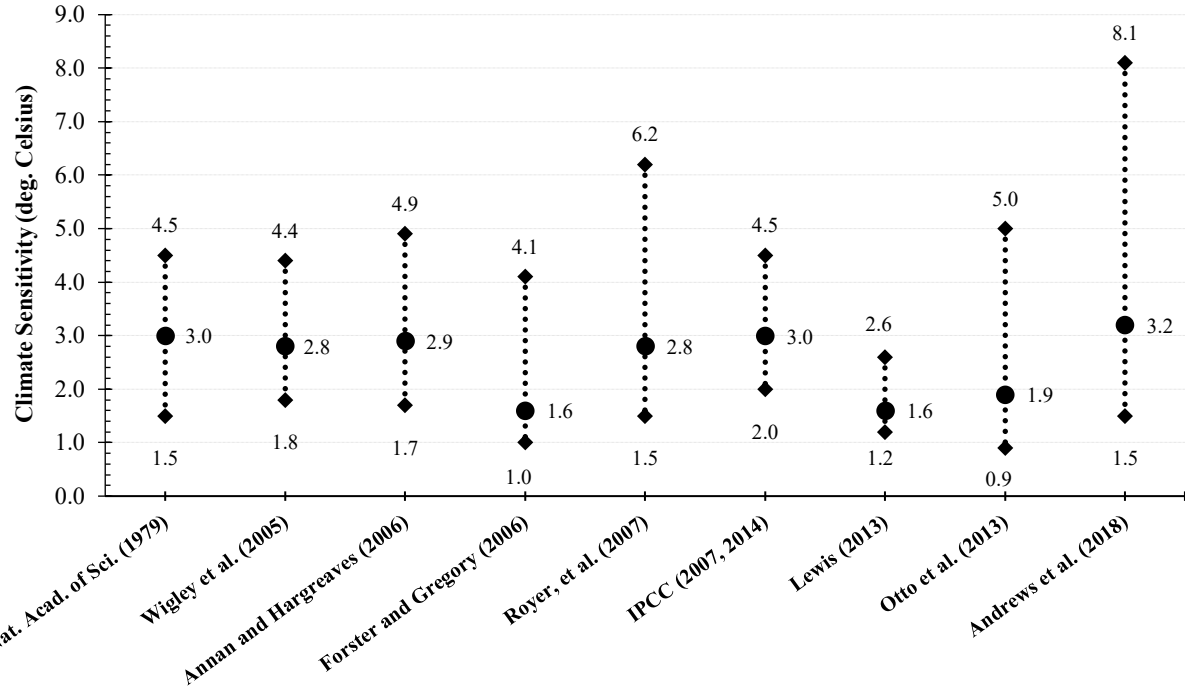

Figure 2.2 Estimations by different studies of the equilibrium climate sensitivity median and 5-95% confidence interval to a doubling of atmospheric carbon dioxide levels and the Earth's radiative response.

Given the very large range of uncertainty involved when addressing climate change, as illustrated by Wilby & Dessai (2010), and because of the limited number of climate-change scenarios used in the traditional approach, some risks may be overlooked. Time and resource constraints forced many authors to limit the number of scenarios being simulated to a manageable number— often only a pessimistic and an optimistic scenario; sometimes an ensemble of scenarios. As a result, the ability to fine-tune adaptation strategies was lost. Obviously, the optimistic and pessimistic scenarios alone would not translate into the upper and lower bounds of the possible impact. For risk-based management, analysis of large datasets employing data mining technologies is encouraged to provide local decision-makers with the likelihood of a large range of outcomes.

The traditionally used *top-down* approaches for assessing climate risk and vulnerability, which has been adopted by the vast majority of researchers, start often by looking into the possible changes in climate conditions in the future based on predetermined scenarios that are parameterized in large-scale models. This is done by downscaling a considerably few scenarios/projections and testing the impacts on a local hydrological system employing rainfall-runoff models. Wilby *et al.,* (2004) refer to these methods as "unintelligent downscaling" approaches. However, hydrological impact models (distributed models in particular) are distinctly sensitive to small-scale climate variations (or even point-scale climate observation) that might be underestimated by large-scale models (Wilby *et al*., 2004). A non-exhaustive list of issues that arise from the use of this approach is presented here. The limited number of RCM projections available to modelers and the lack of methodology to rank RCM outputs were identified as one of the major limitations to the application of the top-down approach. The increasingly growing disastrous extreme hydrological events intensify the urgency to analyze risk associated with climate change on water resource systems differently. A generalized methodology that counts for risk assessment and management

implementing additional levels of post-processing to trace out water system's vulnerability to climate sensitivity deems tremendously needed (Prudhomme *et al.,* 2010).

A key change in perspective to deal with the aforementioned issues has been put forward by so-called *bottom-up* approaches. In contrast to "predict, then directly act" or top-down approach, the bottom-up approach, also referred to as climate sensitivity analysis, is an effective risk-based, decision-making technique that has recently emerged in hydroclimatic modelling aiming at overcoming many limitations encountered by traditional approaches used for water resources planning and project design (Figure 2.3; Brown *et al.,* 2012; Bouwer 2013; Weaver *et al.,* 2013; García *et al.,* 2014; Smid and Costa, 2018). Such approach in the water sector is meant to explore not just outputs from downscaling GCMs for climate adaptation, but rather to achieve a resilient system particularly due to the relatively high uncertainty mainly by climate sensitivity. It uses basically different direction to begin the assessment. To assess the effects of climate change on water resources, for example, bottom-up approach simply reverses the process by assessing vulnerabilities of water resources systems to variations in future climates and determining robustly the prospects of such wide range of changes. The conceptual base for bottom-up approaches was discussed in detail by García *et al.* (2014).

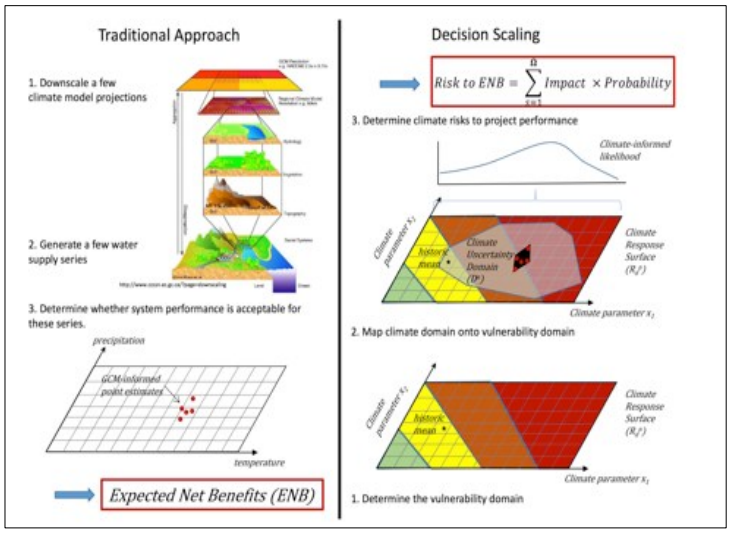

Figure 2.3 Comparison between top-down (traditional approach) and bottom-up (decision-scaling approach) climate change risk assessment (García *et al*., 2014).

2.2.1 Coping with uncertainties in GCMs (better projections or Stochastic climate change projections)

There is a growing focus on risk assessments in the context of climate change for the identification of appropriate planning and operating policy. However, the known limitations of climate change models and their predictions make it very difficult to favour one Global Climate Model (GCM)/Regional Climate Model (RCM) over the others. A significant portion of uncertainties in GCMs comes from underlying physical and social assumptions, as we remain unsure about the future possibility of human population, industry and technology developments. Lenderink *et al.* (2007) and Hayhoe (2010) indicated that a simple method, such as delta method, utilized to refine the raw simulations from the current generation of GCMs would significantly lead to better estimations. That is due to certain inherited systematic errors (known as bias) in GCMs, and their lack of accuracy locally despite the many efforts to refine their outputs (Reichler and Kim, 2008). Overall, such simple correction methods based on the observed data allow for better hydrological

simulations and consequently impact studies compared to using raw RCM data (Chen *et al*., 2013). Yet, this method is not fully capable of correcting the future projections as it prognosticates the same variability of the future climate compared to the historical variability.

More and more climate models and scenarios are made available to impact modellers through collaborative international efforts such as the Coupled Model Intercomparison Project (CMIP5: Taylor *et al.*, 2012), and the Coordinated Regional Climate Downscaling Experiment (CORDEX: Giorgi *et al.*, 2009). However, even large multi-model, multi-scenario ensembles, such as CORDEX and CMIP5, only provide the lower bounds on the maximum range of uncertainty rather than providing forecasts or bounds on uncertainty (Brown *et al*., 2011; Stainforth *et al*., 2007). There is, therefore, a risk of overlooking risky possibilities when the outputs of GCMs/RCMs are the sole imputes to risk discovery. Other limitations of GCM/RCMs include lack of credibility on extremes, even after downscaling and/or bias correction (Seidou *et al*., 2012), lower performance at lower temporal and spatial scales (Knutti 2008; Reichler and Kim 2008; Seidou *et al*., 2012), and a lack of consensus on how to assign probabilities to scenarios that result in a situation of deep uncertainty (Kasprzyk *et al*., 2013; Lempert and Groves 2010; Lempert *et al*., 2003). These limitations led several authors to resort to stochastic or parametric methods to generate a large number of climate scenarios that include but are not constrained by the range of GCM projections (Brown *et al.,* 2011; Brown and Wilby 2012; Prudhomme *et al.,* 2010). To make the computations more efficient, a climate response function is created to relate climate states (described by relevant climate statistics) to risk and/or performance indicators (Brown *et al.,* 2012; Prudhomme *et al.,* 2010). The plausibility of potential climate states that are discovered in the process is then estimated using GCMs or stochastically generated projections (Brown *et al.,* 2012). An unresolved issue is that the weighting of the scenarios is still up to the modeller's judgment. Brown *et al.*

(2012) recommend the development of new stochastic methods combined with robust signals from GCM but have not attempted to do so. A premise of this thesis is that the development of a stochastic method that would start from an initial ensemble of GCM/RCMs-derived climate change scenarios and generate a super-ensemble of scenarios that would cover the range of variability of observed in the historical period would address (or at least mitigate) the above-mentioned issues of ensemble size and scenario probability estimation. Such super-ensemble would be obtained by cloning and perturbing the scenarios in the initial ensemble employing a probabilistic approach. The development of that stochastic method is a key sub-objective in the present thesis.

2.3 Representation in stochastic climate generation

SWGs are often employed for hydrological applications to study impacts of climatic variations based on a single realization, for instance in rainfall-runoff simulations (e.g., Dubrovský *et al*., 2004), erosion simulations (e.g., Zhang and Garbrecht, 2003), the simulation of extreme precipitation events (e.g., Furrer and Katz, 2008; Semenov, 2008) and in climate change studies (e.g., Kilsby *et al*., 2007; Kim *et al*., 2007; Al-Mukhtar *et al*., 2014). Yet unlike observed weather data which provide only one realization, one can generate unlimited number of weather realizations, and statistically it is very improbable that any two realization will be identical. In general, multiple stochastically-generated time series can provide a broad range of weather possibilities to serve detailed sensitivity analysis (Dubrovský *et al*., 2004) such as recently-introduced vulnerability-based methods (e.g., bottom-up approaches) to evaluate uncertainty in projected climate change impacts (e.g., Brown *et al*., 2011; Steinschneider & Brown, 2013; Mukundan *et al*., 2019; Alodah & Seidou, 2019b). An ensemble of multiple realizations is recommended to adequately characterize the whole range of variability of climate data and to

realistically estimate mean values and variances of meteorological variables (Alodah and Seidou, 2019a; Guo *et al.*, 2018; Mehrotra *et al*., 2006; Anyah and Semazzi, 2006; Dubrovský *et al*., 2004).

Multiple realizations of climate series, however, are increasingly becoming the adopted modeling approach in evaluating the variability of the complex climate system and in order to account for rare occurrences of climate variables (Anyah & Semazzi, 2006). This is done by considering an arbitrary (and commonly limited) number of realizations (ranged from 10 to 1000). Examples of some recent works for different applications that utilized multiple runs of weather generators are presented in Table 2.1. It is also common to use SWGs to produce a longer time series than observed ones (e.g., Kou *et al*., 2007; Caron *et al*., 2008; Chen *et al*., 2012; Eames *et al*., 2012) although this might lead to biases resulted from insufficient sampling of the distribution (Mithen and Black, 2011). Therefore, it is recommended (Dubrovský *et al*., 2004; Guo *et al*., 2018) to use multiple realizations with the same length as the training set. However, the use of multiple realizations particularly when used along with a subsequent impact application requires high-performance computational resources. For example, Gitau *et al*. 2012 run a SWAT model 250 times for each of the 172 management scenarios (a total of 43,000 runs) using an extremely large network of computers. They stated, however, that their work could have taken up to 3.3 years to be completed by traditional desktop computer workstations. Thus, given the acknowledged limitations of the prohibitive time and computational expenses, the question related to the required number of realizations to fairly characterize the hydrological space is still open.

Such prolonged process, in particular for large watersheds, may be overcome with the help of expensive supercomputers (which are not always accessible/affordable) or alternatively by identifying the sufficiently representative number of outputs that can capture the random component hydrological modeling and ultimately to reduce the computations. Guo *et al*. (2018)

carried out an investigation to identify the numbers of realizations that can satisfactorily capture a number of statistical characteristics of meteorological variables (i.e., precipitation, and minimum and maximum temperature) synthetically generated by CLIGEN, LARSWG, and WeaGETS. They analyzed increasing *discrete* numbers of realizations (1, 25, 50, and 100) and concluded that a weather generator would well reproduce essential climate characteristics by 25 realizations. The current work generally builds on their ideas. However, the statistics considered in their work belong only to *climatic data space* (precipitation and temperature variables), thus the generalizability of such findings to be applicable also to hydrological variables can be problematic due to the non-linearity of hydrologic response in rainfall-runoff transformation. A variety of diagnostic tools will be applied in chapter five to identify the optimal number of realizations needed for both climatic and hydrologic variables.

Table 2.1 Examples of some recent works that used an ensemble of multiple realizations of weather generators.

Weather Generator(s)	Number of realizations	Timeseries length	Hydrological impacts?	Reference
Met&Roll	30	30-year	SAC-SMA	Dubrovský *et al*. (2004)
WEGN & WeaGETS	30	300-year	HSAMI	Caron *et al*. (2008)
MNHMM	100	22-year	Sacramento	Kwon *et al*. (2011)
WGEN	100	30-year	Several conceptual model	Bastola *et al*. (2012)
Unique SWG	200	25-year	HEC-HMS & VisualBALAN	Candela *et al*. (2012)
WXGEN	250	28-year	SWAT	Gitau *et al*. (2012)
WeaGETS, MulGETS & KNN	1000	41-year	SWAT	Alodah & Seidou (2019a)
MulGETS	250	30-year	SWAT	Alodah & Seidou (2019b)
Unique Stochastic Model	1000	42-year	Crop simulation models	Hansen & Ines (2005)
WGEN, SIMMETEO & SWG	100	71-year	Crop simulation models	Apipattanavis *et al*. (2010)
HMM, KNN, Wilks	100	43-year	Only climate	Mehrotra *et al*. (2006)
Simple resampling method	20	30-year	Only climate	Räisänen and Ruokolainen (2006)
CLIGEN	10	20-year	Only climate	Elliot & Arnold (2001)
MMLR	50	40-year	Only climate	Jeong *et al*. (2012)
Improved KNN	50	62-year	Only climate	Steinschneider & Brown (2013)
CLIGEN, LARS-WG & WeaGETS	50	50-year	Only climate	Mehan *et al*. (2017)
TripleM	30	30-year	Only climate	Breinl *et al*. (2017)
AWE-GEN-2d	50	30-year	Only climate	Peleg *et al*. (2017)
LARS-WG	50	50-year	Only climate	Gitau *et al*. (2018)
CLIGEN, LARS-WG & WeaGETS	100	50-year	Only climate	Guo *et al*. (2018)

2.4 References

Adamowski, K., & Bocci, C. (2001). Geostatistical regional trend detection in river flow data. *Hydrological Processes*, *15*(18), 3331-3341.

Ailliot P, Allard D, Monbet V, Naveau P (2015). Stochastic weather generators: an overview of weather type models. *Journal de la Société Française de Statistique, 156*(1):101–113

Al-Mukhtar M, Dunger V, Merkel B (2014) Evaluation of the climate generator model CLIGEN for rainfall data simulation in Bautzen catchment area, Germany. Hydrol Res 45(4–5):615–630

Alfieri, L., Feyen, L., & Di Baldassarre, G. (2016). Increasing flood risk under climate change: a pan-European assessment of the benefits of four adaptation strategies. *Climatic Change*, *136*(3-4), 507-521.

Alodah, A., & Seidou, O. (2019a). The adequacy of stochastically generated climate time series for water resources systems risk and performance assessment. *Stochastic environmental research and risk assessment*, *33*(1), 253-269.

Alodah, A., & Seidou, O. (2019b). Assessment of Climate Change Impacts on Extreme High and Low Flows: An Improved Bottom-Up Approach. *Water*, *11*(6), 1236.

Anyah, R. O., & Semazzi, F. H. M. (2006). Climate variability over the Greater Horn of Africa based on NCAR AGCM ensemble. *Theoretical and applied climatology*, *86*(1-4), 39-62.

Apipattanavis, S., Bert, F., Podestá, G., & Rajagopalan, B. (2010). Linking weather generators and crop models for assessment of climate forecast outcomes. *Agricultural and forest meteorology*, *150*(2), 166-174.

Bastola, S., Murphy, C., & Fealy, R. (2012). Generating probabilistic estimates of hydrological response for Irish catchments using a weather generator and probabilistic climate change scenarios. *Hydrological processes*, *26*(15), 2307-2321.

Bouwer, L.M. (2013). Projections of Future Extreme Weather Losses Under Changes in Climate and Exposure. *Risk Analysis* 33 (5): 915–30. doi:10.1111/j.1539-6924.2012.01880.x.

Breinl, K., Di Baldassarre, G., Girons Lopez, M., Hagenlocher, M., Vico, G., & Rutgersson, A. (2017). Can weather generation capture precipitation patterns across different climates, spatial scales and under data scarcity? Sci Rep, 7(1), 5449.

Brocca L, Liersch S, Melone F, Moramarco T, Volk M (2013). Application of a model-based rainfall-runoff database as efficient tool for flood risk management. *Hydrol Earth Syst Sci, 17*(8):3159

Brown C, Ghile Y, Laverty M, Li K (2012). Decision scaling: linking bottom up vulnerability analysis with climate projections in the water sector. *Water Resour Res, 48*(9):9537

Brown, C., & Wilby, R. L. (2012). An alternate approach to assessing climate risks. Eos, *Transactions American Geophysical Union*, *93*(41), 401-402.

Brown, C., Werick, W., Leger, W., & Fay, D. (2011). A Decision-Analytic Approach to Managing Climate Risks: Application to the Upper Great Lakes 1. *Journal of the American Water Resources Association*, *47*(3), 524-534.

Brown, C., Werick, W., Leger, W., & Fay, D. (2011). A Decision-Analytic Approach to Managing Climate Risks: Application to the Upper Great Lakes 1. *JAWRA Journal of the American Water Resources Association*, *47*(3), 524-534.

Buishand, T. A. (1978). Some remarks on the use of daily rainfall models. *Journal of Hydrology*, *36*(3-4), 295-308.

Burgueno, A., Martinez, M. D., Lana, X., & Serra, C. (2005). Statistical distributions of the daily rainfall regime in Catalonia (Northeastern Spain) for the years 1950–2000. *International Journal of Climatology: A Journal of the Royal Meteorological Society*, *25*(10), 1381-1403.

Candela, L., Tamoh, K., Olivares, G., & Gomez, M. (2012). Modelling impacts of climate change on water resources in ungauged and data-scarce watersheds. Application to the Siurana catchment (NE Spain). *Science of the total environment*, *440*, 253-260.

Caron A, Leconte R, Brissette F (2008) An improved stochastic weather generator for hydrological impact studies. Can Water Resour J 33:233–256

Chen J, Brissette FP, Leconte R, Caron A (2012). A versatile weather generator for daily precipitation and temperature. *Trans ASABE, 55*(3):895–906

Chen JF, Brissette X, Zhang J (2014). A multi-site stochastic weather generator for daily precipitation and temperature. *Trans ASABE,* 2014:1375–1391. https://doi.org/10.13031/trans.57.10685

Chen, J., F. P. Brissette, D. Chaumont, and M. Braun (2013), Performance and uncertainty evaluation of empirical downscaling methods in quantifying the climate change impacts on hydrology over two North American river basins, J. *Hydrol.*, *479*(4), 200–214.

Dubrovský, M., Buchtele, J., & Žalud, Z. (2004). High-frequency and low-frequency variability in stochastic daily weather generator and its effect on agricultural and hydrologic modelling. *Climatic Change*, *63*(1-2), 145-179.

Eames M, Kershaw T, Coley D (2012) A comparison of future weather created from morphed observed weather and created by a weather generator. *Build Environ* 56:252–264

Elliot W, Arnold C (2001) Validation of the weather generator CLIGEN with precipitation data from Uganda. Trans ASAE 44:53–58

Fowler HJ, Blenkinsop S, Tebaldi C (2007). Linking climate change modelling to impacts studies: recent advances in downscaling techniques for hydrological modelling. *Int J Climatol, 27*:1547–1578

Frich P, Alexander LV, Della-Marta PM, Gleason B, Haylock M, Tank AK, Peterson T (2002). Observed coherent changes in climatic extremes during the second half of the twentieth century. *Clim Res, 19*(3):193–212

Furrer, E. M., & Katz, R. W. (2008). Improving the simulation of extreme precipitation events by stochastic weather generators. *Water Resources Research*, *44*(12).

García, L. E., Matthews, J. H., Rodriguez, D. J., Wijnen, M., DiFrancesco, K. N., & Ray, P. (2014). Beyond downscaling: a bottom-up approach to climate adaptation for water resources management. AGWA Report 01. Washington, DC: World Bank Group.

Geng, S., de Vries, F. W. P., & Supit, I. (1986). A simple method for generating daily rainfall data. *Agricultural and Forest Meteorology*, *36*(4), 363-376.

Giorgi, F., Jones, C., & Asrar, G. R. (2009). Addressing climate information needs at the regional level: the CORDEX framework. World Meteorological Organization (WMO) Bulletin, *58*(3), 175.

Gitau, M. W., Chiang, L. C., Sayeed, M., & Chaubey, I. (2012). Watershed modeling using large-scale distributed computing in Condor and the Soil and Water Assessment Tool model. *Simulation*, *88*(3), 365-380.

Gitau, M. W., Mehan, S., & Guo, T. (2018). Weather generator effectiveness in capturing climate extremes. *Environmental Processes*, *5*(1), 153-165.

Goosse, H., Brovkin, V., Fichefet, T., Haarsma, R., Huybrechts, P., Jongma, J., ... & Deleersnijder, E. (2010). Description of the Earth system model of intermediate complexity LOVECLIM version 1.2. Geoscientific Model Development, *3*, 603-633.

Goyal MK, Burn DH, Ojha CSP (2013). Precipitation simulation based on k-nearest neighbor approach using gamma kernel. *J Hydrol Eng 18*:481–487

Guo, T., Mehan, S., Gitau, M. W., Wang, Q., Kuczek, T., & Flanagan, D. C. (2018). Impact of number of realizations on the suitability of simulated weather data for hydrologic and environmental applications. *Stochastic environmental research and risk assessment, 32*(8), 2405-2421. https://doi.org/10.1007/s00477-017-1498-5

Hansen JW, Ines AV (2005) Stochastic disaggregation of monthly rainfall data for crop simulation studies. Agric For Meteorol 131:233–246

Hanson, L. S., & Vogel, R. (2008). The probability distribution of daily rainfall in the United States. In World Environmental and Water Resources Congress 2008: Ahupua'A (pp. 1-10).

Hayhoe, K. A. (2010). A standardized framework for evaluating the skill of regional climate downscaling techniques (Doctoral dissertation, University of Illinois at Urbana-Champaign).

IPCC, 2007: Climate Change 2007: The Physical Science Basis. Contribution of Working Group I to the Fourth Assessment Report of the Intergovernmental Panel on Climate Change [Solomon, S., D. Qin, M. Manning, Z. Chen, M. Marquis, K.B. Averyt, M. Tignor and H.L. Miller (eds.)]. Cambridge University Press, Cambridge, United Kingdom and New York, NY, USA.

IPCC, 2014: Climate Change 2014: Synthesis Report. Contribution of Working Groups I, II and III to the Fifth Assessment Report of the Intergovernmental Panel on Climate Change [Core Writing Team, R.K. Pachauri and L.A. Meyer (eds.)]. IPCC, Geneva, Switzerland, 151 pp.

Jeong, D. I., St-Hilaire, A., Ouarda, T. B., & Gachon, P. (2012). Multisite statistical downscaling model for daily precipitation combined by multivariate multiple linear regression and stochastic weather generator. Climatic Change, 114(3-4), 567-591.

Kasprzyk, J. R., Nataraj, S., Reed, P. M., & Lempert, R. J. (2013). Many objective robust decision making for complex environmental systems undergoing change. *Environmental Modelling & Software*, *42*, 55-71.

Kilsby, C. G., Jones, P. D., Burton, A., Ford, A. C., Fowler, H. J., Harpham, C., ... & Wilby, R. L. (2007). A daily weather generator for use in climate change studies. *Environmental Modelling & Software*, *22*(12), 1705-1719.

Kim BS, Kim HS, Seoh BH, Kim NW (2007) Impact of climate change on water resources in Yongdam Dam Basin, Korea. Stoch Environ Res Risk Assess 21:355

Kim D, Olivera F, Cho H (2013). Effect of the inter-annual variability of rainfall statistics on stochastically generated rainfall time series: part 1. Impact on peak and extreme rainfall values. *Stoch Env Res Risk Assess, 27*(7):1601–1610

Knutti, R. (2008). Why are climate models reproducing the observed global surface warming so well?. *Geophysical Research Letters*, *35*(18).

Kou, X., Ge, J., Wang, Y., & Zhang, C. (2007). Validation of the weather generator CLIGEN with daily precipitation data from the Loess Plateau, China. *Journal of hydrology*, *347*(3-4), 347-357.

Kwon, H. H., Sivakumar, B., Moon, Y. I., & Kim, B. S. (2011). Assessment of change in design flood frequency under climate change using a multivariate downscaling model and a

precipitation-runoff model. *Stochastic Environmental Research and Risk Assessment*, *25*(4), 567-581.

Lempert, R. J., & Groves, D. G. (2010). Identifying and evaluating robust adaptive policy responses to climate change for water management agencies in the American west. Technological Forecasting and Social Change, *77*(6), 960-974.

Lempert, R. J., Popper, S. W., & Bankes, S. C. (2003). Shaping the next one hundred years: new methods for quantitative, long-term policy analysis. Rand, Santa Monica, CA.

Lenderink, G., Buishand, A., & Deursen, W. V. (2007). Estimates of future discharges of the river Rhine using two scenario methodologies: direct versus delta approach. *Hydrology and Earth System Sciences*, *11*(3), 1145-1159.

Mehan, S., Guo, T., Gitau, M., & Flanagan, D. C. (2017). Comparative study of different stochastic weather generators for long-term climate data simulation. *Climate*, *5*(2), 26.

Mehrotra R, Srikanthan R, Sharma A (2006). A comparison of three stochastic multi-site precipitation occurrence generators. *Journal of Hydrology, 331*(1–2):280–292

Mithen S, Black E (2011) Water, life and civilisation: climate, environment and society in the Jordan Valley, vol Cambridge. University Press, Cambridge

Mukundan, R., Acharya, N., Gelda, R. K., Frei, A., & Owens, E. M. (2019). Modeling streamflow sensitivity to climate change in New York City water supply streams using a stochastic weather generator. *Journal of Hydrology: Regional Studies*, *21*, 147-158.

Peleg, N., Fatichi, S., Paschalis, A., Molnar, P., & Burlando, P. (2017). An advanced stochastic weather generator for simulating 2-D high-resolution climate variables. *Journal of Advances in Modeling Earth Systems*, *9*(3), 1595-1627.

Peleg, N., Fatichi, S., Paschalis, A., Molnar, P., & Burlando, P. (2017). An advanced stochastic weather generator for simulating 2-D high-resolution climate variables. *Journal of Advances in Modeling Earth Systems*, *9*(3), 1595-1627.

Prudhomme, C., R.L. Wilby, S. Crooks, A.L. Kay, and N.S. Reynard. (2010). Scenario-Neutral Approach to Climate Change Impact Studies: Application to Flood Risk. *Journal of Hydrology, 390*(3-4): 198–209. doi:10.1016/j.jhydrol.2010.06.043.

Räisänen, J., & Ruokolainen, L. (2006) Probabilistic forecasts of near-term climate change based on a resampling ensemble technique. *Tellus A: Dynamic Meteorology and Oceanography*, *58*(4), 461-472.

Reichler, T., & Kim, J. (2008). How well do coupled models simulate today's climate?. *Bulletin of the American Meteorological Society*, *89*(3), 303-312.

Richardson CW, Wright DA (1984). WGEN: a model for generating daily weather variables. US Department of Agriculture, Agricultural Research Service, ARS-8

Ritchie, H., & Roser, M. (2017). CO_2 and other greenhouse gas emissions. Our World in Data.

Salas, J. D., Obeysekera, J., & Vogel, R. M. (2018). Techniques for assessing water infrastructure for nonstationary extreme events: a review. *Hydrological Sciences Journal*, *63*(3), 325-352.

Seidou, O., Ramsay, A., & Nistor, I. (2012). Climate change impacts on extreme floods II: improving flood future peaks simulation using non-stationary frequency analysis. *Natural Hazards*, *60*(2), 715-726.

Semenov, M. A. (2008). Simulation of extreme weather events by a stochastic weather generator. *Climate Research*, *35*(3), 203-212.

ŞEN, Z., & Eljadid, A. G. (1999). Rainfall distribution function for Libya and rainfall prediction. *Hydrological sciences journal*, *44*(5), 665-680.

Sharif M, Burn DH (2007). Improved K-nearest neighbor weather generating model. *J Hydrol Eng 12*(1):42–51

Santer, B. D., Thorne, P. W., Haimberger, L., Taylor, K. E., Wigley, T. M. L., Lanzante, J. R., ... & Karl, T. R. (2008). Consistency of modelled and observed temperature trends in the tropical troposphere. *International Journal of Climatology: A Journal of the Royal Meteorological Society*, *28*(13), 1703-1722.

Stainforth, D. A., Downing, T. E., Washington, R., Lopez, A., & New, M. (2007). Issues in the interpretation of climate model ensembles to inform decisions. *Philosophical Transactions of the Royal Society of London A: Mathematical, Physical and Engineering Sciences*, *365*(1857), 2163-2177.

Steinschneider, S., & Brown, C. (2013). A semiparametric multivariate, multisite weather generator with low-frequency variability for use in climate risk assessments. *Water resources research*, *49*(11), 7205-7220.

Stocker, T. F., Qin, D., Plattner, G. K., Tignor, M., Allen, S. K., Boschung, J., ... & Midgley, P. M. (2013). *Climate change* 2013: The physical science basis.

Taylor, K. E., Stouffer, R. J., & Meehl, G. A. (2012). An overview of CMIP5 and the experiment design. *Bulletin of the American Meteorological Society*, 93(4), 485-498.

Thom, H. C. (1951). A frequency distribution for precipitation. *Bull. Am. Meteorol. Soc, 32*(10), 397.

Weaver, C.P., R.J. Lempert, C. Brown, J.A. Hall, D. Revell, and D. Sarewitz. 2013. Improving the Contribution of Climate Model Information to Decision-Making: The Value and

Demands of Robust Decision Frameworks. *Wiley Interdisciplinary Reviews: Climate Change* 4 (1): 39–60. doi:10.1002/wcc.202.

Whitfield, P. H., & Cannon, A. J. (2000). Recent variations in climate and hydrology in Canada. *Canadian Water Resources Journal*, *25*(1), 19-65.

Widmann, M., Bretherton, C. S., & Salathé Jr, E. P. (2003). Statistical precipitation downscaling over the northwestern United States using numerically simulated precipitation as a predictor. *Journal of Climate*, 16(5), 799-816.

Wilby, R. L., & Dessai, S. (2010). Robust adaptation to climate change. *Weather*, *65*(7), 180-185.

Wilby RL, and Fowler HJ (2011). Regional climate downscaling: modelling the impact of climate change on water resources. In: Fai Fung C, Lopez A, New M (eds) Modelling the impact of climate change on water resources. Wiley, Hoboken. ISBN 978-1-405-19671-0

Wilby, R. L., Charles, S. P., Zorita, E., Timbal, B., Whetton, P., & Mearns, L. O. (2004). Guidelines for use of climate scenarios developed from statistical downscaling methods. Supporting material of the Intergovernmental Panel on Climate Change, available from the DDC of IPCC TGCIA, 27.

Wilks DS (1998). Multi-site generalization of a daily stochastic precipitation model. *J Hydrol* 210:178–191

Woolhiser, D. A., & Roldan, J. (1982). Stochastic daily precipitation models: 2. A comparison of distributions of amounts. *Water resources research*, *18*(5), 1461-1468.

Yates D, Gangopadhyay S, Rajagopalan B, Strzepek K (2003). A technique for generating regional climate scenarios using a nearest-neighbor algorithm. *Water Resour Res, 39*(7):1199

Zhang X, Garbrecht JD (2003) Evaluation of CLIGEN precipitation parameters and their implication on WEPP runoff and erosion prediction. *Trans ASAE* 46:311

CHAPTER 3.

*The Adequacy of Stochastically Generated Climate Time Series for Water Resources Systems Risk and Performance Assessment**

Abstract.

Stochastic weather generators are designed to produce synthetic time series that are commonly used for risk discovery, as they would contain rare events that can lead to potentially catastrophic impacts on the environment, or even human lives. These time series are sometimes used as inputs to rainfall-runoff models to simulate the hydrological impacts of these rare events. This paper presents a method that evaluates the usefulness of weather generators by assessing how the statistical properties of simulated precipitation, temperatures, and streamflow deviate from those of observations. This is achieved by plotting a large ensemble of (1) synthetic precipitation and temperature time series in a Climate Statistics Space (CSS), and (2) hydrological indices using simulated streamflow data in a Risk and Performance Indicators Space (RPIS). The performance of the weather generator is assessed using visual inspection and the Mahalanobis distance between statistics derived from observations and simulations. A case study was carried out on the South Nations Watershed, located in Ontario, Canada, using five different weather generators: two versions of WeaGETS (Weather Generator, École de Technologie Supérieure), two versions of MulGETS (Multisite Stochastic Weather Generator, École de Technologie Supérieure) and the K-Nearest Neighbour weather generator (k-nn). Results show that the MulGETS model often outperformed the other weather generators for that particular study area because: a) the observations were well centered within the cloud of points, representing the synthetic time series in both spaces, and b) the points generated using MulGETS had a smaller Mahalanobis distance to the observations than those generated with the other weather generators. The k-nn weather generator performed particularly well in simulating minimum and maximum temperatures, but was the worst for precipitation and streamflow statistics.

Keywords: Weather generator assessment; Stochastic Hydrological modelling; Risk and performance indicators.

---

* This chapter has been published in the journal of *Stochastic Environmental Research and Risk Assessment* (*SERRA*) as "Alodah, A., & Seidou, O. (2019). The adequacy of stochastically generated climate time series for water resources systems risk and performance assessment. *Stoch Env Res Risk A.*, *33*(1), 253-269."

3.1 Introduction

Short or incomplete historical records, either in their length or spatial coverage, can limit hydrological analyses and consequently make water engineering designs more difficult (Loucks *et al*., 1981). A large number of environmental and hydrological applications where hydro-ecological variables are simulated to evaluate alternative designs and policies (Brocca *et al*., 2013) cannot be satisfactorily carried out with sufficient observed hydro-climatic records. Instead, modellers resort to stochastic weather generators to generate long and gap-free time series of atmospheric variables using available historical climate data. The synthetically generated outputs ideally have the same characteristics as observations (e.g., mean or variance) and used to assess the impacts of climate variability (Ailliot *et al*., 2015; Guo *et al*., 2017). The implications of using such outputs as inputs to a hydrological model are investigated in this paper.

A number of weather generators since the 1980s has been put forward to address climate, agricultural, and hydrological problems (e.g., Richardson, 1981; Kavvas and Herd, 1985; Govindaraju and Kavvas,1991), and more recently, also for climate change impact assessment (e.g., Kim *et al.*, 2007; Hashmi *et al.*, 2011; Forsythe *et al.*, 2014; Camera *et al.*, 2017). Interestingly, Let-It-Rain (Kim *et al*., 2017), for example, is a new stochastic weather generator that provides end user with high temporal resolution synthetic rainfall time series easily online. Weather generators are computationally inexpensive tools, designed to produce synthetic time series of weather data for a particular location, by replicating the statistical characteristics of a meteorological variable (Ailliot *et al*., 2015). Weather generators are typically utilized to produce precipitation (PCP), minimum temperature (Tmin) and maximum temperature (Tmax), as well as solar radiation data (Brissette *et al*., 2007) based on a calibration data set but similar sequences of observed climate events are not likely to occur (Wilby & Fowler, 2011). Baigorria and Jones (2010) divided weather generators, based on their structure and mathematical algorithms, into three classes: (1) parametric based on random sampling from parametric distributions (e.g., Wilks, 1998; Brissette *et al*., 2007), (2) non-parametric based on resampling from observations (e.g., Rajagopalan *et al*., 1997; Wilby *et al*., 2003; Sharif

and Burn, 2007), and (3) hybrid approaches (e.g., Palutikof *et al*., 2002; Fowler *et al*., 2005; Shao *et al*., 2015).

The performance of weather generators, however, has been repeatedly criticized. Their drawbacks include their poor performance when modelling inter-annual variability of monthly means, although some recent rainfall generation models (e.g., Kim *et al*., 2013) were presumably able to overcome this issue by incorporating more information about the observed precipitation. They also suffer notoriously from their strictly site-specific nature (Fowler *et al*., 2007), which limits the usefulness of their results and makes them difficult to transferable to other locations and climates. Nevertheless, weather generators are practical and useful for some applications, such as reproducing the number of wet spells and estimating monthly precipitation levels for hydrological applications in developing countries (Wilby & Fowler, 2011). In the face of the recent advances in weather generators, the accuracy of generated weather data has not always been adequately justified. Precise meteorological data cannot be expected from weather generators considering the stochastic uncertainties involved, making any decision for or against the use of a certain weather generator in a decision or design framework particularly challenging. Therefore, the credibility of a given weather generator should be deliberated by quantifying their suitability for a specific field or climate zone.

The present paper proposes a new avenue to build a framework for assessing weather generators realizations by comparing the mapping between observed and generated climate states, and describing statistics that are relevant to the problem at hand. A climate state, represented by a time series X_t, is summarized by a subset of climate statistics, $\mathcal{V}_T$ that are relevant to the problem under investigation (e.g., the mean, and the standard variation of precipitation and temperature), calculated for a period, T (41 years in the present case) as introduced by Brown *et al.* (2012). $\mathcal{V}_T$ is calculated for the observed time series and stochastically generated time series. A climate state will yield a level of risk and performance that can be measured through a set of indicators obtained by feeding an impact model with time series X_t. This was accomplished by using five stochastic weather generators to create plausible daily data series of precipitation and temperatures. Each

one of the generated time series (i.e., realization of climate data) was then used as an input to a rainfall-runoff model to explore their realism in risk and performance indicators for an explicit accounting of streamflow.

With the multitude of numerous available approaches, this paper focuses on three weather generators that apply different methodologies and techniques, namely: WeaGETS, MulGETS, and k-nn. The WeaGETS model (Chen *et al*., 2012) is an extension to the WGEN model (Richardson and Wright, 1984). Unlike WGEN, however, WeaGETS provides a spectral correction approach for a better estimation of low-frequency component and consequently improved simulation of monthly and interannual variability. Yet, WeaGETS is rather more suited to small watersheds wherein a single station can be used to represent the entire watershed (Chen *et al*., 2012), and is thus of limited use for modelling multi-site watersheds within large basins (Mehrotra *et al*., 2006). The selection of weather generators is not exhaustive but since the objective of the paper is to present a framework to evaluate weather generators, the choice is made to work on a small ensemble of schemes.

The so-called Multi-site weather Generator (MulGETS) has been introduced by Chen *et al*. (2014) to provide a weather generator with the capability to account for the spatial attributes of climate data. For the generation of precipitation amounts, a considerable amount of literature has been published on the best-fit probability distribution function of precipitation amounts. The gamma distribution function has been traditionally the most preferred to wet-day daily precipitation (e.g., Thom, 1951; Buishand, 1978; Geng *et al*., 1986; Sen and Eljadid, 1999). Moreover, other distributions have been recommended such as exponential (e.g., Woolhiser and Roldan, 1982; Wilks, 1998; Burgueño *et al*., 2005), Weibull (e.g. Burgueño *et al*., 2005). Hanson and Vogel (2008) recommended the Pearson Type-III (P3) distribution to be applied to the full record of daily precipitation data. Beside WeaGETS and MulGETS, the *K*-nearest neighbor scheme (k-nn) is used for precipitation sequences applying the model by Goyal *et al.* (2012) while the method by Sharif and Burn (2007) was implemented for the generation of temperature sequences. k-nn is a broadly used non-parametric procedure to simulate daily weather variables with no assumptions of the

probability distributions. Its principal concept is to stochastically reshuffle the values from the observed records by looking for a similar pattern to the day of interest (Yates *et al*., 2003).

The hydrological response to the synthetic climate series is a key component for impact assessments. This was evaluated in the Soil and Water Assessment Tool (SWAT-2012). SWAT is a semi-distributed, basin-scale hydrologic model, which has been widely used by hydrologists to address complex water quality and quantity issues and appropriate decisions on water resource management (Srinivasan and Arnold. 1994; Arnold *et al*., 1998; White and Chaubey, 2005; Neitsch *et al*., 2011; Tuppad *et al*., 2011; Arnold *et al*., 2012; Santhi *et al*., 2014). The main physically based input that governs the transformation of precipitation into runoff in SWAT, is weather information (Arnold *et al*., 2012). SWAT's comprehensive physical-process parameterizations strengthen its capability to provide sufficient information for adequate watershed management decisions. To deal with spatial variations in a watershed of interest, a watershed is divided into a number of hydrologic response units (HRUs), each within its own sub-basin. Beside land cover and soil type, each HRU has its own characteristics, such as weather, groundwater, plant growth, land-use, and soil type (Neitsch *et al*., 2011).

The next section introduces briefly the study area and the data used before describing the study methodology. Subsequent sections present the results and a discussion of the main findings, and lastly, a summary of the main points and identifying areas for further research in the conclusion.

3.2 Study Area, and Hydroclimatic Data

3.2.1 Study Area

An example case study was conducted on the South Nation Watershed (Figure 3.1), located in Eastern Ontario, Canada, covering an area about 4000 km^2 between 75°43′ W - 74°22′ W longitude and 44°40′ N - 45°38′ N latitude. The South Nation River, which drains the Watershed, runs northeast from Brockville for 175 km towards Plantagenet. The Watershed is relatively flat as the river has a low topographic gradient of just 80m between its headwaters and the confluence

with the Ottawa River. As a result, the South Nation Watershed is poorly drained, which in turn maximizes the flood risk and boosts the erosion of riverbanks and of topsoil on the agricultural lands.

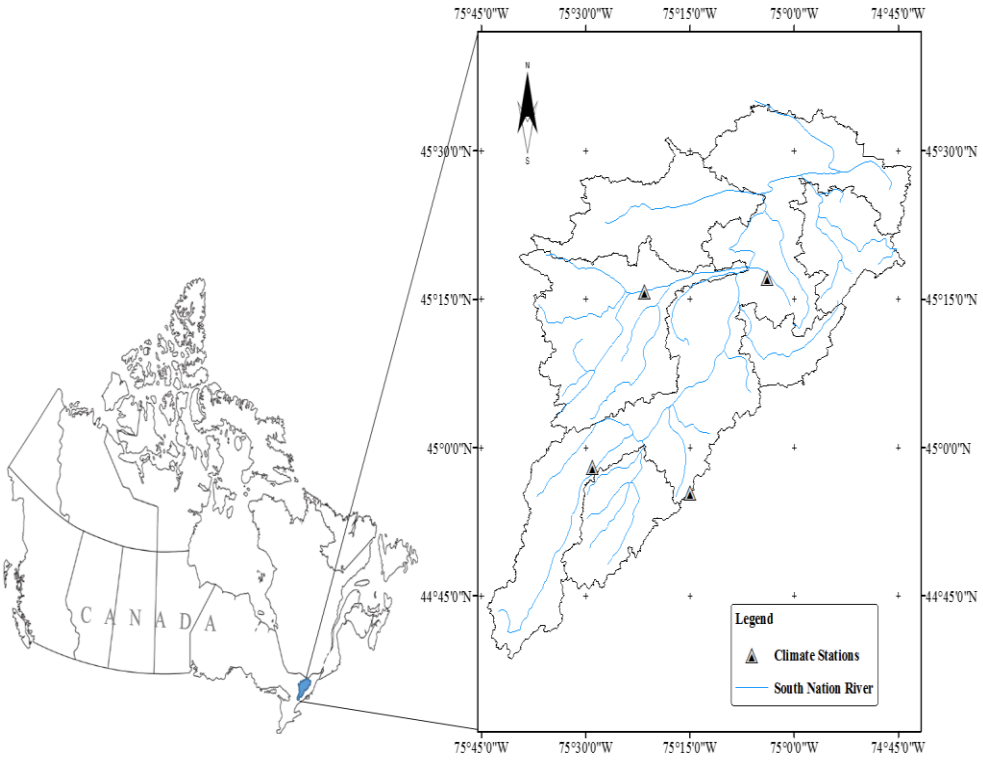

Figure 3.1 The location of the South Nation Watershed and the meteorological gages.

3.2.2 Hydroclimatic Data

Meteorological data were obtained from four gauges over a period of 41 years with locations chosen to be representative of the entire South Nation Watershed (cf., Figure 3.1 and Table 3.1). These stations have complete data series for the period of 1971–2011, namely; St. Albert, Russell, Morrisburg, and South Mountains. On average, the area receives approximately 985mm of precipitation annually, and its annual mean maximum and minimum temperatures are 11.5 and 1.2°C, respectively (Environment Canada, 2012). For the simulations with the weather generators, days with a minimum precipitation of 1mm are considered wet as defined by earlier studies (e.g.,

Frich *et al*., 2002; Sun *et al*., 2006; Klein Tank *et al*., 2009; Polade *et al*., 2014) to neglect small traces of moisture present in the air (i.e., by dew, or fog) (Benestad *et al*., 2012). The length of the generated data set is chosen to match the length of the observed time series.

Table 3.1 Meteorological stations details.

Meteorological Station	CI*	Latitude (N)	Longitude (W)	Elevation (m)	Precipitation **		Tmax **		Tmin **	
					Mean	Stdev	Mean	Stdev	Mean	Stdev
Russell	6107247	45° 15' 46"	75° 21' 34"	76.2	2.63	5.97	11.50	12.54	1.20	11.75
South Mountain	6107955	44° 58' 00"	75° 29' 00"	84.7	2.64	6.07	11.64	12.44	1.46	11.66
Morrisburg	6105460	44° 55' 25"	75° 11' 18"	81.7	2.77	6.17	11.73	12.42	1.21	11.79
St. Albert	6107276	45° 17' 14"	75° 03' 49"	80	2.77	6.06	11.29	12.55	0.79	11.87

*** Climate Identifier (CI) refers to the station number assigned by the Meteorological Service of Canada (MSC).**

**** Daily statistics.**

3.3 Methodology

The main components of the methodology are illustrated in Figure 3.2. A number of weather generators are first used to generate 1000 realizations of precipitation and temperature time series. Each realization of the generated climate time series is then used individually as an input to a hydrological model to obtain streamflow time series. The number of realizations was set to 1000 in order to ensure that the confidence intervals of statistics in the Climate Statistics Space (CSS) and Risk and Performance Indicators Space (RPIS) are calculated with precision. Guo *et al*. (2017) looked into the numbers of realizations that can satisfactorily capture a number of statistical characteristics of precipitation, and maximum and minimum temperatures using three weather generators: CLIGEN, LARSWG, and WeaGETS. They analyzed increasing numbers of realizations (1, 25, 50, and 100) and concluded that a weather generator would well reproduce essential statistical characteristics with 25 realizations. However, the statistics considered in their papers only belong to the CSS. Given that the calculation of statistics in the RPIS involves highly

nonlinear rainfall-runoff transformation, it is speculated that a higher number of realizations would be needed. It was therefore decided to use a number of realizations that is two orders of magnitude higher than the one recommended by Guo *et al.* (2017). A number of statistics (i.e., moments) of the simulated climate as well as SFSD (Simulated Flow using Synthetic data) time series are compared to those of observed climate as well as SFOD (Simulated Flow using Observed data) time series to assess how good the weather generators are. Further, the autocovariance structure of streamflow is analyzed as well. Autocorrelation function measures the stochastic component in a time series by reflecting how the observations in a time series are related to each other. Flow autocorrelation is important factor also for reservoir operation studies.

The different algorithms and submodels applied in the methodology are described in the following sections.

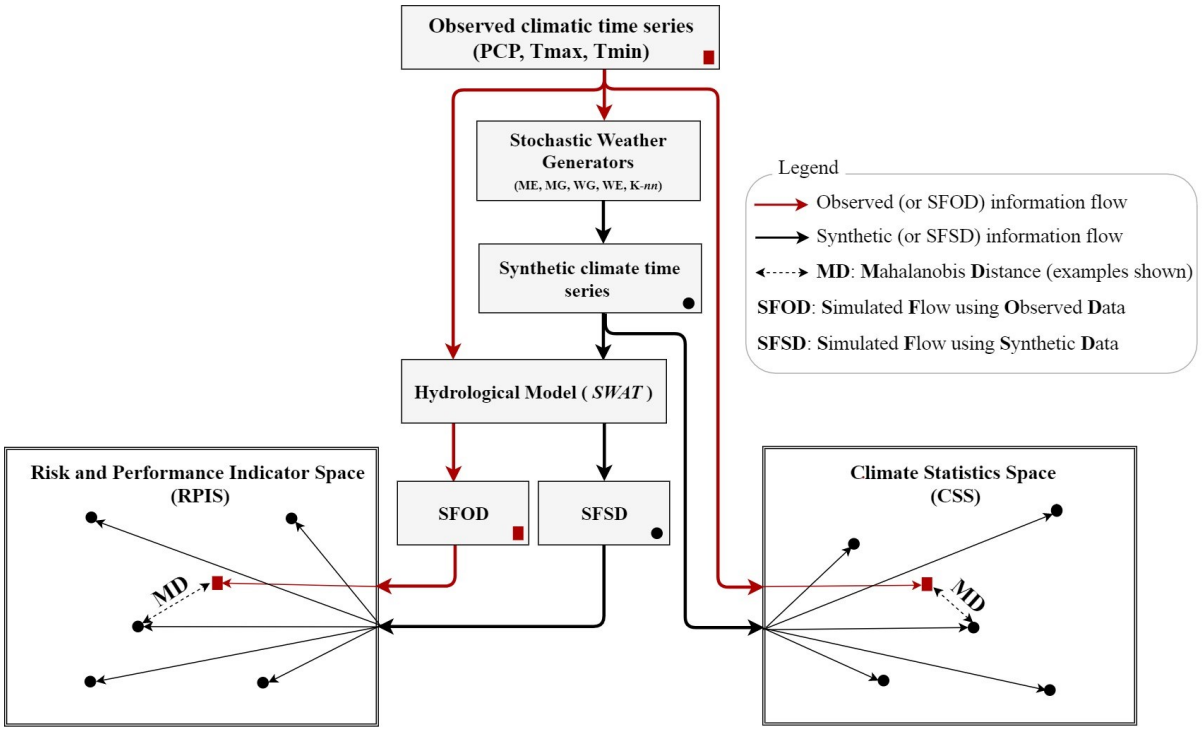

Figure 3.2 A Schematic diagram illustrating the methodology.

3.3.1 Stochastic Weather Generators

The present approach is examined in, but not limited to, several weather generators that apply different methodologies and schemes to generate climatic series. The generation of temperatures in weather generators is relatively simple as it takes a continuous range of values and can be described by a normal distribution (Chen and Brissette, 2014) whereas simulation of precipitation may be an intricate challenge. The stochastic nature of precipitation process is typically simulated in a two-step process for precipitation occurrence and amounts. It is a common practice to use Markov chain (Markov, 1906) models (i.e., precipitation states, wet or dry, of a given day based on the previous state) for daily precipitation occurrence while some weather generators use the alternative renewal process such as LARS-WG (Semenov and Barrow, 2002). The basic input data for tested weather generators in this study include observed precipitation as well as maximum and minimum temperatures data (Figure 3.2).

WeaGETS (version 1.6) provides three orders of Markov chains to precisely account for wet and dry spells (two-state Markov chain with first-, second- and third-order models) and for precipitation amounts (exponential, gamma, skewed normal and mixed exponential distributions) based on a bi-weekly time scale. In this study, daily precipitation sequences are generated using a third-order Markov model without parameter smoothing coupled with exponential (herein called 'WE') and gamma (herein called 'WG') distributions with a minimum precipitation threshold of 0.1mm. A higher-order Markov model, which increases the number of parameters, is chosen to adequately predict lengths of consecutive dry/wet days (Bastola *et al.*, 2011). This selection was adopted routinely by previous works (e.g., Wilks, 1998; Lennartsson *et al.*, 2008; Chen *et al.*, 2012, Ailliot *et al.*, 2015). WeaGETS temperature variables are generated conditional to each other using a normal distribution. The model uses first-order linear auto-regression coupled with constant lag-1 auto correlation and cross correlation to synthetically generate maximum and

minimum temperatures. WeaGETS implements Finite Fourier series with two harmonics to model seasonal cycles.

MulGETS (version 1.2) is a multisite, multivariate weather generator developed by Chen *et al*. (2014) to simulate daily precipitation (based on Brissette *et al*., 2007) and temperature. However, unlike WeaGETS, MulGETS constructs random values that are spatially correlated but temporally independent. This is achieved following a distribution-free approach (Iman and Conover 1982) coupled with an optimization algorithm described by Brissette *et al*. (2007). For precipitation occurrence process, a first-order Markov chain with Cholesky factorization is applied. Wet-day precipitation sequences were reproduced from MulGETS using a multi-Gamma distribution (a combination of several gamma distributions) (herein called 'MG') and multi-Exponential distribution configuration (herein called 'ME'). In terms of generating temperature variables, MulGETS is WeaGETS-like, yet the generation of spatially correlated temperature variables (Tmax and Tmin) is achieved following a distribution-free approach and using a first-order linear autoregressive model.

A simple k-nearest neighbor resampling model as proposed by Goyal *et al.* (2013) is used to generate precipitation sequences. The later seemingly allows producing of unprecedented values in the calibration data set. The procedure involves taking into account the spatial correlation by computing the regional means of precipitation. Some k-nn models that use gamma kernel approaches can prevent producing unrealistic values of less than zero but consequently affect the mean value overall. However, Goyal *et al*. (2013) approach implements gamma kernel perturbation following Salas and Lee (2010) wherein a random value, for a certain day, is perturbed from the kernel density after placing one of the k nearest neighbors to the current value X at the center of a gamma kernel. For precipitation, the temporal window w and the number of nearest

neighbors k are chosen to be 7 days and 13 neighbors. The method by Sharif and Burn (2007) was implemented for the generation of temperature sequences, with no underlying probability distribution assumptions. This approach is based on a traditional autoregressive model, but a random component is added to the individual resampled data points in order to reproduce values that are not in the historical records. For temperature variables, the temporal window and the number of nearest neighbors k are arbitrarily chosen to be 14 days and 7 neighbors. The two k-nn approaches are presumably capable of generating realistic precipitation and temperature sequences. However, since Tmax and Tmin were modeled independently from the precipitation status while they are coextensive with each other in real-world cases, this could affect their efficiency (i.e., by not preserving the correlations between precipitation and temperature). Yet, this should not constrain their individual ability to simulate univariate interannual variability accurately.

Wet-day precipitation sequences were reproduced from WeaGETS and WeaGETS using Gamma and Exponential set-up. The probability density distribution (pdf) of gamma is given by:

$$f(x) = \frac{(x/\beta)^{\alpha-1} \, exp[-x/\beta \,]}{\beta \, \Gamma(\alpha)} \qquad \textbf{Eq. 3.1}$$

where α and β are the shape and scale parameters respectively, and Γ(α) denotes the gamma function calculated at α. The two parameters (α and β) required in order to use the gamma distribution are directly linked to the mean (μ) and the standard deviation (σ). They are defined as follows:

$$\mu = \alpha/\beta \qquad \textbf{Eq. 3.2}$$

$$\sigma = \sqrt{\alpha}/\beta \qquad \textbf{Eq. 3.3}$$

Chen *et al*. (2012) indicated that exponential distribution is easier to calculate but has less performance compared to the gamma distribution. The probability density function (pdf) of the exponential distribution is given by:

$$f(x) = \lambda e^{-\lambda x} \qquad \textbf{Eq. 3.4}$$

where x is the daily precipitation amount and its parameter λ equals 1/mean. The multi-exponential distribution combines several exponential distributions, which each has its own parameter.

3.3.2 Hydrological Modelling

The Soil and Water Assessment Tool (SWAT-2012) is used to evaluate the hydrological response of the watershed to the synthetically generated climate series. In order to adequately simulate the spatial distribution of hydrological processes, the South Nation Watershed was divided into a total of 31 distinct sub-basins, using precipitation and temperature data from the four selected stations representing the Watershed (cf. Figure. 3.1) as well as streamflow data. Calibration based on local conditions was done with SWAT-CUP (Abbaspour *et al.*, 2007) using the SUFI-2 (sequential uncertainty fitting ver. 2) optimization algorithm to reduce the prediction uncertainty.

A set of statistical metrics was used to assess the performance of the calibrated model: the Nash–Sutcliffe efficiency, the RMSE-observations standard deviation ratio, and the percent bias and the criteria by Liew *et al*. (2007) and Moriasi *et al*. (2014) were adopted to evaluate model accuracy. The Nash–Sutcliffe efficiency coefficient (NS), as proposed by Nash and Sutcliffe (1970), is vastly used as an indicator of the hydrological model's efficiency, which can range from - ∞ to 1. The closer NS is to 1, the better the agreement between observations and simulations. The NS can be computed as:

$$NS=1-\left[\frac{\sum_{i=1}^{n}(O_i-P_i)^2}{\sum_{i=1}^{n}(O_i-\overline{O})^2}\right] \quad \textbf{Eq. 3.5}$$

where O stands for observed and P for predicted values, and $\overline{O}$ is the mean of the observed values. The RMSE-observations standard deviation ratio (RSR) was used whenever RMSE (root-mean-square error) values were less than half the standard deviation of the observed data (Singh *et al*., 2005). RSR can be calculated as:

$$RSR=\frac{RMSE}{SRDEV_{obs}}=\frac{\left[\sqrt{\sum_{i=1}^{n}(O_i-P_i)^2}\right]}{\left[\sqrt{\sum_{i=1}^{n}(O_i-\overline{O})^2}\right]} \quad \textbf{Eq. 3.6}$$

The percentage of bias (PBIAS) compares the simulated discharge to observed values, yielding positive/negative values for over-/underestimations, respectively, but ideally a percentage close to zero (Gupta *et al*., 1999). PBIAS percentages are computed as:

$$PBIAS=\frac{\sum_{i=1}^{n}(O_i-P_i)*100}{\sum_{i=1}^{n}(O_i)} \quad \textbf{Eq. 3.7}$$

3.3.3 Performance spaces (CSS and RPIS)

In the present approach, the abovementioned stochastic weather generators have been run for one thousand times (i.e., realizations) for a better chance on capturing essential statistical characteristics of the climate (Hansen and Ines 2005; Guo *et al.*, 2017). Similar to observations in length, 41-year synthetic observed-like weather series were generated for each station. Each realization was represented by its statistics ($\mathcal{V}_T$) in the confidant interval figures. The objective is to discover how popular an observation event to occur in the cluster of experiments or closer the mean of a cloud of points representing the synthetic time series in the CSS. In other words, the observation event is tested against the normal pattern of synthetic weather generator data, using an

adopted threshold. Synthetic climate and streamflow data of a well-behaved weather generator should preserve the observed climate and streamflow statistical moments, namely the mean (μ), standard deviation (σ), skewness (α_3), and kurtosis (α_4). Nonetheless, the proposed approach is not limited to these statistics and further investigation may be necessary to address other characteristics that are relevant to the problem at hand. For example, more analysis based on cross-correlation or log-odd ratios between all stations is suggested to explore the usefulness of multisite modeling of weather generators.

Furthermore, we investigate whether proximity with observations in the CSS translates into proximity in the RPIS. The calibrated SWAT model was forced with each one of the thousand synthetically-generated climate realizations for each weather generator, each realization comprises precipitation, maximum and minimum temperatures data. Other meteorological inputs, such as wind speed, relative humidity, and solar radiation data, were kept constant using observational data. We then compared a set of one thousand simulated streamflow ensemble to simulated streamflow using observed climate data, in order to examine the model performance and their realism in RPIS. The streamflow attributes, or measures of central tendency, were used to evaluate the degree to which a weather generator could reproduce the measured streamflow distributions. When examining the distributions of the mean versus the key attributes, including the standard deviation, skewness, and kurtosis of the observed and stochastically produced climate, the atmospheric variables should be reproduced correctly in a distributional sense.

Given the stochastic nature of streamflow, it is often in the interest of hydrologists to examine flow extremes using statistical models (probability distribution based) in order to assess risk associated with the extreme hydrological events. Two sets of hydrologic risk indicators were used to compare the performance of each weather generator in the RPIS including the traditional case of annual

maxima (*AM* series) and the low flows frequency. The *AM* series was fitted to the three-parameter Generalized Extreme Value (GEV) distribution (Cunnane, 1989), while the three-parameter Weibull (WBL) distribution (Pilon, 1990), also referred to as the Gumbel Type III distribution, was applied to the annual 7-day minima flow (*7Q*), implementing the maximum likelihood estimates (MLE) for parameter distributions. The 7-day minima flow, computed on an annual basis over the smallest flow of 7-consecutive days. The *7Q10*, for example, is the single most commonly employed low flow index with a 10-year return period, and has a non-exceedance probability of 10%.

3.3.3.1 Assessing Similarity in the CSS and RPIS

As stated by Kovalchuk *et al.* (2017), the quality of ensemble-based simulations can be estimated using the relative distance of a group of simulation outputs to its corresponding observations. Kovalchuk *et al*. (2017) listed several potential distance measures such as the Euclidian distance or the Mahalanobis distance. Given the multitude of competitive techniques, the Mahalanobis distance (MD), also known as the generalized squared distance, is the selected probabilistic metric in order to compare observed-to-ensemble of realizations in the CSS and RPIS because of its less sensitive to the differences of magnitudes of the statistics. MD is a tool frequently applied for the detection of anomalous, or for a discriminant analysis to find the probability of a certain sample belonging to a certain group (Huber and Ronchetti, 2009; Fritsch *et al*., 2012; Wang and Zwilling, 2014). The Mahalanobis distance is the quadratic distance of a pre-selected point $x_i \in \mathbb{R}^P$ (an event representing observations) from the origin μ (the centre of a cloud representing ensemble realizations), governed by a covariance matrix Σ (a shape parameter), given by the quantity:

$$MD(\vec{x_i}, \vec{\mu}) = (\vec{x_i} - \vec{\mu})^T \Sigma^{-1} (\vec{x_i} - \vec{\mu}) \qquad \textbf{Eq. 3.8}$$

Moreover, the problem of possible inter-correlation between the original variables is solved through components analysis, which reduces the number of variables to the most relevant.

The set of points that are determined by invariant Mahalanobis distances will form an ellipse (bivariate) or ellipsoid (multivariate) about the mean vector, μ. The orthogonal axes of such an ellipse and their lengths are governed by the eigenvectors (Φ) of the covariance vector (Σ), and the eigenvalues (Λ), respectively. The smaller the MD value, the closer a sample is positioned to a mean value (i.e., a focus) of the ellipse. Outliers can be identified as having large MD values. However, it is important to bear in mind that especially for multi-dimensional multi-variates, an ordinary sample could be falsely identified as an outlier if one attribute is considerably biased. The definition of a particular threshold distance to identify outliers should, therefore, be performed with caution, as it depends on the particular application and type of sample. In theory, the Mahalanobis squared distance describes the distance of a point from the group mean, in units of standard deviation; thus, as dictated by the three-sigma rule, a point with an MD value of 3 or less lies within the boundary of 99% of all data. A tested weather generator is called a good-fit candidate, when the reference point of observations (represented by two of its probability moments) falls within a reasonable distance from the investigated data centre.

The joint density function of two random variables x (μ_x and σ_x) and y (μ_y and σ_y) that hypothetically have a bivariate normal distribution as:

$$f(x,y,\rho)=\frac{1}{2\pi\,\sigma_x\sigma_y\sqrt{1-\rho^2}}\;exp\left\{\frac{-1}{2(1-\rho^2)}\left[\left(\frac{x-\mu_x}{\sigma_x}\right)^2-2\rho\left(\frac{x-\mu_x}{\sigma_x}\right)\left(\frac{y-\mu_y}{\sigma_y}\right)+\left(\frac{y-\mu_y}{\sigma_y}\right)^2\right]\right\} \qquad \textbf{Eq. 3.9}$$

where ρ is the correlation coefficient of x and y ($=\frac{\sigma_{xy}}{\sigma_x\sigma_y}$). An ellipse is formed, centred on the means (μ_x and μ_y), representing a plane of density surface, parallel to the x and y coordinates at a certain

height *K*. If the data is dependent ($\rho \neq 0$), the resulting error ellipse will not be axis aligned. The integral over an ellipse with centre at (μ_x, μ_y) is:

$$\iint_A (\sigma_x \sigma_y)^{-1} f\left(\frac{x-\mu_x}{\sigma_x}, \frac{y-\mu_y}{\sigma_y}, \rho\right) dx\, dy = 1 - e^{-\alpha^2/2} \qquad \textbf{Eq. 3.10}$$

where the equation that describes its area (A) can be parameterized with σ_x , σ_y and ρ as follows (Abramowitz and Stegun, 1972):

$$\left(\frac{x-\mu_x}{\sigma_x}\right)^2 - 2\rho\left(\frac{x-\mu_x}{\sigma_x}\right)\left(\frac{y-\mu_y}{\sigma_y}\right) + \left(\frac{y-\mu_y}{\sigma_y}\right)^2 = (1-\rho^2)\alpha^2 \qquad \textbf{Eq. 3.11}$$

where

$$\alpha^2 = ln\left[4\,\pi^2 K^2 \sigma_y{}^2 \sigma_x{}^2 (1-\rho^2)\right]^{-1} \qquad \textbf{Eq. 3.12}$$

is constant.

The resulting ellipses of constant density (i.e., constant Mahalanobis distance) will not be axis aligned and the rotated new coordinate system is following the principal axes of the ellipse, which are the eigenvectors of the data's covariance matrix. The first principal component lies in the direction of the highest variance in the data. The data projected onto the principal axes ($\dot{x}$ and $\dot{y}$) of the ellipse-shaped cloud are now independent (when ρ is zero), and a point of observations $\bar{X}$ and $\bar{Y}$ is within a constant probability ellipse if,

$$\left(\frac{\bar{X}}{\sigma_x}\right)^2 + \left(\frac{\bar{Y}}{\sigma_y}\right)^2 \leq \alpha^2 \qquad \textbf{Eq. 3.13}$$

The random variable U = $\left(\frac{\bar{X}}{\sigma_x}\right)^2 + \left(\frac{\bar{Y}}{\sigma_y}\right)^2$ follows a chi-square (χ^2) distribution with the number of degrees of freedom (*df*) equivalent to the number of independent variables (Hardin and Rocke, 2005). Therefore, its probability to lie within a certain ellipse is:

$$P[U \leq c^2] = \int_0^{c^2} \frac{e^{-u/2}}{2} du = 1 - e^{-c^2/2} \qquad \textbf{Eq. 3.14}$$

For example, 50% and 99% of samples in a bivariate normal distribution (*df*=2) lie within ellipses that have critical values of the χ^2 distribution of 1.386 and 9.210, respectively. In the current approach, a weather generator is considered a good candidate if the observed data fall within its 99% Confidence ellipse. Caution is advised as certain intervals tend to be larger than others if their variability is large (Helsel and Hirsch, 1992). Graphical representations in combination with a visual examination may, therefore, be useful to obtain a better grasp of the data.

3.3.4 Flow autocovariance

Storage-related statistics are particularly important for water resources reservoir simulation, and these are generally functions of the variance and autocovariance structure of the generated time series (Sveinson *et al*., 2007). Flow autocorrelation is important for reservoir operation studies. Reservoirs are less sensitive to instantaneous extremes such as low and high flow, but their simulation is sensitive to the persistence of low or high values, hence to correlations in flow time series.

For a time series $y_1, y_2..., y_T$ and a sample mean $\bar{y}$, the lag-*h* correlation between y_t and y_{t+1} is given by

$$\hat{\rho}_h = \frac{\sum_{t=h+1}^{T}(y_t - \bar{y})(y_{t+1} - \bar{y})}{\sum_{t=1}^{T}(y_t - \bar{y})^2} \qquad \textbf{Eq. 3.15}$$

Where *h*=1,2,…,N-1,

The standard error SE_ρ and the approximate 95% confidence intervals CI_{95} are estimated as

$$SE_{\rho} = \sqrt{\left(1 + 2\sum_{i=1}^{h-1} \hat{\rho}_i{}^2\right)/N} \qquad \textbf{Eq. 3.16}$$

$$CI_{95} = \hat{\rho}_h \pm 1.96\, SE_{\rho} \qquad \textbf{Eq. 3.17}$$

In this paper, a visual comparison of the autocorrelation functions was drawn at of observed and simulated monthly flows will be used to assess the performance of the weather generators under investigation. A good weather generator is expected to have most of its autocorrelations estimates within the 95% confidence interval bounds.

3.3.5 Dimensions of the CSS and RPIS

Ideally, the CSS and RPIS will have a dimension for each statistic that is of interest to the analysis. Obviously, the number of potential dimensions is potentially unlimited, and it is not obvious to draw a line between meaningful statistics and the others for a particular problem. Furthermore, visual comparison and interpretation of results in a space with more than three dimensions are tricky. For the sake of simplicity and ease of interpretation, only two-dimensional CSS and RPIS are discussed in this paper. We also restricted ourselves to the mean, standard deviation, skewness and kurtosis in the two spaces. The mean controls the magnitude of the variable and is particularly important in hydrological analyses where water volumes are used for reservoir design. The standard deviation is a quantification of the spread about the mean and describes the predictability of a particular variable. The skewness and kurtosis play a crucial role in the distribution of extreme values and impacts the design of flood and drought control structures. Additional dimensions can be added to the CSS and RPIS is the problem at hand warrants it, but the interpretation of the results becomes more difficult with spaces of higher dimensions.

3.4 Results and Discussion

The comparisons between observed and weather generator-driven data, in the CSS and RPIS, allow for quantifying the performances of these weather generators. The relative positions of the mean, standard deviation, skewness, and kurtosis of simulated annual precipitation, maximum and minimum temperature were compared to the ones estimated using observations in the CSS. A similar comparison was carried out for streamflow data in the RPIS space. All statistics were found to be stable in the CSS earlier than those in the RPIS. As an example, the plot of the mean annual precipitation and mean monthly streamflow is shown in Figure 3.3 as a function of the number of realizations. It shows that 25 realizations, as recommended by Guo *et al*. (2017), seem shorter than desired, particularly in the RPIS, to construct robust confidence intervals. These results comforted us in the choice of 1000 for the number of realizations for each weather generators, despite the high computational demand.

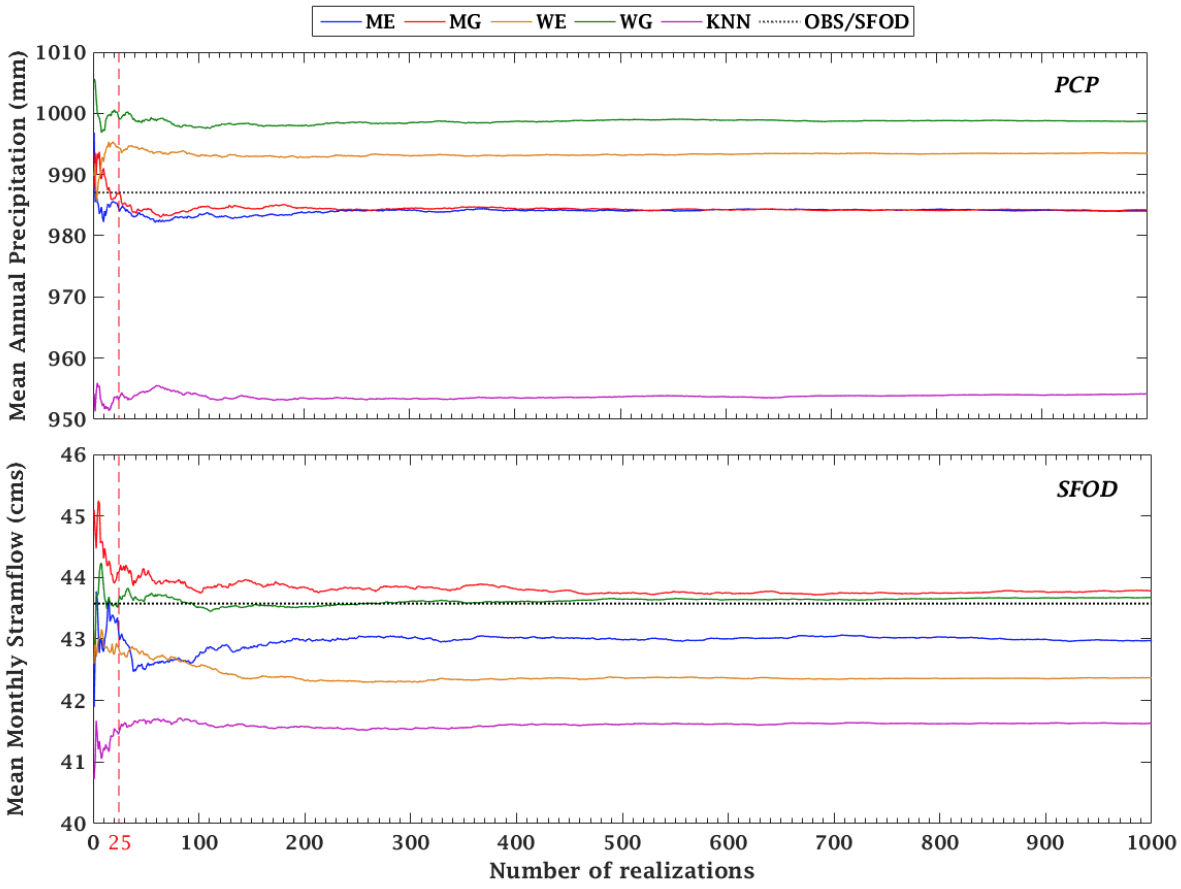

Figure 3.3. Impact of the number of realizations on the accuracy of calculated statistics in the CSS and RPIS.

3.4.1 Climate Statistics Space (CSS)

The analysis of the stochastically generated climatic daily sequences, compared to the reference data, is demonstrated here using lumped approach by averaging the climate data over all locations. The statistics of observed precipitation are shown along with elliptically-shaped confidence intervals from each weather generator dataset, representing 99% and 50% of the data (Figure 3.4). Chen *et al.*, 2012 stated that generating precipitation amounts using the gamma distribution performed reliably better than with the exponential distribution. Yet, Figures 3.4 and 3.5(a) suggest that the two distributions are comparable in the CSS. The generated precipitation amounts, using the exponential distribution in MulGETS, are slightly better than those produced with the gamma

distribution, in terms of retaining observed attributes in the CSS with MD of observed point of 0.45 and located within 9% confident interval of σ and α_3 and located acceptably in 59% of α_4. These findings are partially consistent with the work by Wilks (1998) where the exponential distribution was a better fit than the gamma distribution. The MulGETS no matter the distribution used for precipitation outperformed the WeaGETS where MD of standard deviations of ME, MG, WE and WG, were found to be 0.45, 1.03, 8.4 and 7.2, respectively (Figure 3.6). That possibly indicates the importance of preserving the cross-correlation structure between all stations. Nevertheless, the skewness and kurtosis of both models were within 99% confidence interval.

Compared to other weather generators considered in this study, the k-nearest neighbor approach performed less efficiently in reproducing precipitation attributes, where all precipitation statistics were way above the MD threshold of three. In terms of temperature variables, k-nn appears superior to the other four models in reproducing synthetic temperatures sequences while preserving the statistical features of observed data (Figure 3.5 (b and c), Figure 3.6). These differences in the obtained results can be explained, in part, by differences in the underlying numerical data assimilation algorithms for the land–ocean–atmosphere relations (Warner, 2010). An additional factor may be an inherent limitation of certain weather generators for certain climatic or topographic conditions, depending on the dominant weather systems. Fowler *et al*. (2007) also criticized weather generators for being strictly localized, which implies that they may not be useful in any region or climate. Also, further investigation of weather generators' ability of estimating extreme values of climate variables, as done for rainfall extremes by Ramesh *et al*. (2018), is warranted.

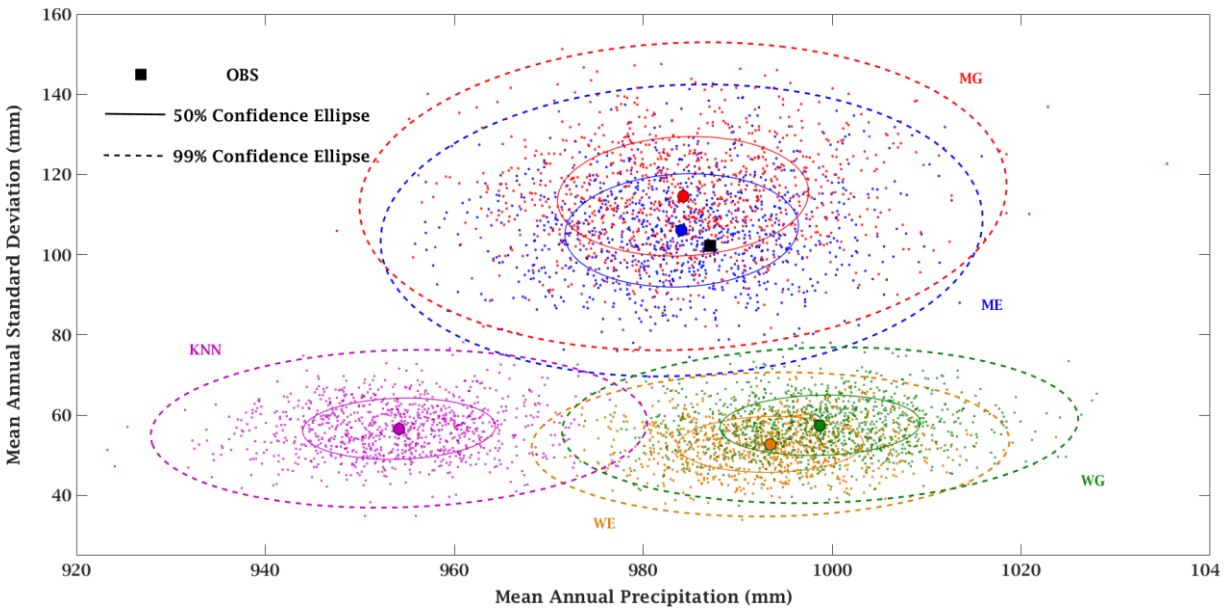

Figure 3.4 Statistics comparison of observed precipitation data (OBS) with 1000 realizations from each weather model, represented as ellipsoidally-shaped clouds around their centers with isolines of the 50% and 99% confidence intervals.

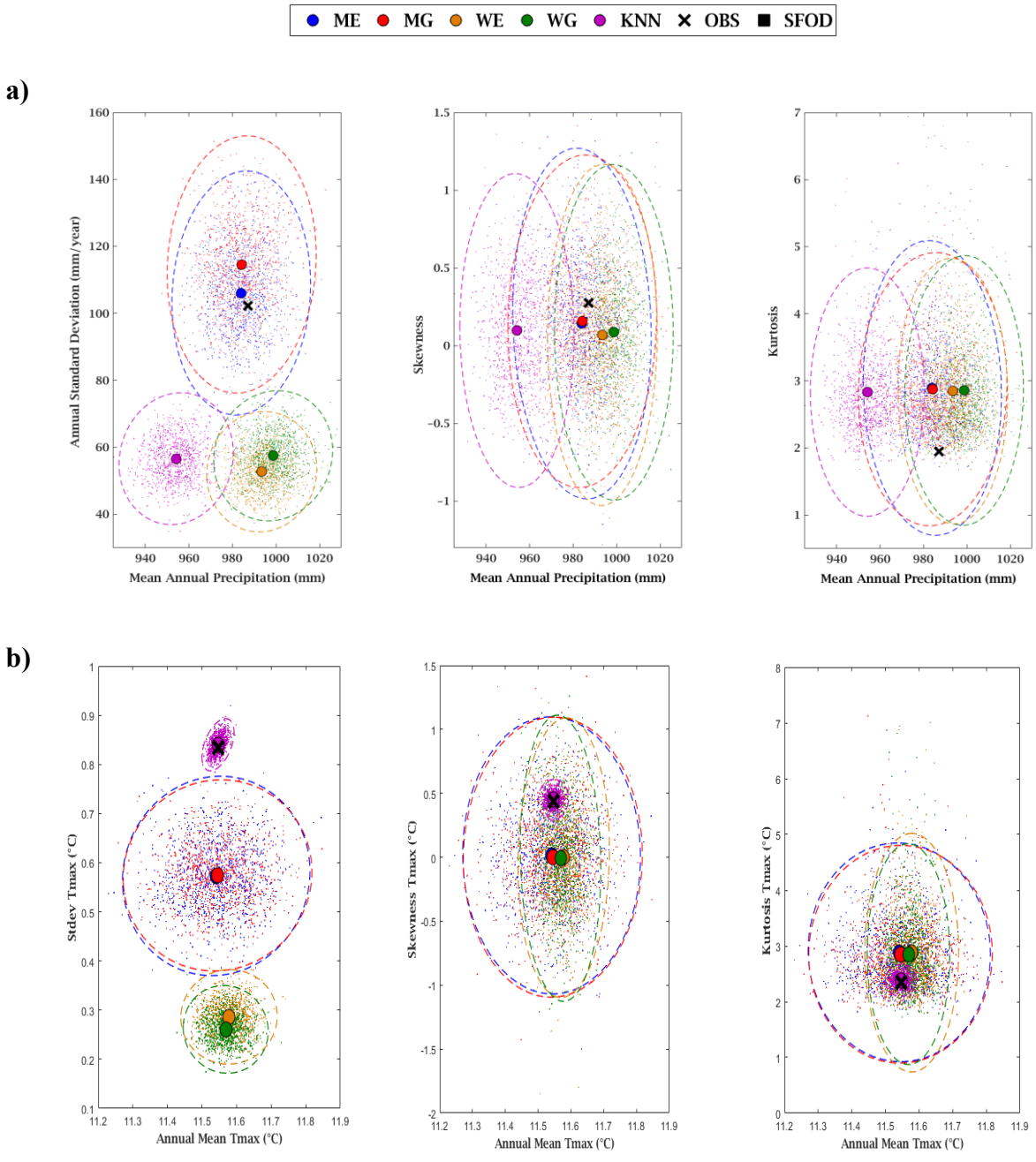
ME MG WE WG KNN OBS SFOD
a)
Annual Standard Deviation (mm/year)
Skewness
Kurtosis
Mean Annual Precipitation (mm)
Mean Annual Precipitation (mm)
Mean Annual Precipitation (mm)
b)
Stdev Tmax (°C)
Skewness Tmax (°C)
Kurtosis Tmax (°C)
Annual Mean Tmax (°C)
Annual Mean Tmax (°C)
Annual Mean Tmax (°C)

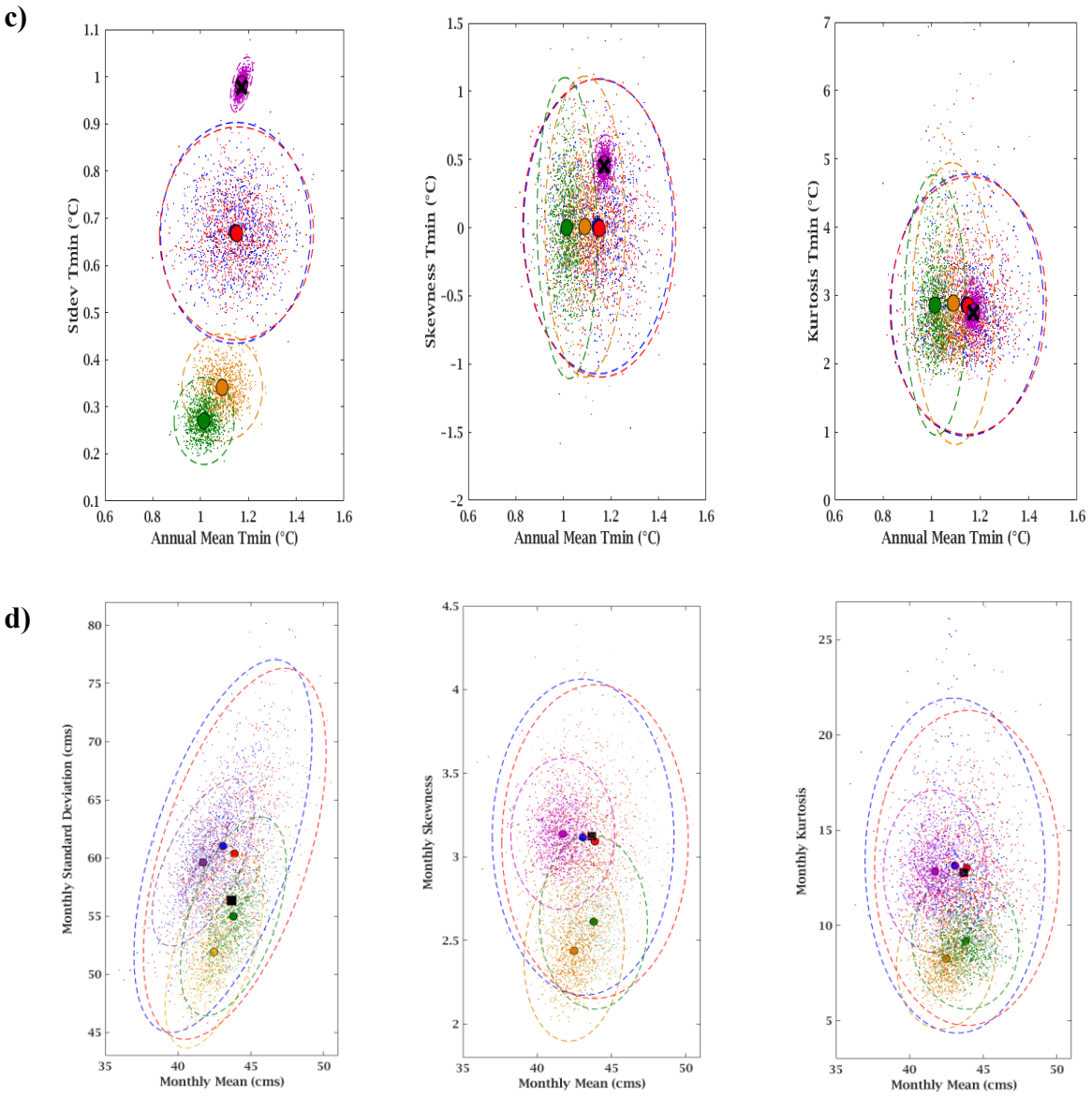

Figure 3.5 Scatter plots of the statistics for the five weather generators for (a) precipitation, (b) maximum temperature, (c) minimum temperature and (d) streamflow.

3.4.2 Risk and Performance Indicator Space (RPIS)

As reflected in the high NS value (0.79), coupled with the low values obtained for PBIAS (3%) and RSR (0.45), the SWAT model fed with observed meteorological information was very capable in simulating monthly streamflow in accordance with the Liew *et al.* (2007) and Moriasi *et al.* (2014) criterions. The lower and upper bounds for the most sensitive parameters, together with the

best fit values from within the prediction uncertainty band, that were then adopted during the subsequent analyses, are provided in Table 3.2.

Table 3.2 Description of SWAT2012 most sensitive parameters calibrated for the South Nation Watershed.

Parameter name*	Description	Initial range		Final selection (the calibrated model values)
		Min	Max	
r__CN2.mgt	Curve number for moisture condition II	-0.2	0.2	-0.06
v__ALPHA_BF.gw	Baseflow alpha factor	0.1	0.9	0.70
v__GW_DELAY.gw	Groundwater delay time	1	499	206.65
v__RCHRG_DP.gw	Deep aquifer percolation fraction	0.01	1	0.64
r__SOL_AWC.sol	Soil available water storage capacity	-0.4	0.4	-0.06
r__SOL_BD.sol	Moist bulk density (Mg/m^3 or g/cm^3)	-0.3	0.3	0.12
v__EPCO.hru	Plant uptake compensation factor	0.01	1	0.34
v__SNOCOVMX.bsn	Minimum snow water content that corresponds to 100% snow cover, SNO_{100}, (mm H_2O).	1	499	381.74
v__SFTMP.bsn	Snowmelt temperature	-19	19	3.18
v__SMFMN.bsn	Melt factor for snow on 21 December	1	20	13.75

* v__: specifies that the default parameter is *replaced by* a given value, while r__ specifies that the existing parameter value is *multiplied by* (1 + a given value) (Abbaspour *et al*., 2007).

One of the main objectives of the current work was to determine how the simulated flow using *observed* climate data (SFOD) comes to lie within the modelled data cluster obtained by feeding SWAT with *synthetic* data (SFSD). There is an infinite number of potential indicators (such as annual, seasonal, and daily indicators) that can be studied, but obviously only a few can be presented herein, and annual data are considered in the analysis. The MulGETS-Gamma set-up appears to be the best weather generator for our study area, in that it preserves the basic SFOD statistics (Figures 3.5 (d) and 3.6), followed by the MulGETS-Exponential configuration. Streamflow driven by the MulGETS-Gamma configuration appears to be satisfactorily consistence with the SFOD with MD values of 0.85, 0.3 and 0.32 respectively for σ, α_3 and α_4, respectively. The MulGETS-Exponential configuration performed less efficiently, yet within the adopted threshold of 3 MD. However, the WeaGETS, implementing both distributions for precipitation generation, as well as the k-nn models were not capable of maintaining the SFOD statistics, in particular the higher moments (α_3 and α_4) (Figure 3.6).

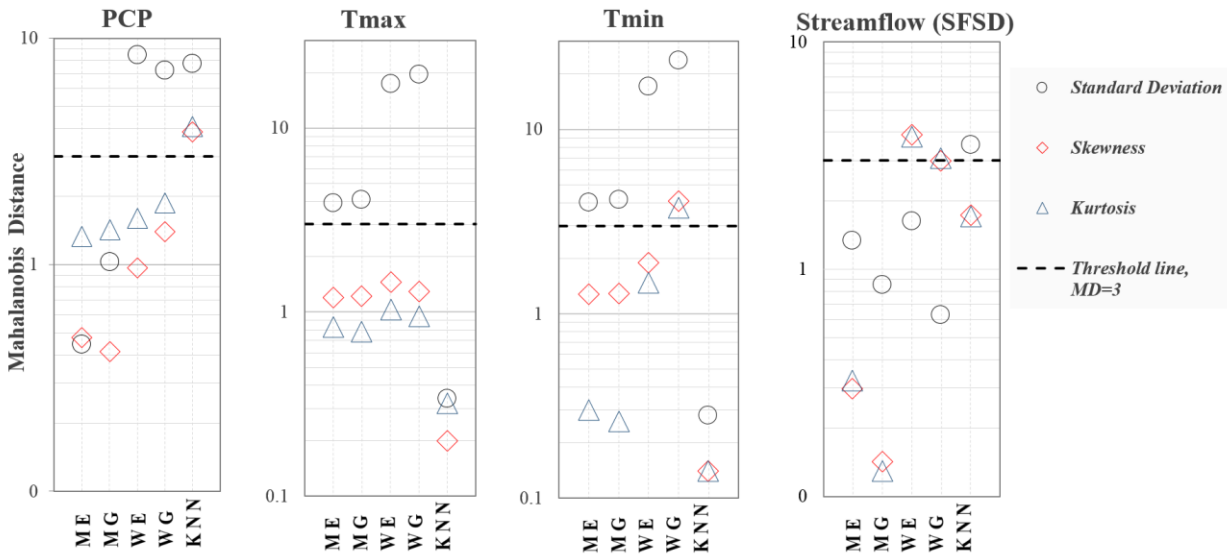

Figure 3.6. Level of adequacy of weather generators using Mahalanobis distance from the observed statistics to the cloud's center of the generated PCP, Tmax, Tmin and SFSD (compared to SFOD) statistics.

The performances of the weather models in terms of reproducing extreme flow are presented in Figure 3.7. Besides the 7-day dry spells (2-, 5-, 10- and 20-year for *7Q2*, *7Q5*, *7Q10* and *7Q20*, respectively), high return period floods (2-, 5-, 10- and 50-year) from the annual maximum series (*AM2*, *AM5*, *AM10*, and *AM50*, respectively) were achieved. No apparent differences were found in the low-flow frequency results, as all tested weather generators performed quite well except for *7Q2* of *k*-nn (Figure 3.7). The high-flow frequency results, on the other hand, were indicative of a convincing performance by the MulGETS models, where all tested recurrence intervals were satisfactorily reproduced with less than two units of standard deviation, as defined by MD. That indicates that they are interesting weather generation models where proximity with observations in the CSS translates very well into proximity in the RPIS. Such results were mainly driven by the accurate generation of streamflow statistics, especially the skewness and kurtosis as indicated previously. The performance of the MulGETS models is not surprising as they are the only ones

with account for spatial dependence between climate variables at different stations. It is well known that the reproduction of hydrologic extremes is dependent of such spatial dependence (i.e., a flood is generally the result of simultaneous high precipitation at various locations; low flow events are more likely to be triggered by low precipitation at several locations).

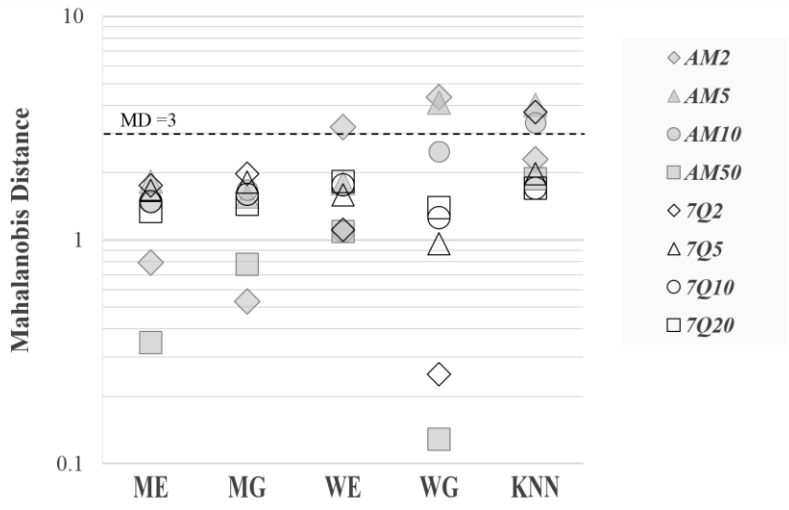

Figure 3.7 The performance of the low and high streamflow indicators of the SFSD compared to the SFOD based on Mahalanobis distance.

The auto-covariance structures of observed and simulated streamflow are shown in Figure 3.8. All weather generators had their autocorrelation within the 95% confidence interval. The reproduction is reasonable but not perfect as the observed autocorrelation is in the interquartile range of the simulated time series only for lags 0 to 3. Visual inspection did not show clear differences in performance in reproducing the autocorrelation function between weather generators.

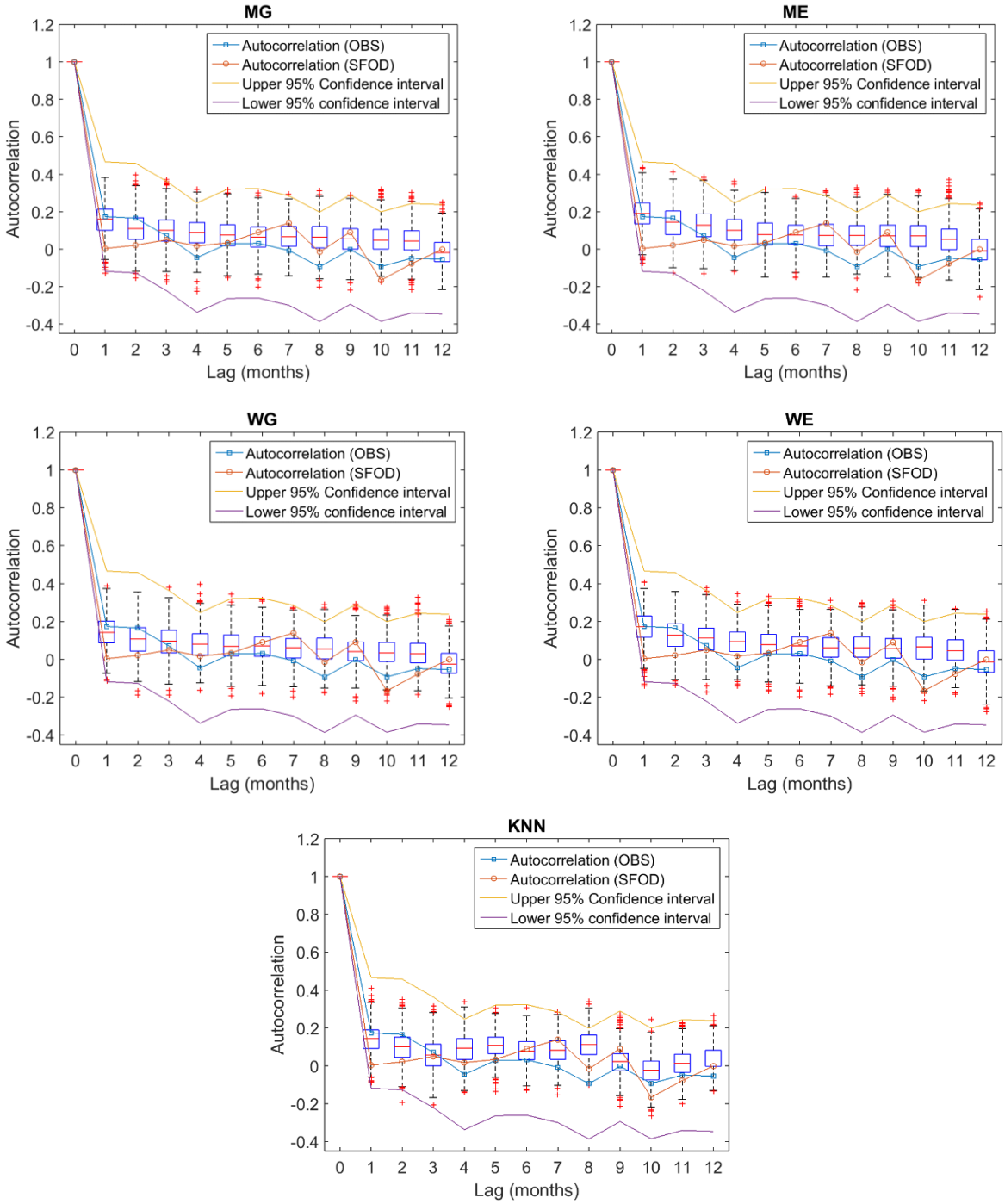

Figure 3.8 Flow autocorrelation of the five weather generators.

The above results show that the choice of a particular weather generator for water resources assessment can have an impact on key statistics of the simulated time series, hence on the estimated level of risk and the selection of management strategies. It is also shown that a given weather generator will perform differently on different variables. In the five weather generators, KNN

would be the recommended weather generator for risks related to temperature (e.g. heat and cold waves, changes growing season, etc.) while MulGETS would be the best for precipitation and streamflow, presumably because of its multisite features. This study is not exhaustive as there are a large number of other weather generators available to the modellers, as well as an infinite number of potential risk indicators. Our recommendation is that for each particular risk assessment problem, once the indicators are selected, the modellers should assess the performance of the weather generators available to them, or at least assess the performance of the weather generator they intend to use.

3.5 Conclusions

In this study, the comparisons between observed and weather generator-driven data, in the CSS and RPIS, allowed for quantifying the performances of these weather generators. The delineated approach was developed to provide a statistical baseline to examine how the observational data come to lie within the modelled data cluster. An explicit accounting of risk and performance indicators was considered to assess uncertainties associated with stochastically generated weather data. Weather generator-derived sequences were compared with the observed climate by training both data series through a calibrated SWAT model. The high NS coefficient, coupled with low values obtained for PBIAS and RSR, implied that the SWAT forced with observed meteorological information was able to predict observed streamflow very satisfactorily. Apart from the *k*-nn approach, we utilized the Matlab-based stochastic weather generators MulGETS and WeaGETS to generate maximum and minimum temperatures, as well as precipitation intensities and occurrences, implementing exponential and gamma distributions for the selected watershed. The current study has examined five families of weather generators, coupled with a hydrological model, while involving more models would lead emphatically to a better comprehensive decision.

A large number of sequence samples (1000 synthetic time-series) was vetted in the CSS and RPIS spaces. Generally, the CSS results demonstrated that MulGETS-models were often the better-performing weather generators for the South Nation area, followed by its counterpart the single site WeaGETS model, and the k-nearest neighbour approach. The statistics of simulated streamflow using observed climatic data were found to lie mostly outside a predefined set of normal behaviour for the WeaGETS and *k*-nn models. The MulGETS model, in its gamma and exponential configurations, thus considered the preferred choice candidates for risk analysis and discovery, mainly due to this model's ability to incorporate covariance for several stations. Low and high flow frequency analyses were conducted on each dataset to examine risk indices. The observed differences between examined weather generators in terms of low flow index results were not statistically significant, and further studies with a particular focus on how low flow indices reproduced by weather generators data are recommended.

While there cannot be a binary black-and-white classification of weather generators, it is possible to quantify their suitability for a specific field or geographical area, based on their individual strengths and weaknesses. The current work should appeal to end users of climate products, to facilitate the appropriate pick of the right weather generators, conditioned on the relevant CSS and RPIS information. It would also be worth looking into verifying these results by versatile models, such as economical, ecological, electricity demand, or crop-yield models.

3.6 References

Abbaspour, K. C., Vejdani, M., Haghighat, S., & Yang, J. (2007, December). SWAT-CUP calibration and uncertainty programs for SWAT. In MODSIM 2007 International Congress on Modelling and Simulation, Modelling and Simulation Society of Australia and New Zealand (pp. 1596-1602).

Abramowitz M, Stegun I A (1972) Handbook of mathematical functions with formulas, graphs, and mathematical tables (Vol. 9). Dover, New York. Chicago

Ailliot, P., Allard, D., Monbet, V., & Naveau, P. (2015). Stochastic weather generators: an overview of weather type models. *Journal de la Société Française de Statistique*, 156(1), 101-113.

Arnold J G, Kiniry J R, Sirinivasan R, Williams J R, Haney E B, Neitsh, S L (2012) SWAT input–output documentation, version 2012. Texas Water Resource Institute. TR-439.

Arnold J G, Moriasi D N, Gassman P W, Abbaspour K C, White M J, Srinivasan R, Santhi C, Harmel R, Van Griensven, A, Van Liew M W, *et al*. (2012) SWAT: Model use, calibration, and validation, Transactions of the ASABE, 55, 1491–1508.

Baigorria G A, & Jones J W (2010) GiST: A stochastic model for generating spatially and temporally correlated daily rainfall data. *J. Climate*, *23*(22), 5990-6008.

Bastola, S., Murphy, C., & Fealy, R. (2012). Generating probabilistic estimates of hydrological response for Irish catchments using a weather generator and probabilistic climate change scenarios. *Hydrological processes, 26*(15), 2307-2321.

Benestad, R. E., Nychka, D., & Mearns, L. O. (2012). Specification of wet-day daily rainfall quantiles from the mean value. *Tellus A: Dynamic Meteorology and Oceanography, 64*(1), 14981.

Brissette F P, Khalili M, Leconte R (2007) Efficient stochastic generation of multi-site synthetic precipitation data. *J. Hydrol., 345*(3-4), 121-133.

Brocca, L., Liersch, S., Melone, F., Moramarco, T., & Volk, M. (2013). Application of a model-based rainfall-runoff database as efficient tool for flood risk management. *Hydrology and Earth System Sciences, 17*(8), 3159.

Brown C, Ghile Y, Laverty M, Li K (2012) Decision scaling: Linking bottom up vulnerability analysis with climate projections in the water sector. *Water Resources Research, 48*(9).

Camera C, Bruggeman A, Hadjinicolaou P, Michaelides S, Lange MA (2016) Evaluation of a spatial rainfall generator for generating high resolution precipitation projections over orographically complex terrain. *Stoch Environ Res Risk Assess 31*: 757

Chen J F, Brissette X, Zhang J (2014) A multi-site stochastic weather generator for daily precipitation and temperature. *Transactions of the ASABE Trans. ASABE*, 2014, 1375-391. doi:10.13031/trans.57.10685.

Chen J, Brissette F (2014) Comparison of five stochastic weather generators in simulating daily precipitation and temperature for the Loess Plateau of China. *Intl. J. Climatol. 34*(10), 3089-3105.

Chen J, Brissette F P, Leconte R, Caron A (2012) A versatile weather generator for daily precipitation and temperature. *Trans. ASABE, 55*(3), 895-906.

Environment Canada. (2012). National climate data and information archive: Climate normals from 1971-2000 Environment Canada.

Forsythe N, Fowler H J, Blenkinsop S, Burton A, Kilsby C G, Archer D R, Harpham C, Hashmi M Z (2014) Application of a stochastic weather generator to assess climate change impacts in a semi-arid climate: The Upper Indus Basin, *Journal of Hydrology, 517*, Pages 1019-1034, ISSN 0022-1694.

Fowler H J, Blenkinsop S, Tebaldi C (2007) Linking climate change modelling to impacts studies: recent advances in downscaling techniques for hydrological modelling. *International Journal of Climatology, 27*: 1547–1578.

Fowler H J, Kilsby C G, O'Connell P E, Burton A (2005) A weather-type conditioned multi-site stochastic rainfall model for the generation of scenarios of climatic variability and change. *J. Hydrol., 308*(1-4), 50-66.

Frich, P., Alexander, L. V., Della-Marta, P. M., Gleason, B., Haylock, M., Tank, A. K., & Peterson, T. (2002). Observed coherent changes in climatic extremes during the second half of the twentieth century. *Climate research, 19*(3), 193-212.

Fritsch V, Varoquaux G, Thyreau B, Poline J, Thirion B (2012) Detecting Outliers in High-Dimensional Neuroimaging Datasets with Robust Covariance Estimators. *Medical Image Analysis, Elsevier, 16,* pp.1359-1370.

Govindaraju, R. S., & Kavvas, M. L. (1991). Stochastic overland flows. *Stochastic Hydrology and Hydraulics, 5*(2), 105-124.

Goyal MK, Burn DH, Ojha CSP (2013) Precipitation simulation based on k-nearest neighbor approach using gamma kernel. *J Hydrol Eng, 18*:481–487.

Guo, T., Mehan, S., Gitau, M. W., Wang, Q., Kuczek, T., & Flanagan, D. C. (2017) Impact of number of realizations on the suitability of simulated weather data for hydrologic and environmental applications. *Stoch Environ Res Risk Assess*. https://doi.org/10.1007/s00477-017-1498-5.

Gupta H, Sorooshian S, Yapo P (1999) Status of Automatic Calibration for Hydrologic Models: Comparison with Multilevel Expert Calibration. *Journal of Hydrologic Engineering, 4*(2), 135-143.

Hansen JW, and Ines AV (2005) Stochastic disaggregation of monthly rainfall data for crop simulation studies. *Agric For Meteorol 131*:233–246

Hardin J and Rocke D M (2005) The distribution of robust distances. *Journal of Computational and Graphical Statistics 14*, 928–946.

Hashmi MZ, Shamseldin AY, Melville BW (2011) Comparison of SDSM and LARS-WG for simulation and downscaling of extreme precipitation events in a watershed. *Stoch Environ Res Risk Assess 25*:475–484.

Helsel DR and Hirsch R M (1992) Statistical Methods in Water Resources, *Studies in Environmental Science, 49*, Elsevier, Amsterdam, 529 pages.

Huber P J and Ronchetti E M (2009) Robust Tests, in Robust Statistics, Second Edition, John Wiley & Sons, Inc., Hoboken, NJ, USA. doi: 10.1002/9780470434697.ch13

Iman, R. L., & Conover, W. J. (1982). A distribution-free approach to inducing rank correlation among input variables. *Communications in Statistics-Simulation and Computation, 11*(3), 311-334.

Kavvas, M. L., & Herd, K. R. (1985). A Radar- Based Stochastic Model for Short- Time-Increment Rainfall. *Water Resources Research, 21*(9), 1437-1455.

Kim, B.S., Kim, H.S., Seoh, B.H. Kim N W (2007) Impact of climate change on water resources in Yongdam Dam Basin, Korea. *Stoch Environ Res Risk Assess, 21*: 355.

Kim, D., Cho, H., Onof, C., & Choi, M. (2017). Let-It-Rain: a web application for stochastic point rainfall generation at ungaged basins and its applicability in runoff and flood modeling. *Stochastic Environmental Research and Risk Assessment, 31*(4), 1023-1043.

Kim, D., Olivera, F., & Cho, H. (2013). Effect of the inter-annual variability of rainfall statistics on stochastically generated rainfall time series: part 1. Impact on peak and extreme rainfall values. *Stochastic environmental research and risk assessment, 27*(7), 1601-1610.

Klein Tank, A. M. G., Zwiers, F. W. & Zhang, X. (2009). Guidelines on Analysis of extremes in a changing climate in support of informed decisions for adaptation. World Meteorological Organization. 72 and WMO Tech. Doc. 1500, 56 pp.

Kovalchuk, S. V., Krikunov, A. V., Knyazkov, K. V., & Boukhanovsky, A. V. (2017). Classification issues within ensemble-based simulation: application to surge floods forecasting. *Stochastic Environmental Research and Risk Assessment, 31*(5), 1183-1197.

Lennartsson J, Baxevani A, Chen D (2008) Modelling precipitation in Sweden using multiple step Markov chains and a composite model. Journal of Hydrology, 363(1):42–59.

Liew M W, Veith T L, Bosch D D, Arnold J G (2007) Suitability of SWAT for the conservation effects assessment project: A comparison on USDA-ARS experimental watersheds. *J. Hydrologic Eng. 12*(2): 173-189.

Loucks D, Stedinger J, Haith D (1981) Water Resource Systems Planning and Analysis, Prentice-Hall, Englewood Cliffs, N.J.

Mahalanobis P C (1936) On the generalised distance in statistics. Proceedings of the National Institute of Science of India, 12 (1936), pp. 49-55

Markov, A. A. (1906). Rasprostranenie zakona bol'shih chisel na velichiny, zavisyaschie drug ot druga. Izvestiya Fiziko-matematicheskogo obschestva pri Kazanskom universitete, 15(135-156), 18.

Mehrotra R, Srikanthan R, Sharma A (2006) A comparison of three stochastic multi-site precipitation occurrence generators. *J. Hydrol., 331*(1-2), 280-292.

Moriasi, D. N., Arnold, J. G., Van Liew, M. W., Bingner, R. L., Harmel, R. D., & Veith, T. L. (2007). Model evaluation guidelines for systematic quantification of accuracy in watershed simulations. *Transactions of the ASABE, 50*(3), 885-900.

Nash J E, Sutcliffe W H (1970) River flow forecasting through conceptual models: Part 1. A discussion of principles. *J. Hydrol., 10*(3), 282–290.

Neitsch, S. L., Arnold, J. G., Kiniry, J. R., & Williams, J. R. (2011). Soil and water assessment tool theoretical documentation version 2009. Texas Water Resources Institute.

O. G. B. Sveinsson, J. D. Salas, W. L. Lane, and D.K. Frevert (2007). Stochastic Analysis, Modeling, and Simulation (SAMS) Version 2007 USER's MANUAL. Technical report No. 11. Computing Hydrology Laboratory, Department of Civil and Environmental Engineering. Colorado State University, Fort Collins, Colorado

Palutikof J P, Goodess C M, Watkins S J, Holt T (2002) Generating rainfall and temperature scenarios at multiple sites: Examples from the Mediterranean. *J. Climate, 15*(24), 3529- 3548.

Polade, S. D., Pierce, D. W., Cayan, D. R., Gershunov, A., & Dettinger, M. D. (2014). The key role of dry days in changing regional climate and precipitation regimes. *Scientific reports, 4*, 4364.

Rajagopalan, B., Lall, U., Tarboton, D. G., & Bowles, D. S. (1997). Multivariate nonparametric resampling scheme for generation of daily weather variables. *Stochastic Hydrology and Hydraulics, 11*(1), 65-93.

Ramesh, N.I., Garthwaite, A.P. & Onof, C. (2018) A doubly stochastic rainfall model with exponentially decaying pulses. *Stoch Environ Res Risk Assess. 32*: 1645.

Richardson C W (1981) Stochastic simulation of daily precipitation, temperature, and solar radiation. *Water Resour. Res., 17*(1), 182-190.

Richardson C W, Wright D A (1984) WGEN: A Model for Generating Daily Weather Variables. U. S. Department of Agriculture, Agricultural Research Service, ARS-8, 83 p.

Salas, J. D., and Lee, T. S. (2010) Nonparametric simulation of single-site seasonal streamflows. *J. Hydrol. Eng., 15*(4), 284–296.

Santhi C, Arnold J, Williams J, Dugas W, Srinivasan R, Hauck L (2001) Validation of the Swat Model on a Large Rwer Basin with Point and Nonpoint Sources 1. *Journal of the American Water Resources Association, 37*(5), 1169-1188.

Semenov MA, Barrow EM. 2002. LARS-WG, A Stochastic Weather Generator for Use in Climate Impact Studies, User Manual. http://www.rothamsted.ac.uk/mas-models/download/LARS-WGManual.pdf

Shao, Q., Zhang, L., & Wang, Q. J. (2016). A hybrid stochastic-weather-generation method for temporal disaggregation of precipitation with consideration of seasonality and within-month variations. *Stoch Environ Res Risk Assess, 30*(6), 1705-1724.

Sharif M, Burn D H (2007) Improved K-nearest neighbor weather generating model. J Hydrol Eng 12(1):42–51

Singh, J., Knapp, H. V., Arnold, J. G., & Demissie, M. (2005). Hydrological modeling of the Iroquois River watershed using HSPF and SWAT. *JAWRA Journal of the American Water Resources Association, 41*(2), 343-360.

Srinivasan R, Arnold J G (1994) Integration of a basin-scale water quality model with GIS. *Water Resour. Bull. 30*(3): 453-462.

Sun, Y., Solomon, S., Dai, A., & Portmann, R. W. (2006). How often does it rain?. *Journal of Climate, 19*(6), 916-934.

Sveinsson, O. G., Salas, J. D., Lane, W. L., & Frevert, D. K. (2007). Stochastic analysis, modeling, and simulation (sams) version 2007, user's manual. Computing Hydrology Laboratory, Department of Civil and Environmental Engineering, Colorado State University, Fort Collins, Colorado.

Tuppad P, Douglas-Mankin K R, Lee T, Srinivasan R, Arnold J G (2011) Soil and Water Assessment Tool (SWAT) hydrologic/water quality model: Extended capability and wider adoption. *Trans. ASABE 54*(5): 1677-1684.

Wang, M. Y., & Zwilling, C. E. (2015). Multivariate computing and robust estimating for outlier and novelty in data and imaging sciences. In Advances in Bioengineering. InTech.

Warner T (2010) Climate modeling and downscaling. Numerical Weather and Climate Prediction (pp. 407-455). Cambridge: Cambridge University Press. doi:10.1017/CBO9780511763243.017

White K L, Chaubey I (2005) Sensitivity analysis, calibration, and validations for a multisite and multivariable SWAT model. *J. American Water Resour. Assoc. 41*(5): 1077-1089.

Wilby R L, Fowler H J (2011) Regional Climate Downscaling: Modelling the Impact of Climate Change on Water Resources. Edited by Fai Fung, Ana Lopez and Mark New, Blackwell Publishing Ltd. ISBN: 978-1-405-19671-0.

Wilby R W, Tomlinson O J, Dawson C W (2003) Multisite simulation of precipitation by conditionalresampling. *Climate Res., 23*(3), 183-194.

Wilks D S (1998) Multi-site generalization of a daily stochastic precipitation model. *J. Hydrol. 210*, 178–191.

Yates D, Gangopadhyay S, Rajagopalan B, Strzepek K (2003) A technique for generating regional climate scenarios using a nearest-neighbor algorithm. *Water Resources Research, 39*(7).

CHAPTER 4.

*Assessment of Climate Change Impacts on Extreme High and Low Flows: An Improved Bottom-Up Approach**

Abstract.

A quantitative assessment of the likelihood of possible future states is lacking in both the traditional top-down and the alternative bottom-up approaches to climate change impacts assessment. The issue is tackled herein by generating a large number of representative climate projections using weather generators calibrated with the outputs of regional climate models. A case study is performed on the South Nation Watershed, Ontario, Canada using climate projections generated by four climate models and forced with medium- to high-emission scenarios (RCP4.5 and RCP8.5) for the future 30-year period (2071-2100). These raw projections are corrected using two downscaling techniques. Large ensembles of future series are created by perturbing downscaled data with a stochastic weather generator, then used as inputs to a hydrological model that was calibrated using observed data. Risk indices calculated with the simulated streamflow data are converted into probability distributions using Kernel Density Estimations (KDE). The results are dimensional joint probability distributions of risk-relevant indices that provide estimates of the likelihood of unwanted events under a given watershed configuration and management policy. The proposed approach offers a more complete vision of the impacts of climate change and opens the door to a more objective assessment of adaptation strategies.

Keywords: hydrological risk assessment, extreme hydrologic events, climate change impacts, downscaling, uncertainty, ensembles, water resource systems

---

* This chapter has been published in *Water* journal as "Alodah, A., & Seidou, O. (2019). Assessment of Climate Change Impacts on Extreme High and Low Flows: An Improved Bottom-Up Approach. *Water*, *11*(6), 1236."

4.1 Introduction

Climate change has forced the research community to revisit assumptions and theories used for the design, planning, and management of water resource systems (Stocker *et al.*, 2013). Hydrological processes depend to a great degree on the climate regime (Manabe, 1969; Gleick, 1989; Arora and Boer, 2001; Frich *et al.*, 2002; Bierkens *et al.*, 2008). Perturbing the climate regime inevitably results in a perturbed hydrological regime which in turn affects water-related risk and water resource system performance. Numerous researchers and practitioners have been working intensely to develop methodologies to identify future climate change impacts and viable adaptations strategies (e.g., Panagoulia, 1991, 1992; Panagoulia *et al.*, 2008).

The most frequently used approach in climate impact assessments is the top-down approach, which is constrained by the availability of Global Circulation Models (GCM) and Regional Climate Models (RCM). Typically, it considers possible future changes in climatic conditions based on predetermined scenarios that are parameterized in large-scale models. This is achieved by downscaling a distinctly few projections to be able to determine the impacts on the local hydrological system. However, a critical limitation of this approach is that it ignores plausible risks by not covering all possible future conditions despite using multi-model and multi-scenario projections. For example, while multidecadal GCM simulations are the main derive of climate projections, they poorly account for many natural climate forcing, such as volcanic eruptions, which leads to added uncertainty, particularly when estimating local and regional impacts (Pielke *et al.*, 2012). Also, all downscaled scenarios are equally likely which makes it impossible to choose one scenario over another.

The alternative bottom-up approach uses a wide range of possible conditions to assess the sensitivity of water resource systems to climate change and identify potentially risky situations (García *et al.*, 2014). This approach was only recently introduced to the field of climate

adaptations in water research where it has been gaining traction, particularly in risk assessment and planning (Alodah and Seidou, 2017; Guo *et al*., 2017; Culley *et al*., 2016; Bhaye *et al*., 2014; Wilby, 2011). However, the bottom-up approach creates large and uncertain vulnerability domains that are inconvenient for decision-maker. In addition, both approaches suffer from the limited availability of GCM/RCM projections at a given watershed and there is no existing methodology to rank their outputs (Panagoulia *et al*., 2008). These limitations are real hindrances when considering such projections in a decision or design framework and need to be improved.

By using modelled climate data, precipitation-runoff models are frequently used to simulate hydrological processes, quantify potential impacts of climate change, and identify water availability issues, particularly under extreme conditions. There are two common types of extreme streamflow that are usually considered in impact studies: peak events (causing flooding) using frequency analysis (FA) and low streamflow indices (causing drought) (Panagoulia, 2006; Sapač *et al*., 2019). Extreme high and low flow indicators based on return periods are used for efficient and safe engineering designs. The importance of an engineering structure and consequences of its potential failure determine the choice of the return period (e.g., dams are designed based on a 1000-year return period). Besides the use of low-flow information in typical water sector applications such as energy, irrigation, and navigation, there are also noticeably increasing efforts to study risks imposed upon aquatic habitat and to regulate minimum environmental flow requirements and sustain water quantity and quality (e.g., Tharme, 2003; Arthington *et al*., 2006; Linnansaari *et al*., 2012; Pastor *et al*., 2014). Also, low-flow indices are used to prevent deterioration of freshwater ecosystems, which are very vulnerable to climate change.

In order to address the aforementioned unresolved issues, this paper proposes a methodology to generate a large number of climate change projections by combining the outputs of stochastic

weather generators and regional climate models to create an ensemble of projections with quantifiable probabilities. This new set of projections provides better coverage of the risk space and can facilitate the implementation of a bottom-up approach by considering the plausibility of risk which may lead to informed decisions and robust adaptation plans.

4.2 Materials and Methods

One of the major limitations of the top-down approach is that the number of scenarios is too low to fully explore the climate-related risk space. The problem can be partially mitigated by cloning projections generated by corrected climate models and slightly perturbing them through a stochastic weather generator to obtain a larger set of scenarios that cover the same statistical space as the synthetic time series. Here is a brief explanation of the 'ensemble generation process' used herein for risk discovery. We firstly used downscaling methods to correct biased (i.e., raw) regional climate model data. Secondly, using corrected (i.e., downscaled) climate data, the stochastic weather generator (MulGETS) was utilized to generate 30 years of daily precipitation and minimum and maximum temperature data. The second step is repeated to generate a large number of climate projections (i.e., we run MulGETS 250 with each corrected RCM data). Thirdly, the calibrated SWAT model was forced with these climate projections individually to generate "ensemble" of streamflow projections. Subsequently, the newly-generated ensemble will be utilized to determine the risk space that is largely overlooked by top-down methods. This is done to consider the inherent randomness of hydroclimatic variables. Figure 4.1 presents a schematic representation of all datasets used in this study and relationships between different time series in the proposed framework.

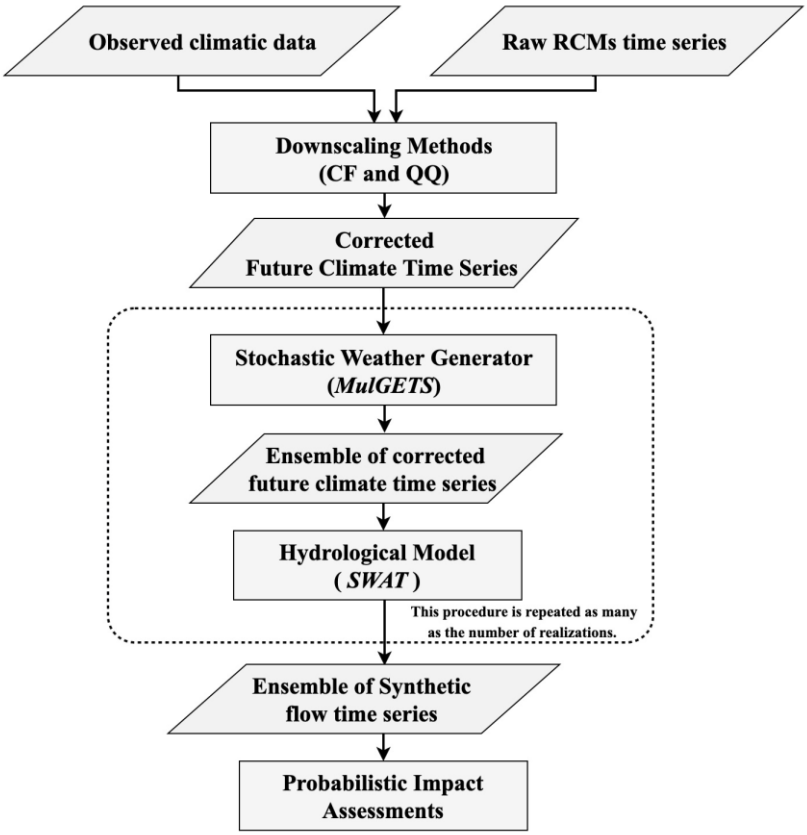

Figure 4.4 Schematic representation of the proposed approach.

4.2.1 Study Area

The South Nation Watershed (SNW) of about 4000 in Eastern Ontario is used as a showcase. It is characterized by multigauge climatic data (from St. Albert, Russell, Morrisburg, and South Mountains metrological stations) and downstream daily discharge data (collected at Plantagenet gauging station (ID: 02LB005)) (Figure 4.2). Hydrogeological investigations have indicated that an impermeable overburden watershed and a lack of streambed gradients in parts of the South Nation River pose a prominent flooding risk (Chin *et al*., 1980). The average maximum and minimum air temperatures are 11.5 and 1.2, respectively, with a mean annual precipitation of around 1000 mm. A more detailed description of the watershed has been presented previously (Alodah and Seidou, 2019).

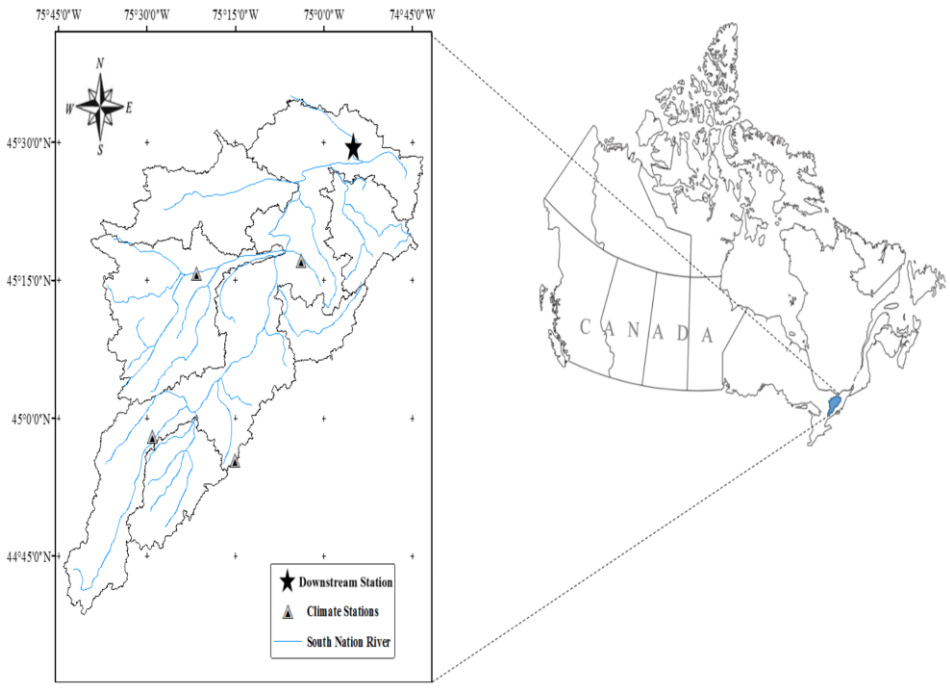

Figure 4.5 Map of the South Nation Watershed.

4.2.2 Regional Climate Model Data

The availability of daily climatic variables at fine spatial scales is essential for hydrological impact studies (Semenov, 2007). The gridded daily data of precipitation, maximum near-surface air temperature, and minimum near-surface air temperature were extracted from the NA-CORDEX project archive (North American domain of Coordinated Regional Climate Downscaling Experiment) driven by state-of-the-art GCMs as part of the CMIP5 experiment (the Coupled Model Inter-comparison Project Phase 5) (Table 4.1). The CORDEX project was initiated by the World Climate Research Program (WCRP) to provide reliable predictions of regional future climate change. The four independent models are forced with medium- to high-emission scenarios RCP4.5 and RCP 8.5 (resulting in 8 different projections). They are originally based on outputs from the CanESM2 and EC-EARTH Global Circulation Models, whose outputs are downscaled with three Regional Climate Models: CanRCM4, RCA4, and HIRHAM5. The horizontal spatial resolution was chosen to be 0.44° or approximately 50 km (NAM-44).

Table 4.2 List of Regional Climate Models used in the study.

Global Circulation Models (GCM) (Driver)	Regional Climate Model (RCM)	Grid (spatial resolution)	Representative Concentration Pathways	Variables
Second-generation Canadian Earth System Model (CanESM2)	Canadian Regional Climate Model (CanRCM4)	NAM-44 (0.44 deg)	RCP4.5 RCP8.5	pr tasmax tasmin
Second-generation Canadian Earth System Model (CanESM2)	Rossby Centre Regional Atmospheric Climate Model (RCA4)	NAM-44 (0.44 deg)	RCP4.5 RCP8.5	pr tasmax tasmin
European Earth System Model (EC-EARTH)	Danish Climate Centre model (HIRHAM5)	NAM-44 (0.44 deg)	RCP4.5 RCP8.5	pr tasmax tasmin
European Earth System Model (EC-EARTH)	Rossby Centre Regional Atmospheric Climate Model (RCA4)	NAM-44 (0.44 deg)	RCP4.5 RCP8.5	pr tasmax tasmin

4.2.3 Downscaling Methods

Downscaling is a procedure undertaken to reconcile the large-scale data representativeness of observations and produce climate change data at a finer resolution. This study makes use of two statistical downscaling techniques, namely Change Factors (CF) and Quantile-Quantile transformation (QQ), to produce more reliable station-level climatic information to be used later as inputs to a distributed impact model.

The linear correction method applied in this study, namely CF, requires three time series: observations (or synthetic climate series), historical and future raw RCM data. The primary assumption in this method is that the relationship between historical and future projections is the same as the relation between historical RCM data and observed time series. However, the Quantile-Quantile method applies a different concept that is based on the distribution of raw simulations and observations. For a given variable, downscaling is conducted using a monthly time-step. Observed precipitation and temperature variables of 30 years (1981 to 2010) were

used to define a reference climatology and to spatially downscale the coarse-scale climate data in the future (2071–2100).

4.2.3.1 Change Factor Method

The Change Factors (CF) method is a commonly used approach to linearly downscale a variable (e.g., precipitation) by calculating the difference between the control and future GCM simulations before scaling the baseline observations accordingly (Lenderink *et al*., 2007). Yet, the conventional CF method is usually used a top-down approach and as such not always reliable. Nevertheless, it has been used excessively in recent climate change assessments (Luo *et al*., 2018; Hansen *et al*., 2017; Harris *et al*., 2014; Lafon *et al*., 2013; Teutschbein and Seibert, 2012; van Roosmalen *et al*., 2011; Mpelasoka and Chiew, 2009; Diaz-Nieto and Wilby, 2005). The CF approach lacks the ability to correct future projections as it predicts the same variability for the future climate by keeping the same historical temporal structure, which is unrealistic (Hayhoe, 2010; Lenderink *et al*., 2007; Diaz-Nieto and Wilby, 2005). One of its limitations is that it produces the exact same temporal structure of wet days (occurrences) in the future (Seidou *et al*., 2012), which is by no means certain for a stochastic variable such as precipitation. Furthermore, extreme events that are vital in risk assessments cannot be adequately corrected by such a method when using only one observational dataset. To alleviate these disadvantages, we employ stochastic weather generators as they are capable of capturing climate variability. We explore the potential risks by producing a new set of weather data and applying factors of change obtained from raw daily RCM outputs between the reference period and the future.

Each climate station is perturbed using the simplest version of the CF method, i.e., we apply the following deterministic transformation to downscaled climate model outputs:

$$PCP_t^{RCM,\,CF} = PCP_t^{OBS} \frac{AVG_{historical}\left(PCP_t^{RCM}\right)}{AVG_{future}\left(PCP_t^{RCM}\right)}, \qquad \textbf{Eq. 4.1}$$

where $PCP_t^{RCM,\,CF}$ is the perturbed RCM output, PCP_t^{RCM} is the original RCM output, and PCP_t^{OBS} denotes the observed data. Analogously for temperature, we use:

$$TMP_t^{RCM,\,CF} = TMP_t^{OBS} + \left[AVG_{future}\left(TMP_t^{RCM}\right) - AVG_{historical}\left(TMP_t^{RCM}\right)\right], \qquad \textbf{Eq. 4.2}$$

where $TMP_t^{RCM,\,CF}$ is the perturbed RCM output, TMP_t^{RCM} is the original RCM output, and TMP_t^{OBS} is the observed climate. The expectation is that after transformation, the means of $PCP_t^{RCM,\,CF}$ and $TMP_t^{RCM,\,CF}$ will each be closer to the respective means of PCP_t^{OBS} and TMP_t^{OBS} over the reference period.

4.2.3.2 Quantile-Quantile Transformation

Quantile-Quantile (QQ) transformation is an empirical routine applied to correct systematic errors in regional climate models (Maraun, 2016; Lafon *et al*., 2013; Themβel *et al*., 2010). The raw RCM outputs typically do not have the same distribution as the observations (Sarr *et al*., 2015) and both distributions must be reconciled. It is more sophisticated than mean-based methods and its procedure includes remapping the probability density function (PDF) of uncorrected RCM data onto the PDF of observations. Corrected RCM simulations, X_{CORR}, of the future are produced by applying the following transformation to their cumulative distribution functions (F):

$$X_{CORR} = F_{OBS}^{-1}\left(F_{RCM}\left(X_{RCM}\right)\right), \qquad \textbf{Eq. 4.3}$$

where X_{RCM} refers to the climate variable extracted from raw RCM data. This technique has been proven to be more accurate for reproducing a valid agreement between the corrected and observed PDFs than the linear method discussed earlier (Angelina *et al*., 2015; Sarr *et al*., 2015; Themβel *et al*., 2010; Lenderink *et al*., 2007). However, one of the main drawbacks of the QQ

technique is its inability to predict values beyond the original range of historic extremes (Wilby and Fowler, 2011) which may ultimately affect risk analysis.

4.2.4 Generating an Ensemble of Corrected-RCM-Like Realizations

The Change Factors and Quantile-Quantile downscaling methods lack the ability to produce more than one possible future state and underestimates the impact variability (Wilks, 1998). The variability issue is tackled in this paper by generating an ensemble of corrected-RCM-like realizations, as illustrated in Figure 4.1, which consists of multiple runs (the number of realizations is 250) of a given stochastic weather generator fed with corrected future climate for a 30-year period. This produces a total of 2000 unique future climate projections (=250*4*2) for each downscaling method (=2000*2). Methods involving stochastic weather generators are generally capable of creating a limitless number of sequences of weather data with novel scenarios which helps with the uncertainty analysis (Hansen *et al*., 2017). The selection of an adequate stochastic weather generator is crucial to efficiently explore a wide range of climate risk scenarios for water resource systems (Sapač *et al*., 2019).

This study made use of MulGETS (Multi-site weather Generator of École de Technologie Supérieure) (Chen *et al*., 2014), a multisite, multivariate weather generator that correctly reproduced historical climatic and hydrological characteristics for the SNW (Alodah and Seidou, 2019). Wet-day precipitation sequences were reproduced using a multi-Gamma distribution (a combination of several gamma distributions). MulGETS can account for the coherency among multiple climate variables. Climatic data and MulGETS configuration have been presented in Alodah and Seidou (2019). The final result is a super-ensemble combining all ensembles containing a large number of scenarios (hereafter the “ensemble”) that inherit the trends projected by climate models while covering the range of variability from the historical period.

Given that the variability range of the historical period is matched, the assumption that all scenarios are equally probable will now be more defendable.

4.2.5 Hydrological Response

Ultimately, the development of such new future-climate scenarios, essentially driven by corrected GCM/RCM projections, enables us to discover the risks presented by changing hydrology using altered flows at a local scale. The Soil and Water Assessment Tool (SWAT-2012) was used to simulate hydrological variables and utilizing the semi-automated SUFI-2 optimization algorithm (sequential uncertainty fitting ver. 2) to evaluate the most accurate simulation based on an uncertainty analysis routine (Abbaspour *et al*., 2007). SWAT is a semi-distributed, watershed-scale hydrological model that has been extensively utilized to address water quality and quantity issues (Neitsch *et al*., 2011). Hydrologists, conservationists, and policy makers have extensively used SWAT to predict a variety of water-related issues and their environmental impacts (e.g., Tan *et al*., 2019; Arnold *et al*., 2012; Neitsch *et al*., 2011; Tuppad *et al*., 2011; White and Chaubey, 2005; Santhi *et al*., 2001; Arnold *et al*., 1998; Srinivasan and Arnold, 1994). Weather information is the main physically based input that controls the transformation of precipitation into runoff in SWAT (Abbaspour *et al*., 2007).

The SNW was partitioned into 31 different Hydrologic Response Unit (HRU), each HRU has its land, management, and soil characteristics. A detailed description of the SWAT model configuration and parameterization used in this study has been presented previously (Alodah and Seidou, 2019). A set of different statistic measures was used to assess the goodness of fit of the calibrated model, including the Nash–Sutcliffe efficiency, the RMSE-observations standard deviation ratio, and the percent bias (Table 4.2). Hydrological impact models, distributed models in particular (e.g., SWAT), are particularly sensitive to small-scale climate variations that might

be underestimated by large-scale models (Wilby *et al*., 2004), and it could be reasonably argued that relying on a selected few models, either in a top-down or bottom-up approach, cannot be adequately justified.

Table 4.2 Goodness-of-Fit metrics used for SWAT model performance evaluation.

Statistic Measure	Formula [1]
The Nash–Sutcliffe efficiency coefficient (NSE)	$\mathrm{NSE} = 1 - \frac{\sum_{i=1}^{n} (O_i - P_i)^2}{\sum_{i=1}^{n} (O_i - \bar{O})^2}$
The RMSE-observations standard deviation ratio (RSR)	$\mathrm{RSR} = \frac{\sqrt{\sum_{i=1}^{n} (O_i - P_i)^2}}{\sqrt{\sum_{i=1}^{n} (O_i - \bar{O})^2}}$
The percentage of bias (PBIAS)	$\mathrm{PBIAS} = \frac{\sum_{i=1}^{n} (O_i - P_i) \times 100}{\sum_{i=1}^{n} (O_i)}$

[1] where O_i stands for observed and P_i for predicted values; $\bar{O}$ is the mean of the observed values.

4.2.6 Quantifying the Risk Spaces

Because the goal is to build on the bottom-up approach, the same framework as Brown *et al*. (2012) is adopted. A climate state represented by a time series is summarized by subsets of climate and hydrological statistics that are relevant to the problem under investigation. These subsets can be calculated for any observational time series, or downscaled climate model outputs. A climate state will yield a level of risk and performance that is measured by a set of risk/performance indicators. These indicators are obtained by feeding SWAT with the perturbed time series data, each of which is unique. We placed a greater focus on hydrological risks due to their direct impacts on the watershed systems. This includes analyzing extreme values based on statistical models and investigating the timing and intensity of peak spring flow.

4.2.6.1 Extreme Value Statistical Probability Models (AM and 7Q)

The 3-parameter Generalized Extreme Value (GEV) and 2-parameter Weibull (WBL) distribution functions were fitted to the annual maximum streamflow (*AM*) and minimum extreme events (the lowest 7-day average flow, or *7Q*), respectively, based on seven time-

intervals (2, 5, 10, 20, 50, 100, and 500 years). The cumulative distribution functions (CDFs) of the GEV and WBL models are (Jenkinson, 1955):

$$F_{GEV}(x) = exp\left\{-\left[1+\xi\left(\frac{x-\mu}{\sigma}\right)\right]^{-1/\xi}\right\}, \text{ where } \left[1+\xi\left(\frac{x-\mu}{\sigma}\right)\right] > 0, \qquad \textbf{Eq. 4.4}$$

$$F_{WBL}(x) = 1- exp\left\{-\left[\frac{x}{\sigma}\right]^{\xi}\right\} \qquad \textbf{Eq. 4.5}$$

where ξ, μ, and σ are the shape, location, and scale parameters, respectively. Maximum likelihood (ML) estimators, as recommended by Das *et al*. (2013), are used to compute the parameters of these statistical models based on 95% confidence intervals (α=0.05).

4.2.6.2 Spring Flow Timing and Intensity

Another important phenomenon with significant impacts on the hydrology of many river systems in temperate regions is the timing of the annual snowmelt and changes to river-ice conditions. In the SNW, the most common flooding events are caused by snowmelt-driven runoff. Hence, future changes in the spring snowmelt and river-ice breakup, particularly at high latitudes or in large mountain regions, seem inevitable. These changes in river-ice processes are useful indicators of climate change because of their sensitivity to air temperature (Karl *et al*., 1993; Huntington *et al*., 2003). Warmer winters may promote dramatic alterations in discharge patterns and in the severity and timing of the snowmelt. A threshold amount of energy, including the mean daily temperature and soil heat flux, as well as the areal coverage of snow are critical in controlling the release of the stored water. In the SWAT model, the snowmelt starts when the daily maximum temperature (SMTMP) is above 0 C° and its uniformly released water is considered as precipitation (Neitsch *et al*., 2011). For simplicity, the peak spring flow is defined as the event of maximum daily flow in the spring season from January 1 to May 31.

4.2.7 Likelihood Estimation Using KDE

It is assumed that the synthetically generated time series will be a fair representation of the natural climate variability. Using all sample data, we employ a nonparametric density estimation function, or the kernel density estimator (KDE) to build a continuous probability density function (PDF) without making any a priori assumptions with regard to the underlying distribution. This approach involves exploring the extent of possible changes to hydroclimatic variables in the context of climate change. This includes analyzing the main characteristics of hydrological variables. The kernel density estimator of a sample of a d-variate random vector $(x_1, x_2, \ldots, x_n)$, drawn from an unknown distribution, is given by:

$$\hat{f}_h(x) = \frac{1}{n}\sum_{i=1}^{n} K(x - x_i), \qquad \textbf{Eq. 4.6}$$

where K is a non-negative kernel smoothing function, and h the non-negative bandwidth. The bivariate kernel density estimation in this study was based on a diagonal bandwidth matrix and a Gaussian kernel (Botev *et al.*, 2010).

4.3 Results

4.3.1 SWAT Calibration and Validation

The results of the proposed method for the South Nation Watershed under changing climate conditions using a stochastic data-oriented approach are presented. Applying the two downscaling methods described above to different CORDEX data, corrected daily time series of precipitation, maximum and minimum temperature from four RCMs under the conditions of RCP4.5 and RCP8.5 emission scenarios were generated for every metrological station. The SWAT model was calibrated with 15 years of observed streamflow at a monthly resolution for the period from Jan. 1981 to Dec. 1995 and validated on the period from Jan. 1996 to Dec. 2005.

Tables 4.3 provides results of a set of statistics that show a satisfactory agreement between observed and simulated streamflow in both periods.

Table 4.3 SWAT model performance in the calibration and validation periods.

Statistic measure	Preferred Ranges*	Period	
		Calibration	Validation
The Nash–Sutcliffe efficiency coefficient (NSE)	NSE ≥ 0.75	0.90	0.81
The RMSE-observations standard deviation ratio (RSR)	RSR ≤ 0.5	0.31	0.43
The percentage of bias (PBIAS)	−10% ≤ PBIAS ≤ 10%	-10.0%	-8.3%

* According to Liew *et al*. (2007) and Moriasi *et al*. (2010).

4.3.2 Time Series Generation for the Reference and Future Periods

The weather generator, MulGETS, was used to generate 250 30-year climate datasets for each climate scenario. Then, the SWAT model, calibrated on historical climate data, was forced with the corrected future climate information to investigate hydrological changes. This resulted in 4000 realizations of future daily streamflow sequences, each consisting of 30 years of predictions. The exact number of simulations is presented in Table 4.4. To account for uncertainties, the total of 480,000 years of predictions are summarized using extreme-streamflow indicators that describe the associated risks and allow for comparisons against observations.

Table 4.3 Details of models and number of future projections used in the study.

Downscaling methods	RCMs	RCPs	Variables (daily)	Weather Generator	Hydrological model	Period length	
Change Factor (CF) Quantile-Quantile (QQ)	CanRCM4 RCA4 HIRHAM5 RCA4	RCP4.5 RCP8.5	PCP TMAX TMIN Streamflow	MulGETS	SWAT	30 (yrs) (2071-2100)	**Total (yrs)**
Total = 2	4	2	4	250*	1	30	**= 480,000**

* Number of realizations used.

4.3.3 Representation of the Sensitivity Space

4.3.3.1 Flood and Drought Indicators

Hydrologically-based extreme streamflow metrics simulated by SWAT, including the design flood and 7-day low flow based on selective return periods, were analyzed. These results are compared to the equivalent SWAT-estimated extreme indices on the historical period to quantify possible changes (Figure 4.3). The isolines in Figure 4.3 depict the intensity of projections as the probability scale is given by the colour varying smoothly from yellow (higher intensity) to blue (less intensity). Results of the ensemble (Figure 4.3e) imply significant decreases in the annual maximum flows and increasing summer minimum flows by mostly all data configurations (i.e., RCMs, RCPs, and downscaling methods).

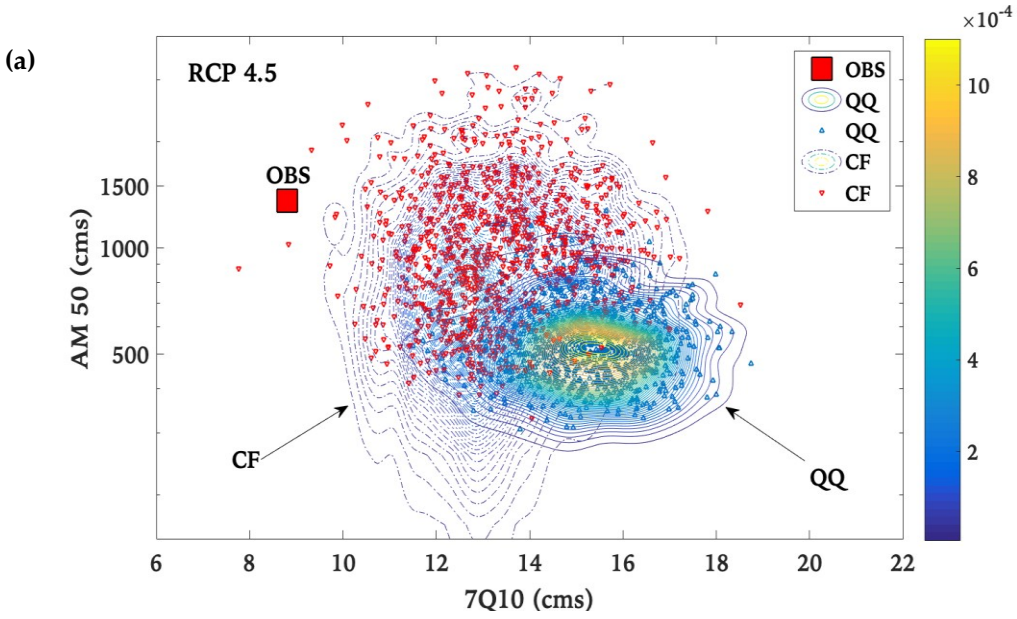

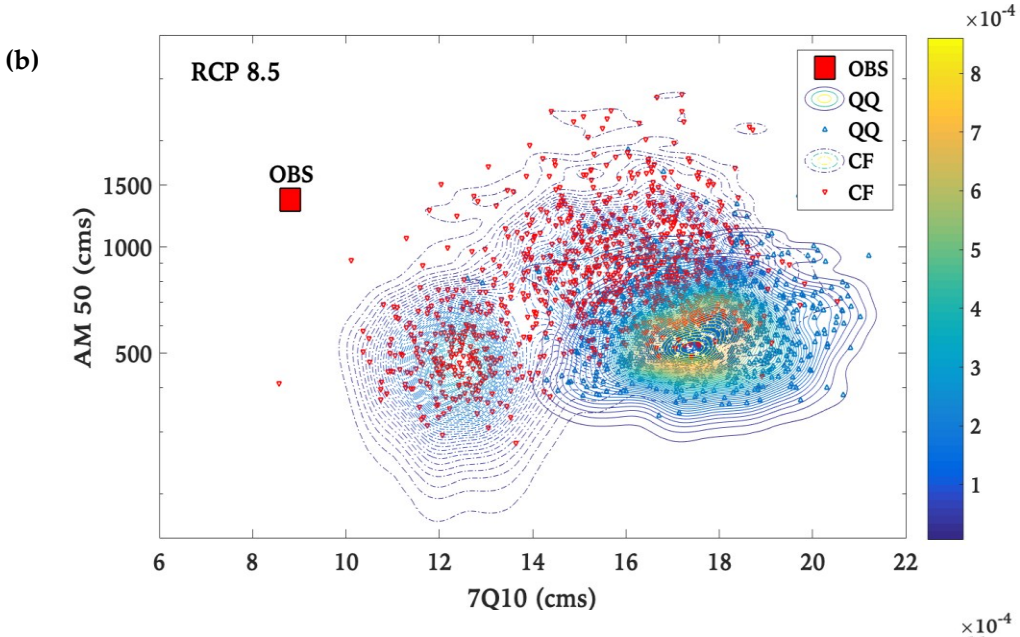
(b)
RCP 8.5
OBS
QQ
QQ
CF
CF
OBS
AM 50 (cms)
7Q10 (cms)
×10^-4

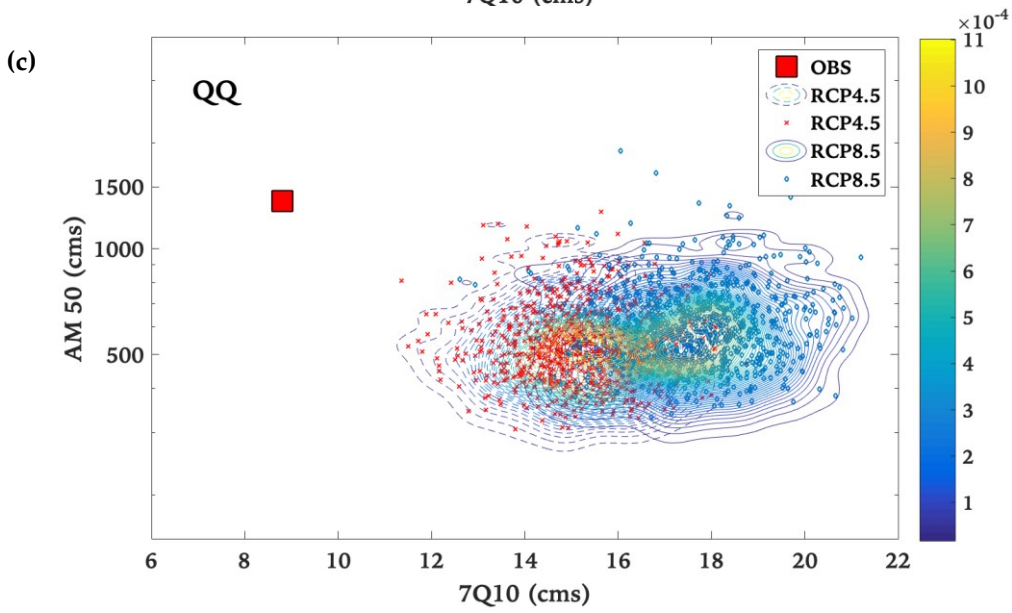
(c)
QQ
OBS
RCP4.5
RCP4.5
RCP8.5
RCP8.5
AM 50 (cms)
7Q10 (cms)
×10^-4

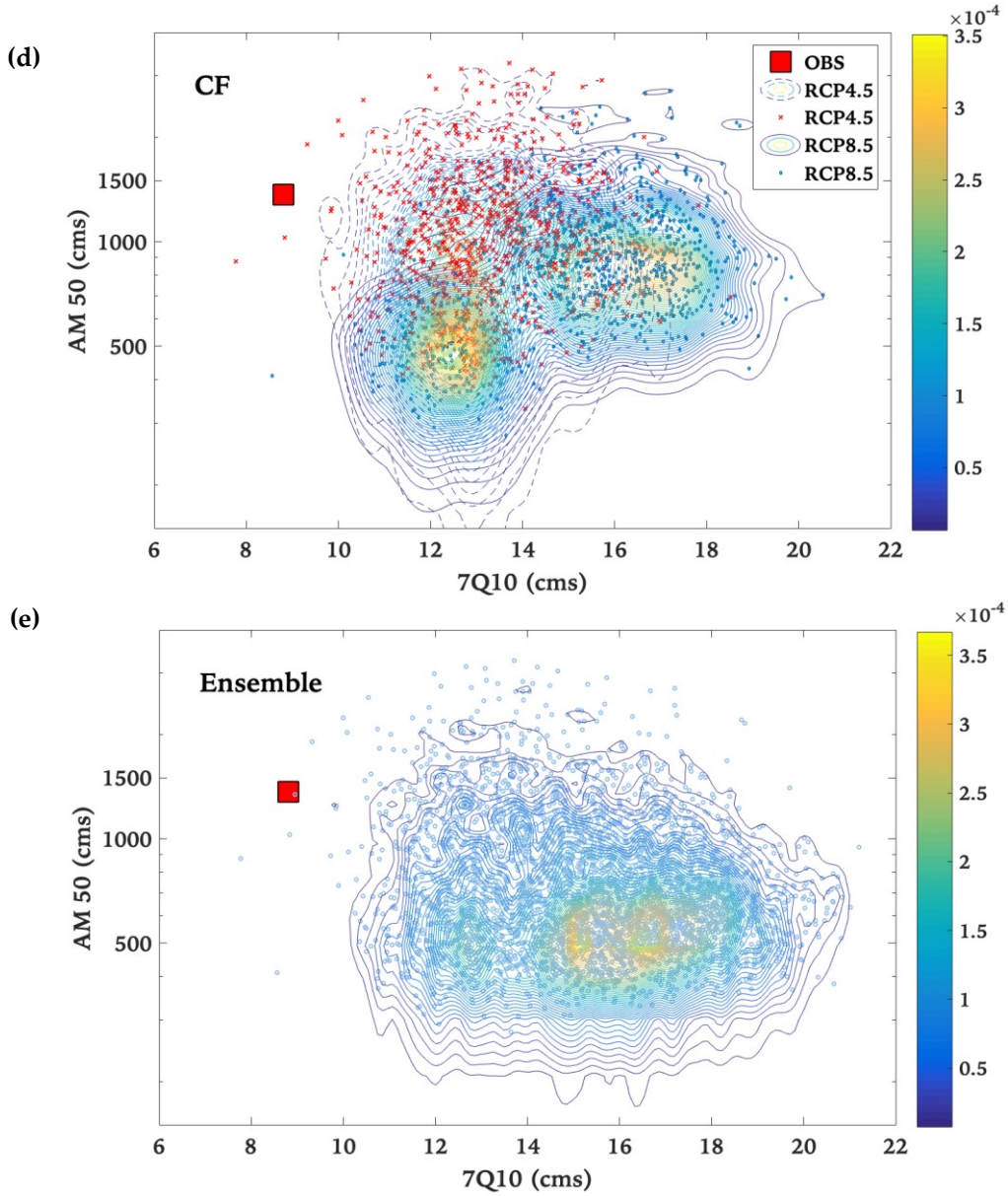

Figure 4.6 Bivariate kernel density estimations of the 50-year flooding event (*AM50*) and the 7-day low flow of 10-year return period (*7Q10*) based on (**a**) RCP4.5 and (**b**) RCP8.5 scenarios, derived from ensembles of downscaled climate data using (**c**) QQ method, (**d**) CF method, and (**e**) the ensemble of all simulations. Each point represents a hydrological response to a climate-change realization (projection) and isolines represent their probability where isoline-values coded by color from yellow (higher intensity) to blue (less intensity). Results are compared to observed data (red square).

Further analysis was conducted on extreme values by combining all simulations by each downscaling method, resulting in 30,000 years of simulated streamflow data. Drought indices

(*7Q*) and design floods (*AM*) of these time series were compared to observed ones (Figure 4.4). The comparison indicates that higher air temperatures lead to reduced summer low-flows and less intense high flows. The ensemble results indicate similar trends in both indices, i.e., fewer droughts and extreme flooding events.

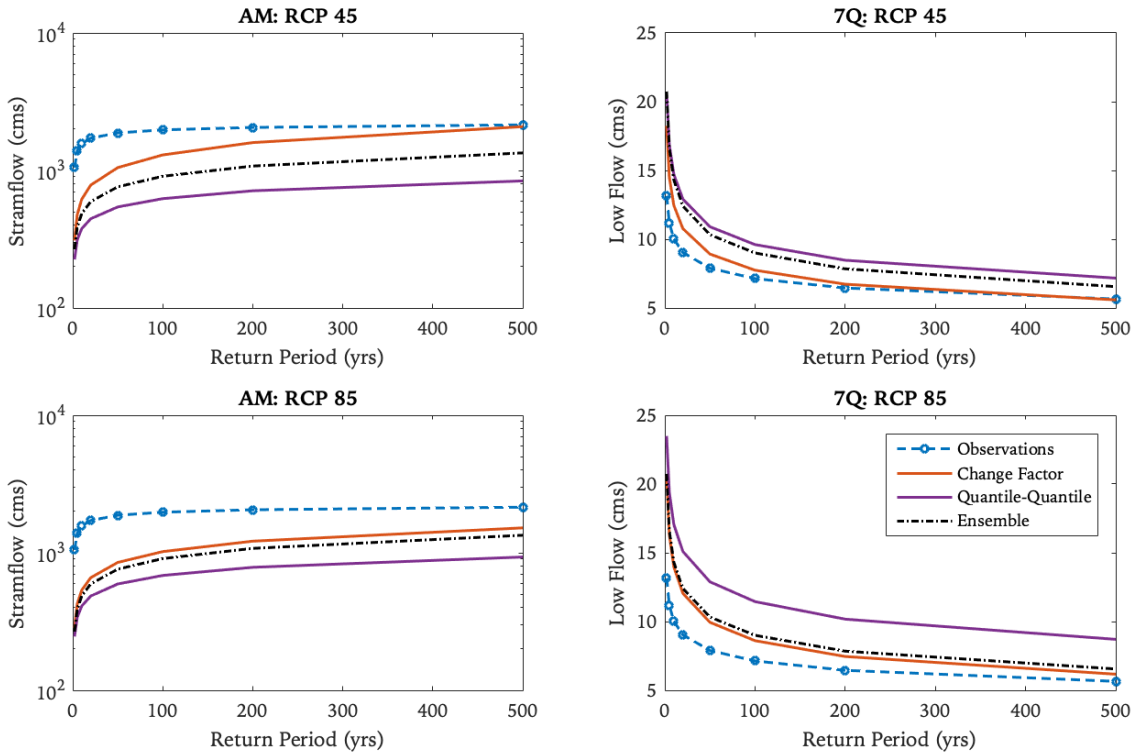

Figure 4.7 Estimations of future drought indices (*7Q*) and design floods (*AM*) based on RCP4.5 and RCP8.5 constructed from prolonged corrected climate time series, compared to observed and ensemble series.

4.3.3.2 Spring Flow Variability

Increasing temperatures have a direct effect on the hydrology of the watershed by changing to the snowmelt-driven runoff that occurs in late winter/early spring. Shorter duration of snowpack and an increase in stream flow in the winter are projected, triggered by a warming winter, particularly in cold regions. This is predicted by most models and scenarios with some variations in timing and magnitude of the largest flow with more substantial warming occurring

in the winter months. Figure 4.5 shows the disparity between the timing of the largest flow in the historical period and in the late-21st century. Between 1981 and 2010, the median date of the largest spring flow was March 12th (red dashed line in Figure 4.5b). The domination of most of the models and downscaling methods suggests that the peak spring flow will occur earlier, which is consistent with an earlier spring warming. As a result, the intensity of the annual spring flow at the outlet of the SNW is expected to significantly decrease by up to 60% (Figure 4.5a). The ensemble results suggest a 50% decrease in the quantity and the occurrence of the peak spring flow to be before the month of March.

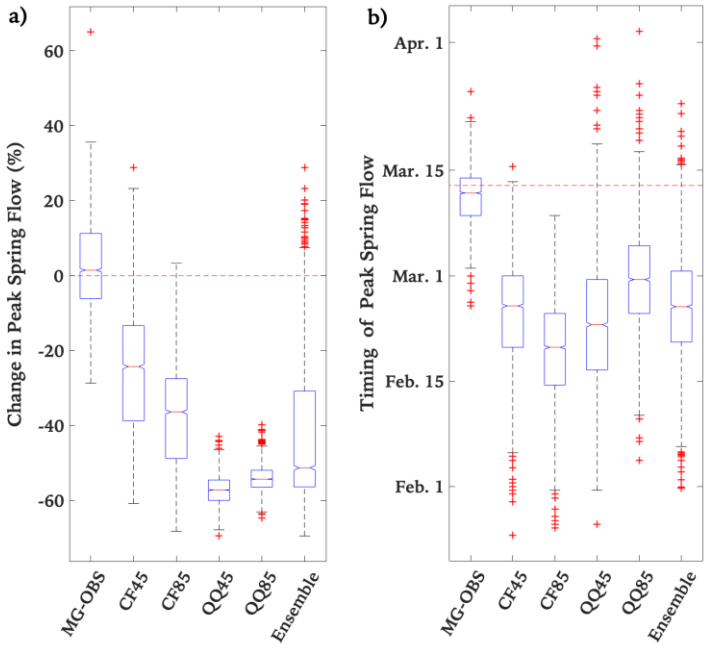

Figure 4.8 Estimations Projected changes in (**a**) the magnitude (%) and (**b**) timing of the peak spring flow event at the outlet of the SNW using two downscaling methods (Change Factor {CF}, and Quantile-Quantile method {QQ}) and forced with two climate scenarios (RCP4.5 {45} and RCP8.5 {85}). "Ensemble" represents all simulations combined and compared to the range of variability observed in the reference period (MG-OBS).

4.4 Discussion

The main contribution of this paper is to represent the variability of future outcomes through ensembles of realizations of climate time series that are converted into an ensemble of impacts. The spread of these ensembles is a representation of the uncertainty in future climate and impacts. The uncertainty comes from the fact that there is no consensus approximation of climate response to a doubling of atmospheric carbon dioxide (or climate sensitivity) although the initial estimation by National Academy of Sciences (1979) to be in the range of 1.5-4.5 °C is still adopted by the recent reports of the Intergovernmental Panel on Climate Change (IPCC) (2007, 2014). Andrews *et al*. (2018) suggested that the response of global temperature might be greater and more uncertain than previously estimated, specifically at the upper end. The ensemble also covers the range of variability observed during the baseline period. The spread of the ensemble depends on the climate model, emission scenario and the choice of downscaling methods. The following sections discuss the impacts of these factors on the results.

4.4.1 Comparison of Downscaling Methods

By comparing downscaling methods in Figures 4.3 and 4.5, it becomes apparent that the QQ technique outperformed the mean-based CF by correcting the distributions of RCM data rather than a single statistic. The cloud of points is denser (yellow-contours) where the probability is higher. QQ outcomes have a tendency to consistent clouds representing different climate models and scenarios. Indeed, the convergence in the projected QQ results across RCMs with different parameterization and climate sensitivity may suggest a more refined and skillful representation of future climate and hydrological systems, especially in the estimation of extreme daily precipitation (Sarr *et al*., 2015). However, in the context of risk analysis, Daniels *et al*. (2012) stated that one cannot utterly exclude an outlier scenario as it may characterize some underlying physical processes that were missed by other models or scenarios.

The mean-based downscaling method used in this study provides more diverse results (Figure 4.3). Results, however, are scattered, suggesting that the choice of the downscaling method will greatly affect the estimated impacts and thus adaptation strategies. In the absence of evidence that one method is better than another, the safest approach is to use all available methods. Several researchers or practitioners use one downscaling method without justification, neglecting that their results will be tainted by that choice. Research is needed to assess the relative credibility of downscaling methods in order to choose the most reliable approach.

4.4.2 Sensitivity Domains Assessment

Based on the probabilistic assessment of climate change, the 7-day mean annual minima and annual maxima indices suggested positive changes in the future period compared to the reference period. While low streamflow is a product of a complex combination of several factors in the physical processes, a possible reason of such projected changes in low flow is attributed to enhanced evapotranspiration (due to increased air temperature) from the wet-land surfaces of the watershed in summer (Abdel-Fattah and Krantzberg, 2014) which leads to increased precipitation frequency through more intense convective storms and consequently increasing flows during the summer months. These projected changes of volume in low flows would be welcome especially in terms of their impacts on aquatic habitat and water quality.

Higher values of future low flows compared to the baseline period due to increased rainfall intensity in North America were reported by Shrestha *et al.* (2019) based on SWAT simulations forced by data from ten GCMs from CMIP5 archives in response to RCP 4.5 and RCP 8.5 scenarios in a river located in southwest Ohio, USA. Similar conclusions of extremely low flow conditions to occur less frequently in the future were reported by modeling studies applied to different watersheds across Europe (Laaha *et al*., 2016; Gunawardhana *et al*., 2012) and Asia

(Tian *et al*., 2017; Gain *et al*., 2011). In fact, these projections are also in agreement with previously reported findings of upward trends in observed low flow values across Canada (Ehsanzadeh and Adamowski, 2007; Yue *et al*., 2003). For example, Khaliq *et al*. (2008) investigated observed values of 1-, 7-, 15-, and 30-day annual low-flow indicators in some Canadian rivers and found significantly increasing trends in southern Ontario. Similarly, Moore *et al*. (2007) found a statistically large positive trend in streamflow during low flow season in southwest British Columbia. Moreover, Novotny and Stefan (2007) found 7-day low flows to be increasing at a significant rate in three major river basins of Minnesota during both the summer and winter. In general, both low- and high-flows have been investigated in various regional studies with no consistent conclusions in terms of how they will be altered by climate change (Sapač *et al*., 2019). Rather, it is believed that such extremes are very localized and dependent on the selected GCMs and hydrological models; thus, results cannot be simply generalized.

On the other hand, spring peak flow is generally a product of average air temperature and snowmelt runoff. Most of the ensemble data suggest an early occurrence of peak spring flow. This result is consistent with the finding of Gunawardhana and Kazama (2012), who projected an early occurrence of peak spring flow in Italy by approximately 12 days during the 2080s in comparison to the baseline period. Also, it is supported by observed and projected changes in spring streamflow-timing across parts of western North America (Stewart *et al*., 2004). An advance in the timing of spring peak flow could negatively affect water supply, ecosystem and reservoirs' storage management (Stewart *et al*., 2004). However, such change in timing implies a reduction in snowmelt runoff severity (and hence the magnitude of the largest daily mean flows in spring), and the economic impacts will be apparent particularly in Canada (Beltaos, 2000). These findings can likely explain the projected reduction in annual maxima values in a mainly snowmelt dominated river, where typically the highest flow occurs in early spring each year

caused by snowmelt-generated runoff. These results are also consistent with previous works done in some Canadian watersheds that detected the same behaviour in the past such as Zhang *et al*. (2001).

When multiple RCMs and downscaling approaches are used, the best hydrological estimate can be constructed based on weighting of combined results of rainfall-runoff modelling. By adopting the versatile methodology considered herein, it is believed that the risk of extremes and their consequent losses under an uncertain climate can be significantly reduced, as risk cannot be completely eliminated. Ideally, further improvement to the super-ensemble can be achieved by considering more stochastic weather generators, climate-change models, and downscaling methods to ensure a thorough evaluation. To overcome the high computational requirements to construct the super-ensemble, further research is needed to determine the optimal length of the chain containing realizations needed to represent observed data in climatic and hydrological modelling.

4.5 Conclusions

This paper proposed a novel approach to associate a credibility measure to the climate and sensitivity measure in a bottom-up approach by combining synthetically generated climate series with downscaled climate model output to populate the climate and sensitivity spaces. The large number of projections allowed us to quantify future uncertainties and provided better coverage of the risk space based on a probabilistic assessment of climate change. Furthermore, the likelihood measure provides a more practical assessment of the plausibility of future risks to serve infrastructure design and allow more confidence in water-related management decisions. Ideally, the generation of such ensembles should contain - to a feasible extent - as many uncertainty elements as possible. Given that the choice of climate models, downscaling techniques, and weather generator affects the results, a super-ensemble of future climate series

was used to derive flooding and drought indices, while bearing in mind the uncertainties inherent in the extreme value modelling under a changing climate at regional scales. The results of the modelled risk analysis on the South Nation Watershed located in Ontario, Canada, indicate a marginal increase in the 7-day low flow, whereas design floods will noticeably weaken. A shorter and warmer winter is expected to result in an earlier disappearance of accumulated winter snow cover, early onset of snowmelt and consequently an earlier and less intensive peak spring flow. While an application was centered in one pilot watershed, the methodology delivers new insights into hydrological processes under changing climate conditions in general and will be of interest for Canada and beyond. The need is also manifest for examining a broader range of hydrologic indicators. Finally, the broader natural uncertainty posed by climate change and land-use, and their implicit disruptions to various agro-socioeconomic and water sectors at an operational level, may constitute an interesting and worthwhile extension of this study.

4.6 References

Abbaspour, K. C.; Yang, J.; Maximov, I.; Siber, R.; Bogner, K.; Mieleitner, J.; ... & Srinivasan, R. (2007). Modelling hydrology and water quality in the pre-alpine/alpine Thur watershed using SWAT. *J. Hydrol.*, *333(2-4)*, 413-430.

Abdel-Fattah, S.; Krantzberg, G. (2014). A review: Building the resilience of Great Lakes beneficial uses to climate change. *Sustainability Water Qual. Ecol.*, *3*, 3-13.

Alodah, A.; Seidou, O. (2017). The realism of Stochastic Weather Generators in Risk Discovery. *WIT Trans. Ecol. Envir.*, *220*, 239-249. DOI: 10.2495/WRM170231

Alodah, A.; Seidou, O. (2019). The adequacy of stochastically generated climate time series for water resources systems risk and performance assessment. *Stoch. Environ. Res. Risk. Assess.*, *33(1)*, 253-269. doi: 10.1007/s00477-018-1613-2

Andrews, T.; Gregory, J. M.; Paynter, D.; Silvers, L. G.; Zhou, C.; Mauritsen, T.; ... & Titchner, H. (2018). Accounting for changing temperature patterns increases historical estimates of climate sensitivity. *Geophys. Res. Lett.*, *45(16),* 8490-8499.

Angelina, A.; Gado Djibo, A.; Seidou, O.; Seidou Sanda, I.; Sittichok, K. (2015). Changes to flow regime on the Niger River at Koulikoro under a changing climate. *Hydrolog. Sci. J.*, *60(10),* 1709-1723.

Arnold JG, Moriasi DN, Gassman PW, Abbaspour KC, White MJ, Srinivasan R, Santhi C, Harmel R, Van Griensven A, Van Liew MW *et al*. (2012). SWAT: model use, calibration, and validation. *T. ASABE*, *55,* 1491–1508

Arnold JG, Srinivasan R, Muttiah RS, Williams JR. (1998). Large area hydrologic modeling and assessment part I: model development 1. *J. Am. Water. Resour. Assoc.*, *34(1)*, 73–89

Arora, V. K.; Boer, G. J. (2001). Effects of simulated climate change on the hydrology of major river basins. *J. Geophys. Res. Atm.*, *106(D4),* 3335-3348.

Arthington, A. H.; Bunn, S. E.; Poff, N. L.; Naiman, R. J. (2006). The challenge of providing environmental flow rules to sustain river ecosystems. *Ecol. Appl.*, *16(4)*, 1311-1318.

Beltaos, S. (2000). Advances in river ice hydrology. *Hydrol. Process.*, *14(9)*, 1613-1625.

Bhave, A.; Mishra, A.; Raghuwanshi, N. (2014). A combined bottom-up and top-down approach for assessment of climate change adaptation options. J. Hydrol., 518, 150-161. DOI: 10.1007/s10584-014-1061-z

Bierkens, M. F.; Dolman, A. J.; Troch, P. A. (Eds.). (2008). Climate and the hydrological cycle, *8*. International Association of Hydrological Sciences.

Botev, Z. I.; Grotowski, J. F.; Kroese, D. P. (2010). Kernel density estimation via diffusion. *Ann. Stat.*, *38(5)*, 2916-2957.

Brown C.; Ghile Y.; Laverty M.; Li K. (2012). Decision scaling: linking bottom up vulnerability analysis with climate projections in the water sector. *Water Resour. Res.*, *48(9)*, 9537

Brown, C.; Werick, W.; Leger, W.; Fay, D. (2011). A Decision-Analytic Approach to Managing Climate Risks: Application to the Upper Great Lakes. *J. Am. Water. Resour. As.*, *47(3)*, 524–534. DOI: 10.1111/j.1752-1688.2011.00552.x

Chen, J.; Brissette, F.P.; Zhang, X.J. (2014). A multi-site stochastic weather generator for daily precipitation and temperature. *T. ASABE*, *57*(5), pp.1375-1391.

Chin, V.I.; Wang, K.T. and Vallery, O.J. (1980). Water resources of the South Nation River Basin. Ont. Min. Environ., Toronto, Ont., Rep. No. 13.

Culley, S.; Noble, S.; Yates, A.; Timbs, M.; Westra, S.; Mair, H.R.; Giuliani, M.; Castelletti, A. (2016). A bottom-up approach to identifying the operational adaptive capacity of water resources systems to a changing climate. *Water Resour. Res*, *52(9)*, 6751 - 6758. DOI: 10.1002/2015WR018253/full

Daniels, A.E.; Morrison, J.F.; Joyce, L.A.; Crookston, N.L.; Chen, S.C.; McNully, S.G. (2012). Climate projections FAQ. General Technical Report. Department of Agriculture, Forest Service, Rocky Mountain Research Station, Fort Collins, CO, U.S.A, 2012; pp. 1-32.

Das, S.; Millington, N.; Simonovic, S. P. (2013). Distribution choice for the assessment of design rainfall for the city of London (Ontario, Canada) under climate change. *Can. J. Civil Eng.*, *40(2)*, 121-129.

Diaz-Nieto, J.; Wilby, R. L. (2005). A comparison of statistical downscaling and climate change factor methods: impacts on low flows in the River Thames, United Kingdom. *Climatic Change*, *69(2-3)*, 245-268.

Ehsanzadeh, E.; Adamowski, K. (2007). Detection of trends in low flows across Canada. *Can. Water Resour. J.*, *32(4)*, 251-264.

Frich P.; Alexander L.V.; Della-Marta P.M.; Gleason B.; Haylock M.; Tank A.K.; Peterson T. (). Observed coherent changes in climatic extremes during the second half of the twentieth century. *Clim. Res.* 2002, *19(3)*, 193–212

Gain, A. K.; Immerzeel, W. W.; Sperna Weiland, F. C.; Bierkens, M. F. P. (2011). Impact of climate change on the stream flow of the lower Brahmaputra: trends in high and low flows based on discharge-weighted ensemble modelling. *Hydrol. Earth Syst. Sc.*, *15(5)*, 1537-1545.

García, L. E.; Matthews, J. H.; Rodriguez, D. J.; Wijnen, M.; DiFrancesco, K. N.; Ray, P. (2014). Beyond downscaling: a bottom-up approach to climate adaptation for water resources management. World Bank Publications.

Gleick, P. H. (1989). Climate change, hydrology, and water resources. *Rev. Geophys. 27(3),* 329-344.

Gunawardhana, L. N.; Kazama, S. (2012). A water availability and low-flow analysis of the Tagliamento River discharge in Italy under changing climate conditions, *Hydrol. Earth Syst. Sci.*, *16*, 1033-1045, https://doi.org/10.5194/hess-16-1033-2012.

Guo, D.; Westra, S.; Maier, H.R. (2017). Use of a scenario-neutral approach to identify the key hydro-meteorological attributes that impact runoff from a natural catchment. *J. Hydrol.*, *554*, 317-330. DOI: 10.1016/j.jhydrol.2017.09.021

Hansen, C. H.; Goharian, E.; Burian, S. (2017). Downscaling precipitation for local-scale hydrologic modeling applications: comparison of traditional and combined change factor methodologies. *J. Hydrol. Eng.*, *22(9)*, 04017030.

Harris, C. N. P.; Quinn, A. D.; Bridgeman, J. (2014). The use of probabilistic weather generator information for climate change adaptation in the UK water sector. *Meteorol. Appl.*, *21(2)*, 129-140.

Hayhoe, K. A. (2010). A standardized framework for evaluating the skill of regional climate downscaling techniques, Doctoral dissertation, University of Illinois at Urbana-Champaign, Illinois.

Huntington, T. G.; Hodgkins, G. A.; Dudley, R. W. (2003). Historical trend in river ice thickness and coherence in hydroclimatological trends in Maine. *Climatic Change*, 61(1-2), 217-236.

IPCC, 2007: Climate Change 2007: Synthesis Report. Contribution of Working Groups I, II and III to the Fourth Assessment Report of the Intergovernmental Panel on Climate Change [Core Writing Team, Pachauri, R.K and Reisinger, A. (eds.)]. 2007, IPCC, Geneva, Switzerland, 104 pp.

IPCC, 2014: Climate Change 2014: Impacts, Adaptation, and Vulnerability. Part A: Global and Sectoral Aspects. Contribution of Working Group II to the Fifth Assessment Report of the Intergovernmental Panel on Climate Change [Field, C.B.; V.R. Barros, D.J. Dokken, K.J. Mach, M.D. Mastrandrea, T.E. Bilir, M. Chatterjee, K.L. Ebi, Y.O. Estrada, R.C. Genova, B. Girma, E.S. Kissel, A.N. Levy, S. MacCracken, P.R. Mastrandrea, and L.L. White (eds.)]. 2014, Cambridge University Press, Cambridge, United Kingdom and New York, NY, USA, 1132 pp.

Jenkinson, A. F. (1955). The frequency distribution of the annual maximum (or minimum) values of meteorological elements. *Q. J. Roy. Meteor. Soc.*, *81(348)*, 158-171.

Karl, T. R.; Groisman, P. Y.; Knight, R. W.; Heim Jr, R. R. (1993). Recent variations of snow cover and snowfall in North America and their relation to precipitation and temperature variations. *J. Climate*, *6(7)*, 1327-1344.

Khaliq, M. N.; Ouarda, T. B.; Gachon, P.; Sushama, L. (2008). Temporal evolution of low-flow regimes in Canadian rivers. *Water Resour. Res.*,*44(8)*.

Laaha G.; Parajka J.; Viglione A.; Koffler D.; Haslinger K.; Schöner W.; *et al*. (2016). A three-pillar approach to assessing climate impacts on low flows. *Hydrol. Earth Syst. Sc.*, *20(9)*, 3967–3985.

Lafon, T.; Dadson, S.; Buys, G.; Prudhomme, C. (2013). Bias correction of daily precipitation simulated by a regional climate model: a comparison of methods. *Int. J. Climatol.*, *33(6)*, 1367-1381.

Lenderink, G.; Buishand, A.; Deursen, W. V. (2007). Estimates of future discharges of the river Rhine using two scenario methodologies: direct versus delta approach. *Hydrol. Earth. Syst. Sc.*, *11(3)*, 1145-1159.

Liew MW, Veith TL, Bosch DD, Arnold JG. (2007). Suitability of SWAT for the conservation effects assessment project: a comparison on USDA-ARS experimental watersheds. *J. Hydrol. Eng.*, *12(2),* 173–189

Linnansaari, T.; Monk, W. A., Baird, D. J.; Curry, R. A. (2012). Review of approaches and methods to assess Environmental Flows across Canada and internationally. *DFO Can. Sci. Advis. Sec. Res. Doc.*, *39*, 1-74.

Luo, M.; Liu, T.; Frankl, A.; Duan, Y.; Meng, F.; Bao, A.; ... & De Maeyer, P. (2018). Defining spatiotemporal characteristics of climate change trends from downscaled GCMs ensembles: how climate change reacts in Xinjiang, China. *Int. J. Climatol.*, *38(5)*, 2538-2553.

Manabe, S. (1969). Climate and the ocean circulation: I. The atmospheric circulation and the hydrology of the earth's surface. *Mon. Weather Rev*. *97(11)*, 739-774.

Maraun, D. (2016). Bias correcting climate change simulations-a critical review. *Current Climate Change Reports*, *2(4)*, 211-220.

Moore, R. D.; Allen, D. M.; Stahl, K. (2007). Climate change and low flows: influences of groundwater and glaciers. Final Report for Climate Change Action Fund Project A, 875, 211.

Moriasi DN, Arnold JG, Van Liew MW, Bingner RL, Harmel RD, Veith TL. (2007). Model evaluation guidelines for systematic quantification of accuracy in watershed simulations. *T. ASABE*., *50(3)*, 885-900.

Mpelasoka, F. S.; and F. H. S. Chiew. (2009). Influence of rainfall scenario construction methods on runoff projections, *J. Hydrometeorol*., *10*, 1168–1183.

National Academy of Sciences. (1979). Carbon Dioxide and Climate: A Scientific Assessment, Washington, D. C.

Neitsch, S. L.; Arnold, J. G.; Kiniry, J. R.; Williams, J. R. (2011). Soil and water assessment tool theoretical documentation version 2009. Texas Water Resources Institute.

Novotny, E. V.; Stefan, H. G. (2007). Stream flow in Minnesota: Indicator of climate change. *J. Hydrol.*, *334(3-4)*, 319-333.

Panagoulia D. (1991). Hydrological response of a medium-sized mountainous catchment to climate changes, *Hydrolog. Sci. J.*, *36(6)*, pp. 525-547.

Panagoulia D. (1992). Impacts of GISS-modelled climate changes on catchment hydrology, *Hydrolog. Sci. J.*, 37(2), pp. 141-163.

Panagoulia D., (2006). Artificial neural networks and high and low flows in various climate regimes, *Hydrolog. Sci. J.*, *51(4)*, pp. 563-587.

Panagoulia D., Bárdossy A., and Lourmas G., (2008). Multivariate stochastic downscaling models generating precipitation and temperature scenarios of climate change based on atmospheric circulation, *Global Nest J.*, *10 (2)*, pp. 263-272.

Panagoulia D.; Bárdossy A.; Lourmas G. (2008). Multivariate stochastic downscaling models generating precipitation and temperature scenarios of climate change based on atmospheric circulation, *Global Nest J.*, *10 (2)*, pp. 263-272.

Pastor, A. V.; Ludwig, F.; Biemans, H.; Hoff, H.; Kabat, P. (2014). Accounting for environmental flow requirements in global water assessments. *Hydrol. Earth. Syst. Sc.*, *18(12)*, 5041-5059.

Pielke Sr, R. A.; Wilby, R.; Niyogi, D.; Hossain, F.; Dairuku, K.; Adegoke, J.; ... & Suding, K. (2012). Dealing with complexity and extreme events using a bottom-up, resource-based vulnerability perspective. Extreme Events and Natural Hazards: The Complexity Perspective, *Geophys. Monogr. Ser*, *196*, 345-359.

Santhi C, Arnold J, Williams J, Dugas W, Srinivasan R, Hauck L. (2001). Validation of the SWAT model on a large river basin with point and nonpoint sources 1. *J. Am. Water. Resour. Assoc.*, *37(5)*, 1169–1188

Sapač, K.; Medved, A.; Rusjan, S.; Bezak, N. (2019). Investigation of Low- and High-Flow Characteristics of Karst Catchments under Climate Change. *Water*, *11*, 925.

Sarr, M. A.; Seidou, O.; Tramblay, Y.; El Adlouni, S. (2015). Comparison of downscaling methods for mean and extreme precipitation in Senegal. *J. Hydrol. Reg. Stud.*, *4*, 369-385.

Seidou, O.; Ramsay, A.; Nistor, I. (2012). Climate change impacts on extreme floods II: improving flood future peaks simulation using non-stationary frequency analysis. *Nat. Hazards*, *60(2)*, 715-726.

Semenov V. A. (2007). Structure of temperature variability in the high latitudes of the Northern Hemisphere. *Izv. Atmos. Ocean. Phy.*, *43(6)*, 687-95.

Shrestha, S.; Sharma, S.; Gupta, R.; Bhattarai, R. (2019). Impact of global climate change on stream low flows: A case study of the great Miami river watershed, Ohio, USA. *Int. J. Agric. & Biol. Eng.*, *12(1)*, 84-95.

Srinivasan R, Arnold JG. (1994). Integration of a basin-scale water quality model with GIS. *Water Resour. Bull.*, *30(3)*, 453–462

Stewart, I. T.; Cayan, D. R.; Dettinger, M. D. (2004). Changes in snowmelt runoff timing in western North America under abusiness as usual'climate change scenario. *Clim. Change*, *62(1-3)*, 217-232.

Stocker, T. F.; Qin, D.; Plattner, G.-K.; Tignor, M.; Allen, S. K.; Boschung, J.; Nauels, A.; Xia, Y.; Bex, V.; Midgley, P. M. (2013). Climate Change 2013: The Physical Science Basis. Intergovernmental Panel on Climate Change, Working Group I Contribution to the IPCC Fifth Assessment Report (AR5). Cambridge University Press: New York USA; 159–254.

Tan, M.L.; Gassman, P.W.; Srinivasan, R.; Arnold, J.G.; Yang, X. (2019). A Review of SWAT Studies in Southeast Asia: Applications, Challenges and Future Directions. *Water*, *11*, 914.

Teutschbein, C.; Seibert, J. (2012). Bias correction of regional climate model simulations for hydrological climate-change impact studies: Review and evaluation of different methods. *J. Hydrol.*, *456*, 12-29.

Tharme, R. E. (2003). A global perspective on environmental flow assessment: emerging trends in the development and application of environmental flow methodologies for rivers. *River. Res. Appl.*, *19(5-6)*, 397-441.

Themβel, M. J.; A. Gobiet, and A. Leuprecht. (2010). Empirical statistical downscaling and error correction of daily precipitation from regional climate models, *Int. J. Climatol.*, *31*, 1530–1544, DOI: 10.1002.joc.2168.

Tian Y.; Xu Y P.; Ma C.; Wang G. (2017). Modeling the impact of climate change on low flows in Xiangjiang River Basin with Bayesian averaging method. *J Hydrol Eng.*, *22(9)*, 04017035.

Tuppad P, Douglas-Mankin KR, Lee T, Srinivasan R, Arnold JG. (2011). Soil and Water Assessment Tool (SWAT). hydrologic/water quality model: extended capability and wider adoption. *T. ASABE*, *54(5)*, 1677–1684

van Roosmalen L.; T. O. Sonnenborg, K. H. Jensen, and J. H. Christensen. (2011). Comparison of hydrological simulations of climate change using perturbation of observations and distribution-based scaling, Soil Science Society of America, *Vadose Zone J.*, *10*, 136–150, doi:10.2136/ vzj2010.0112

White KL, Chaubey I. (2005). Sensitivity analysis, calibration, and validations for a multisite and multivariable SWAT model. *J. Am. Water. Resour. Assoc.*, *41(5)*, 1077–1089

Whitfield, P. H.; Cannon, A. J. Recent variations in climate and hydrology in Canada. *Can. Water Resour. J.* 2000, *25(1),* 19-65.

Wilby R.L.; Fowler H.J. (2011). Regional climate downscaling: modelling the impact of climate change on water resources. Fung, F.; Lopez, A.; New, M.; Eds.; Wiley-Blackwell: Chichester, West Sussex, UK; Hoboken, NJ, ISBN 978-1-4051-9671-0

Wilby, R. L.; Charles, S. P.; Zorita, E.; Timbal, B.; Whetton, P.; Mearns, L. O. (2004). Guidelines for use of climate scenarios developed from statistical downscaling methods. Supporting material of the Intergovernmental Panel on Climate Change, available from the DDC of IPCC TGCIA, 27.

Wilby, R.L. (2011). Adaptation: Wells of wisdom. *Nat. Clim. Change*, *1(6)*, 302–303. DOI: 10.1038/nclimate1203

Wilks DS. (1998). Multi-site generalization of a daily stochastic precipitation model. *J. Hydrol.*, *210*, 178–191

Yue, S.; Pilon, P.; Phinney, B. O. B. (2003). Canadian streamflow trend detection: impacts of serial and cross-correlation. *Hydrolog. Sci. J.*, *48(1)*, 51-63.

Zhang, X.; Harvey, K. D.; Hogg, W. D.; Yuzyk, T. R. (2001). Trends in Canadian streamflow. *Water Resour. Res.*, *37(4),* 987-998.

CHAPTER 5.

*Influence of the Output Size of Stochastic Weather Generators on the Accuracy of Common Climate and Hydrologic Statistical Indices**

Abstract.

While Stochastic Weather Generators (SWGs) are used intensively in climate and hydrological applications to simulate hydroclimatic time series and estimate risks and performance measures linked to climate variability, there have been few investigations into how many realizations are required for a robust estimation of these measures. Given the computational cost and time necessary to force climate-sensitive systems with multiple realizations, the estimation of the optimal number of synthetic time series to generate with a particular SWG for a predefined accuracy when estimating a particular risk or performance measure is particularly important. In this paper, the required number of realizations of five SWGs coupled with a SWAT model (the Soil and Water Assessment Tool) needed in order to achieve a predefined Relative Root Mean Square Error is investigated. The statistical indices used are the mean, standard deviation, skewness, and kurtosis of four hydroclimatic variables: precipitation, maximum and minimum temperature, and annual streamflow. While the results vary somewhat across SWGs and indicators, they overall show that the marginal improvement decreases dramatically after 25 realizations. The results also indicate that the benefit of generating more than 100 realizations of climate and streamflow data is very minimal.

Keywords: *stochastic weather generators; stochastic hydrological modeling; hydrometeorology; hydrological risk assessment; climate ensemble; climate sensitivity; climate realizations; hydrological realizations*

---

* This chapter is currently under consideration.

5.1 Introduction

Stochastic weather Generators (referred to as SWGs hereafter) are numerical tools that are used broadly to simulate the statistical characteristics of observed climate variables and generate random time series that can be used as inputs for climate-sensitive hydrological models (Wheater *et al*., 2005). The variability in the input translates into variability in the generated hydrological time series. The risk associated with and performance of the modeled water system is assessed by estimating the statistics for the simulated variables. The use of SWG outputs in such studies is convenient, as SWGs can generate long and gap-free synthetic sequences based on historical observations and can be used for water resources planning and management (Vu *et al*., 2018). A large ensemble of long and gap-free time series is assumed to represent the internal variability of hydroclimatic variables, consisting mostly of precipitation, maximum temperature, minimum temperature, solar radiation, and relative humidity (Santer *et al.,* 2008) at different spatial and temporal scales (Ailliot *et al.*, 2015). According to Guenni (1994), SWGs are mainly useful in: (1) extending insufficient or incomplete records that constrain the modeling approach (e.g., Fodor *et al.*, 2013; Fatichi *et al*., 2016), (2) developing datasets for ungauged sites via spatially interpolating model parameters from adjacent areas with sufficient records (e.g., Baffault *et al.*, 1996; Fodor *et al.*, 2013), and, recently, (3) accounting for the uncertainty that arises from natural variability along with anthropogenic forcing in climate-change simulations (e.g., Räisänen and Ruokolainen, 2006; Minville *et al.*, 2008; Deser *et al.*, 2012; Thompson *et al.*, 2015).

SWGs were introduced initially for hydrological applications requiring long sequences of daily weather data (Gabriel and Neumann, 1962; Todorovic and Woolhiser, 1975) and have since been used consistently in various applications, such as the assessment of anthropogenic climate change impacts (e.g., Zwiers, 1996; Eames *et al*., 2012; Kilsby *et al*., 2007; Candela *et al*., 2012), crop

yield estimates (e.g., Vesely *et al*., 2019), ecosystem and food security models (e.g., Stevens and Madani, 2016), and in streamflow simulations (e.g., Zhang and Garbrecht, 2003; Dubrovský *et al*., 2004; Alodah and Seidou, 2019a) mainly to characterize internal atmospheric variability (or climate noise) (Räisänen and Ruokolainen, 2006; Santer *et al.,* 2008; Deser *et al.*, 2012). The use of observed climate data in hydrological modeling is always preferable; however, SWGs provide a suitable alternative, as some localized risky events that are not covered fully in the observed set can be underestimated (Räisänen and Ruokolainen, 2006; Ivanov *et al.,* 2007; Santer *et al.,* 2008; Vu *et al*., 2018).

SWGs are often employed to study the impacts of climatic variations based on a single realization, for instance, in rainfall-runoff simulations (e.g., Dubrovský *et al*., 2004), erosion simulations (e.g., Zhang and Garbrecht, 2003), simulations of extreme precipitation events (e.g., Furrer and Katz, 2008; Semenov, 2008), and in climate-change studies (e.g., Kilsby *et al*., 2007; Kim *et al*., 2007; Al-Mukhtar *et al*., 2014). Yet, unlike observed weather data which provide only one realization, an unlimited number of weather realizations can be generated (Kim *et al*., 2018; Vu *et al*., 2018), and it is very improbable statistically that any two realization will be identical (i.e., uncorrelated data from a realization to the next one). In general, multiple stochastically-generated time series can provide a broad range of weather possibilities for a detailed sensitivity analysis (Dubrovský *et al*., 2004; Santer *et al.,* 2008), such as the recently introduced vulnerability-based methods (e.g., bottom-up approaches) for evaluating uncertainty in projected climate change impacts (e.g., Brown *et al*., 2011; Steinschneider and Brown, 2013; Mukundan *et al*., 2019; Alodah & Seidou, 2019b). An ensemble of multiple realizations is recommended in order to characterize the variability in climate data adequately and estimate realistic mean values and variances of

meteorological variables (Alodah and Seidou, 2019a; Guo *et al.*, 2018; Mehrotra *et al*., 2006; Anyah and Semazzi, 2006; Dubrovský *et al*., 2004).

Multiple realizations of climate series are increasingly becoming the adopted modeling approach when evaluating the variability of complex climate systems in order to account for rare occurrences of climate variables (Anyah and Semazzi, 2006). Typically, an arbitrary (and commonly limited) number of realizations (ranged from 10 to 1000) are used. Examples of some recent publications utilizing multiple runs of weather generators are presented in Table 5.1. It is also common to use SWGs to produce a time series that is longer than observed ones (e.g., Kou *et al*., 2007; Caron *et al*., 2008; Chen *et al*., 2012; Eames *et al*., 2012), although this might lead to biases due to an insufficient sampling of the distribution (Mithen and Black, 2011). Therefore, it is recommended that multiple realizations with the same lengths as the training set be used (Dubrovský *et al*., 2004; Guo *et al*., 2018). However, the use of multiple realizations requires high-performance computational resources, especially when used in conjunction with a complex impact model. For example, Gitau *et al*. (2012) analyzed 172 management scenarios and ran a SWAT model 250 times for each of them, for a total of 43,000 runs, using an extremely large computing Condor framework. However, they stated that their work could have taken up to 3.3 years to complete via a traditional desktop computer workstation. Thus, given the acknowledged limitations imposed by time and computational expenses, the question related to the required number of realizations to characterize the hydrological space fairly is still open.

This prolonged process, particularly for large watersheds, may be overcome with the help of expensive supercomputers or by identifying a sufficiently representative number of outputs needed to capture the random component of the hydrological model and ultimately reduce the computations. Guo *et al*. (2018) investigated identifying the numbers of realizations necessary for

capturing several statistical characteristics of meteorological variables satisfactorily (i.e., for precipitation, and minimum and maximum temperature) generated synthetically by CLIGEN, LARSWG, and WeaGETS. They analyzed increasing discrete numbers of realizations (1, 25, 50, and 100) and concluded that a weather generator would reproduce essential climate characteristics well by 25 realizations. The current work builds generally on their ideas. However, the statistics considered in their work belong to the climatic data space only (precipitation and temperature variables); thus, their findings may not be applicable for hydrological variables, especially due to the non-linearity of the hydrologic response in rainfall-runoff transformations.

Table 5.1 Some recent publications using an ensemble of multiple realizations

Stochastic Weather Generator(s)	Number of realizations	Time series length	Hydrological impacts?	*Reference*
Met & Roll	30	30-year	SAC-SMA	Dubrovský *et al*. (2004)
WEGN & WeaGETS	30	300-year	HSAMI	Caron *et al*. (2008)
MNHMM	100	22-year	Sacramento	Kwon *et al*. (2011)
WGEN	100	30-year	Several conceptual models	Bastola *et al*. (2012)
Unique SWG	200	25-year	HEC-HMS & VisualBALAN	Candela *et al*. (2012)
WXGEN	250	28-year	SWAT	Gitau *et al*. (2012)
WeaGETS, MulGETS, & KNN	1000	41-year	SWAT	Alodah & Seidou (2019a)
MulGETS	250	30-year	SWAT	Alodah & Seidou (2019b)
Unique Stochastic Model	1000	42-year	Crop simulation models	Hansen & Ines (2005)
WGEN, SIMMETEO, & SWG	100	71-year	Crop simulation models	Apipattanavis *et al*. (2010)
CLIGEN	10	20-year	Climate only	Elliot & Arnold (2001)
HMM, KNN, &Wilks	100	43-year	Climate only	Mehrotra *et al*. (2006)
Simple resampling method	20	30-year	Climate only	Räisänen & Ruokolainen (2006)
MMLR	50	40-year	Climate only	Jeong *et al*. (2012)
Improved KNN	50	62-year	Climate only	Steinschneider & Brown (2013)
CLIGEN, LARS-WG, & WeaGETS	50	50-year	Climate only	Mehan *et al*. (2017)
TripleM	30	30-year	Climate only	Breinl *et al*. (2017)
AWE-GEN-2d	50	30-year	Climate only	Peleg *et al*. (2017)
LARS-WG	50	50-year	Climate only	Gitau *et al*. (2018)
CLIGEN, LARS-WG, & WeaGETS	100	50-year	Climate only	Guo *et al*. (2018)
AWE-GEN	100	30-year	Climate only	Kim *et al*. (2018)

Frequently, synthetically generated climate sequences are fed to hydrological models and used thereafter to examine some risk spaces. This study aims to analyze how the accuracy of the estimates of key statistics evolves with the number of realizations of SWGs. Five SWGs were used to generate ensembles of daily precipitation occurrences and amounts (PCP) and daily maximum (Tmax) and minimum (Tmin) temperatures coupled with a hydrological model (SWAT) to simulate streamflow. A variety of diagnostic tools were then applied to identify the optimal number of realizations needed for both the climatic and hydrologic variables.

5.2 Materials and methods

5.2.1 Study area and available hydro-climatic data

The study area is the South Nation Watershed (SNW), located in Eastern Ontario, Canada. The SNW has a relatively flat area of about 4000 km^2 between 74°22′ to 75°43′ W longitude and 44°40′ to 45°38′ N latitude. The watershed is drained by the South Nation River, which runs northeast for 175km towards Plantagenet, with a low topographic gradient of only 80m between its headwaters and the confluence with the Ottawa River. This characteristic maximizes the flood risk and boosts the erosion of riverbanks and agricultural topsoil. Climate data were collected for a 41-year period, based on the availability and consistency of the observed data, between 1971 and 2011 at four metrological stations, namely, Russell Station (Climate Identifier (CI): 6107247, Latitude: 45° 15' 46"N, Longitude: 75° 21' 34"W, Elevation: 76.2m), South Mountain Station (CI: 6107955, Latitude: 44° 58' 00"N, Longitude: 75° 29' 00", Elevation: 84.7m), Morrisburg Station (CI: 6105460, Latitude: 44° 55' 25"N, Longitude: 75° 11' 18"W, Elevation: 81.7m), and St. Albert Station (CI: 6107276, Latitude: 45° 17' 14"N, Longitude: 75° 03' 49"W, Elevation: 80m). In addition, the observed downstream daily discharge data were collected at the Plantagenet Gauging Station (ID: 02LB005, Latitude: 45° 31' 01" N, Longitude: 74° 58' 41" W). There was no missing

data in either dataset for the reference period. A detailed description of the observed hydroclimatic data has been presented previously in Alodah and Seidou (2019a).

5.2.2 Stochastic Weather Generators

The observed 41-year climate series for maximum air temperature, minimum air temperature, and precipitation from the four metrological stations were fed into five SWGs, namely, the WeaGETS implementing multi-Gamma (referred to as *WG* hereafter) and multi-Exponential (referred to as *WE* hereafter) distributions for wet-day sequences (Chen *et al*., 2012), MulGETS implementing multi-Gamma (referred to as *MG* hereafter) and multi-Exponential (referred to as *ME* hereafter) distributions for wet-day sequences (Chen *et al*., 2014), and k-nearest neighbor resampling models (Sharif and Burn, 2007; Goyal *et al*., 2013). WeaGETS, a uni-site weather generator from the École de Technologie Supérieure (ÉTS), is a multivariate parametric model that simulates temperature variables conditional to each other based on a normal distribution and using first-order linear auto-regression coupled with constant lag-1 autocorrelation and cross-correlation. It also considers seasonal cycles with the help of Finite Fourier series with two harmonics. The MulGETS, a multi-site weather generator also from ÉTS, is an extension of WeaGETS and has the ability to take into account the spatial attributes of climate data, which is crucial in most hydrological models. For the simulation of a precipitation occurrence, MulGETS uses a two-state (dry or wet) first-order Markov chain with Cholesky factorization, whereas WeaGETS uses a third-order Markov model without parameter smoothing. A higher-order Markov model is used in WeaGETS since it is recommended for better predicting long dry and wet spells (Bastola *et al*., 2012; Chen *et al*., 2012), whereas a first-order Markov chain is the only option in MulGETS. Both models (WeaGETS and MulGETS) were used twice to simulate the daily wet-day precipitation sequences while implementing two probability distribution functions: a multi-Gamma distribution

(a combination of several gamma distributions) and multi-Exponential distribution. The probability distribution functions (PDFs) of the Gamma and Exponential models are:

$$f_{Gamma}(x) = \frac{(x/\beta)^{\alpha-1}\ exp[-x/\beta\ ]}{\beta\ \Gamma(\alpha)} \quad \textbf{Eq. 5.1}$$

$$f_{Exp}(x) = \lambda e^{-\lambda x} \quad \textbf{Eq. 5.2}$$

The k-nearest neighbor resampling model (*KNN*) is a daily generator that applies different methodologies based on the nonparametric resampling of an observed climate dataset. Since it is nonparametric, KNN has the advantage of being able to generate unprecedented values in the historical period but within the sampled values. For further information, the reader is referred to a previous paper (Alodah and Seidou, 2019a) for a full description of the configurations of the abovementioned stochastic models and their performances.

5.2.3 Rainfall-runoff model

The Soil and Water Assessment Tool (SWAT) is a well-known hydrological model that has been used widely for many applications, including the simulation of sediment and nutrient flow but mainly for streamflow simulations (Neitsch *et al*., 2011). SWAT is a semi-distributed watershed-scale model that relies on hydrologic response units (HRUs) of uniform land and climate characteristics. The SWAT model for this study was first calibrated and validated with the observed climate data using a daily time step and based on the Nash-Sutcliffe efficiency (NSE), the RMSE-observations standard deviation ratio (RSR), and the percent bias (PBIAS). The results of the calibration and validation of the model indicate a good fit between the observed and simulated flows (Metric: *Calibration*, *Validation*; NSE: *0.90*, *0.81*; RSR: *0.31*, *0.43*; PBIAS: *−10.0%*, *−8.3%*). The reader is referred to Alodah and Seidou (2019a) for an enhanced description of the SWAT configuration and parameter selection. Next, synthetic climate time series were fed independently into the SWAT model to generate synthetic daily streamflow time series. To

examine the hydrological responses to various synthetic climate scenarios, all SWAT parameters were kept unchanged except for the climate input when synthetic climate time series replaced the observed ones, enabling the effect of climate variability on hydrological variables to be tracked.

5.2.4 Definitions and notations

For additional clarity, the definitions of some terms used herein are given below:

- ***A realization*** is a random output generated by running a SWG (climate) or the SWAT model with synthetic climate data (streamflow) for a number of years (a 41-yr cycle herein), where all realizations are considered equally plausible for a given SWG (the terms "*realization*", "*run*", and "scenario" are frequently interchangeable in the literature).
- ***A cloud*** is an ensemble of separately-generated realizations (i.e., one thousand herein) of climate (or streamflow) time series generated by running a given SWG (coupled with SWAT) 1000 sperate times.
- ***A sample*** is a set of *N realizations* (for example: a 10-realization sample), where this set of length *N* is reproduced randomly 10,000 times from the cloud.

The following sections provide a more enhanced description of the main steps involved in the integrated framework: (a) the generation of multiple realizations of climate and streamflow data, and (b) the evaluation criteria used to define the number of realizations needed in hydrological simulations. A schematic illustration of the overall modeling framework is presented in Figure 5.1.

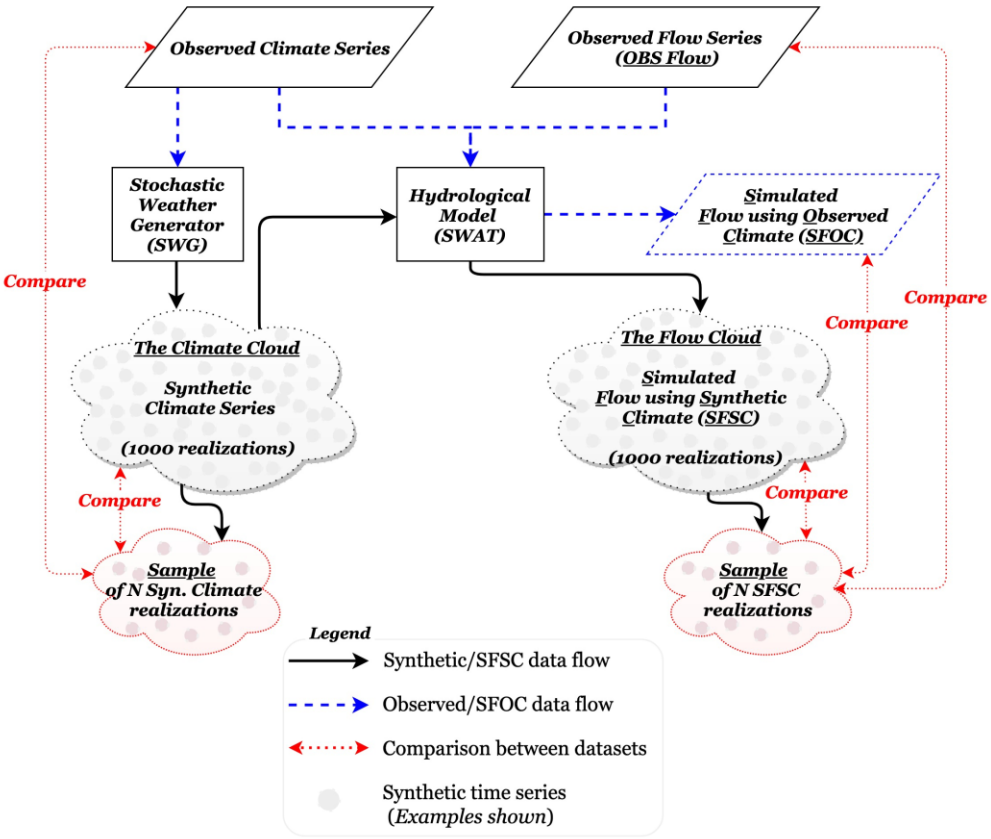

Figure 5.1 Schematic representation of the current work, where *N* ranges from 1 to 1000 unique realizations.

To ease comprehension, the following notations are adopted:

- Index *s* goes from 1 to *S* and represent the metrological stations listed below:

    1. Russell
    2. South Mountain
    3. Morrisburg
    4. St. Albert

    where, *S* is the number of stations (4).

- T is the length in years of all climatic and hydrological time series (41-yr series).
- The observed climate and flow time series are denoted as:

- $PCP_t^{obs,s}$, $t=1,...,T$; $s=1,..,S$, which represents the observed precipitation at time t at meteorological station s
- $Tmax_t^{obs,s}$, $t=1,...,T$; $s=1,..,S$, which represents the observed maximum temperature at time t at meteorological station s
- $Tmin_t^{obs,s}$, $t=1,...,T$; $s=1,..,S$, which represents the observed minimum temperature at time t at meteorological station s
- Q_t^{obs}, $t=1,...,T$, which represents the observed discharge (OBS Flow) at time t at the outlet for the SNW.

- The flow time series at the outlet for the SNW obtained by forcing the SWAT model using observed climate data, called *Simulated Flow using Observed Climate*, is denoted as:
  - $SFOC_t$, $t=1,...,T$.

5.2.5 Climate and flow cloud generation

In this work, 41 years of records (1971-2011) are used for the definitions of the observed climate and streamflow from which the deviations are calculated. While 30 years of weather means comprise the standard definition of a climatic mean, reproduced synthetic precipitation and temperatures data were produced fora 41-year period to permit an adequate risk analysis to be conducted (Semenov and Barrow, 1997; Elliot and Arnold, 2001). Each stochastic model was run 1000 separate times to generate a total of 5000 41-year realizations of weather sequences (matching the length of the observed climate data) at daily temporal resolutions. That is, a total of 205,000 synthetic weather years were generated (5 SWGs *x* 41 yrs *x* 1000 realizations). Similarly, the SWAT model was run 5000 separate times, with each run producing a unique 41-year realization of the climate. The choice of 1000 for the number of realizations for each weather generator, despite the excessive computational demand, particularly for the hydrological modeling, was done in order to form a dense *cloud* of realizations and thus identify a satisfactory number of realizations. The 1000 synthetic time series for precipitation, minimum temperature,

and maximum temperature generated using SWGs and representing the climate at station *s* (referred to as *the climate cloud* hereafter) are denoted:

- $PCP_t^{i,s}$, *t=1,...,T; s=1,.., S for the precipitation time series,*
- $Tmax_t^{i,s}$, *t=1,...,T; s=1,.., S for the maximum temperature time series,*
- $Tmin_t^{i,s}$, *t=1,...,T; s=1,.., S for the minimum temperature time series.*

The 1000 streamflow time series obtained by forcing the SWAT model with the synthetic climate time series (referred to as *the flow cloud* hereafter) are each called *Simulated flow using synthetic climate (SFSC)* and denoted as:

- $SFSC_{t,SWG}^{i}$, *t=1,...,T; i=1,...,1000,* $SWG \in \{ME, MG, WE, WG, KNN\}$.

5.2.6 Estimation of a statistic V using N realizations

The following algorithm is used to estimate a statistic *V* using N realizations. For *k* between 1 and 10,000:

- Sample without repetition from a subset of size N of indices between 1 and 1000, i.e., $\left\{j_1^k, j_2^k, ..., j_N^k\right\}$.
- A *k*th estimate of the mean value of a statistic *V* is,

$$\mu_k = \frac{1}{N}\sum_{m=1}^{N}\left(\frac{\sum_{t=1}^{T} V_t^{j_m,s}}{T}\right) \qquad \textbf{Eq. 5.3}$$

The more variability in $\{\mu_k\}, k = 1,...,10000$, the less precise the estimate. The variability in these estimated means can be illustrated using a boxplot graph. The deviations from Y_{ref} quantify the biases of the estimates.

5.2.7 Evaluation criteria

Given that a series of samples generated by the SWGs will not be identical, the impact of such variations between the samples is investigated visually using time series graphs of the simulated sequences, such as sequence plots, running mean plots, and boxplots of the samples at a certain number of realizations, following the methodology presented by Guo *et al.* (2018).

5.2.7.1 Visual convergence assessment

An examination using proper graphical techniques can produce a general idea concerning the variable of interest (Ott and Longnecker, 2015). Plots of each parameter and the running mean are used to examine the simulation process as the number of realizations increases. A time series plot of the running mean is simple and easy to implement and used to check when a new stochastic generation of flow data is no longer deviating significantly from the mean of previous realizations. The running mean is computed as the mean of all sampled values up to and including the current realization. The plot then shows whether the running mean stabilizes at a realization (randomly ordered) against the mean of all realizations (Smith 2007). These plots will eventually converge to a constant value, which is the mean of all realizations according to the Central Limit Theorem. These visual evaluations should provide general insights, yet they are not sufficient indicators and further statistical analyses must be conducted.

5.2.7.2 Quantitative assessment

The four key statistics to be estimated from the time series are the mean (μ), standard deviation (σ), and the skewness (α_3) and kurtosis (α_4) coefficients of the climate or flow variable of interest. For the sake of simplicity, Y will be used herein to indicate any of the estimates of the above statistics. The statistical measures considered are the Relative Error (RE) and the Relative

Root Mean Squared Error ($RMSE_r$). The relative error (RE) refers to the magnitude of the difference between an experimental (sample) value (Y_i) and the known or accepted value (Y_{ref}):

$$\text{RE}(\%) = \left(\frac{Y_{ref} - Y_i}{Y_{ref}}\right) \text{X } 100 \qquad \textbf{Eq. 5.4}$$

The root mean squared error (RMSE), also called root-mean-square deviation, is one of the most common metrics used to measure the accuracy of continuous variables via measuring the average magnitude of the error. It is a negatively-oriented score that has a range between 0 to ∞, meaning that values closer to 0 are preferable. This metric is particularly useful when a large error cannot be tolerated, as the errors are squared when computing it. The RMSE and relative RMSE ($RMSE_r$) are computed as:

$$RMSE = \sqrt{\frac{1}{KN}\sum_{j=1}^{K}\sum_{i=1}^{N}(Y_{ref} - Y_j)^2} \qquad \textbf{Eq. 5.5}$$

$$RMSE_r(\%) = \left(\frac{RMSE}{Y_{ref}}\right) X\ 100, \qquad \textbf{Eq. 5.6}$$

where $\hat{Y}_i$ and Y_m are, respectively, the sample and accepted (cloud) means from the training set, and n is the number of samples in the set of data being examined. The improvement in the $RMSE_r$ value obtained by adding one more realization ($RMSE_{r,\ improvement}$) and the marginal improvement ($RMSE_{r,\ mar.\ improvement}$) are defined as:

$$RMSE_{r,\ improvement} = RMSE_{r,n-1} - RMSE_{r,n} \qquad \textbf{Eq. 5.7}$$

$$RMSE_{r,\ mar.\ improvement} = RMSE_{r,n=1} - RMSE_{r,n}, \qquad \textbf{Eq. 5.8}$$

where n=2, 3, …., *N*, and *N*=1000.

For any given statistic, several reference statistics can be used to calculate both the RE and the RRMSE. The three reference values for the key *climate* statistics are:

- The statistics calculated from observations ($V_{ref,Y,OBS}$), and
- The average of the statistics calculated from the 1000 realizations in the synthetic climate ($V_{ref,Y,SC}$).

The three reference values for the key *flow* statistics are:

- The estimates of statistics V calculated with observations, denoted by ($V_{ref,OBS}$);
- The estimates of statistics V calculated from the time series simulated via SWAT using the observed climate, denoted by ($V_{ref,SFOC}$); and
- The average of statistics V calculated from the 1000 realizations in the flow cloud, denoted by ($V_{ref,SFSC}$).

5.3 Results and discussion

The results are presented and discussed in two parts: first, a visual assessment of the synthetically generated climate and flow time series is presented using graphical methods. Second, the effect of the number of SWGs realizations on the accuracy of basic annual climatic indices is assessed. Variability is presented via boxplots and graphics of the running mean, the RMSEr, and the RE, where the x-axis in each case represents the number of realizations, which goes from 1 to 1000. The same analysis is performed for each climate and flow variable, each performance index, and each reference value.

5.3.1 Visual convergence assessment

Figures 5.2 and 5.4 show that the mean annual precipitation estimated via the MulGETS and WeaGETS realizations is reasonably close to the mean of observed values ($\mu_{ref,\,PCP,\,OBS}$), but that the observed values are underestimated by KNN. However, the WeaGETS models (WE and WG) and KNN underestimated the standard deviation $\sigma_{ref,\,PCP,OBS}$ of the annual precipitation, while both the MulGETS models (ME and MG) were able to capture σ adequately (Figure 5.2). The kurtosis

coefficients for the synthetic annual precipitation were consistently higher than those for the observed precipitation (Figure 5.2). Thus, the results are consistent with the findings of Chen and Brissette (2014), who reported that the kurtosis coefficient of the mean annual precipitation is poorly reproduced by SWGs. The differences among the five models in terms of generating α_3 for the synthetic annual precipitation were not notable.

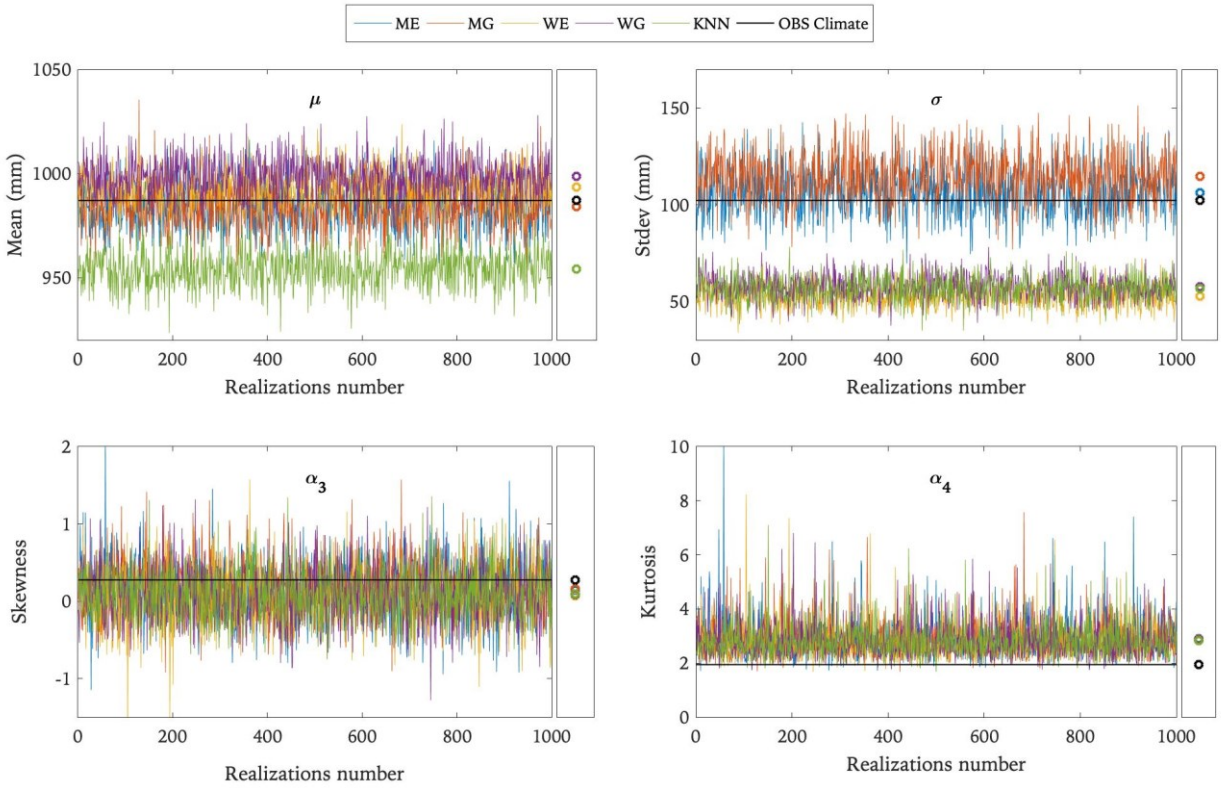

Figure 5.2 Plots of the *precipitation* statistics generated by five SWGs, where the observed climate values are indicated by the black lines. The mean values of all realizations are shown in the side boxes.

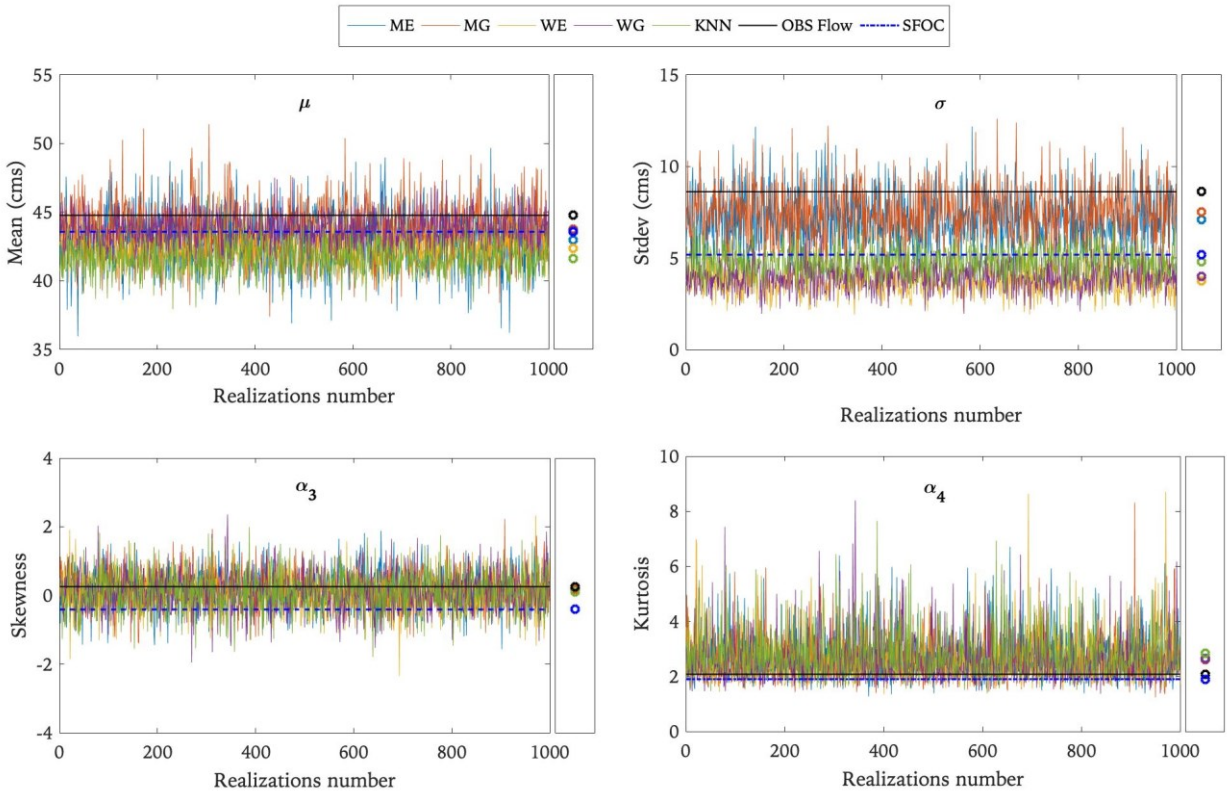

Figure 5.3 Plots of mean annual streamflow statistics generated by five SWGs. The observed flow and SFOC values are shown by the black and blue dashed lines, respectively. The mean values of all realizations are shown in the side boxes and compared to reference data.

The interannual σ's of $SFSC_{WE}$ and $SFSC_{WG}$ were underestimated compared to the observed flow and –to a lesser degree– the SFOC (Figure 5.3). The inter-annual variability of $SFSC_{KNN}$ closely matched that of SFOC, while $SFSC_{ME}$ and $SFSC_{MG}$ were between the two reference datasets (mostly underestimated the observed flow but overestimated the SFOC). Interestingly, the *SFSC*s of all SWGs performed similarly in well reproducing the α_3 of the OBS Flow and overestimating the α_3 of the SFOC. Similar to precipitation results, the poor performance (overestimation) of most outputs of the tested SWGs in replicating the α_4 of the annual streamflow was observed when compared to both the OBS Flow and SFOC data (Figure 5.3). In general, it is fairer to compare the

SFSC to the SFOC than to the observed flow, as the first two were both simulated by SWAT and inherited the biases within the model itself.

The annual precipitation and streamflow statistics are plotted as a function of the number of realizations in Figures 5.4 and 5.5. The running mean plots demonstrate the mean of previous realizations up to and including each iteration displayed on the x-axis. Such figures show how the running mean highly fluctuates at the beginning of the sequence, making it difficult to construct robust confidence intervals. The statistics for the outputs of the five weather generators, however, do not differ much after 100 realizations. That is, almost all parameter estimates appear to stabilize around 100 realizations. Biases caused by the stochastic generation of the cloud are clearly outweighed eventually by the increased number of realizations, as stated in Räisänen and Ruokolainen (2006).

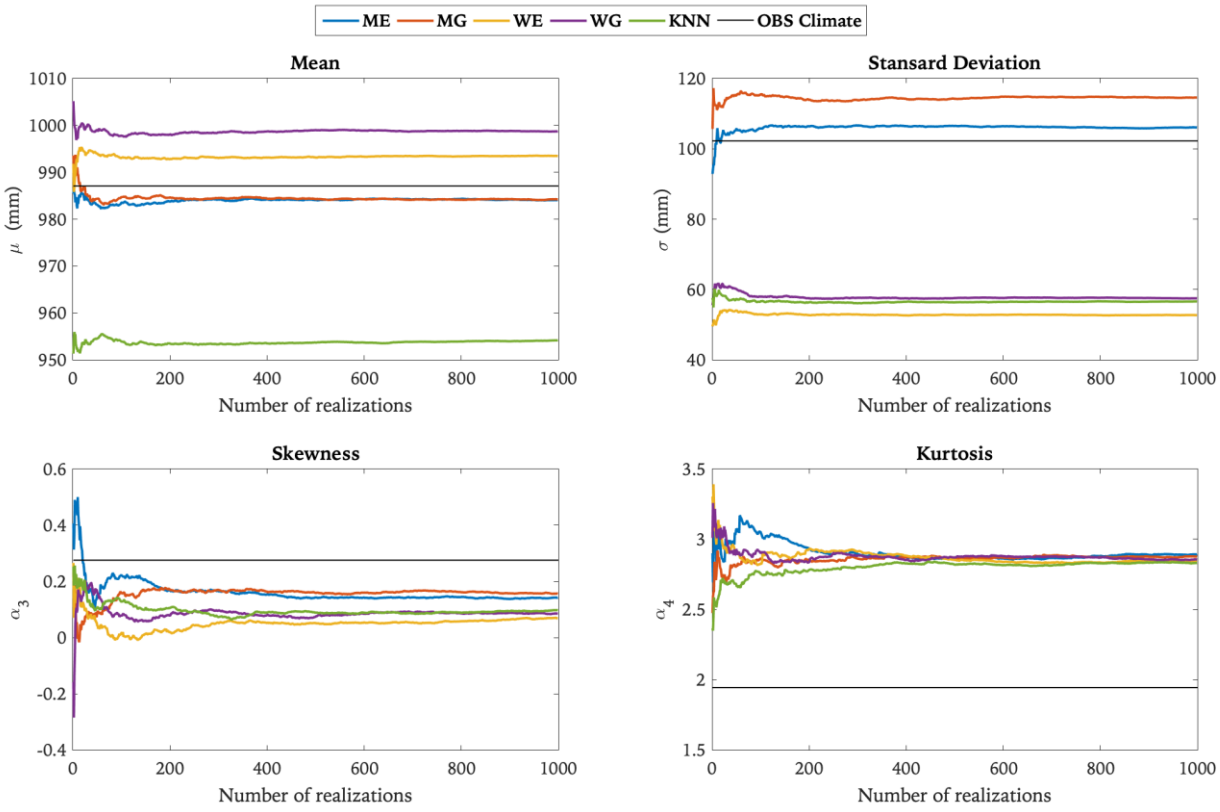

Figure 5.4 Running mean plots for the mean annual **precipitation** statistics generated by five SWGs in which the order of the realizations is random. The black dashed lines indicate the observed climate values.

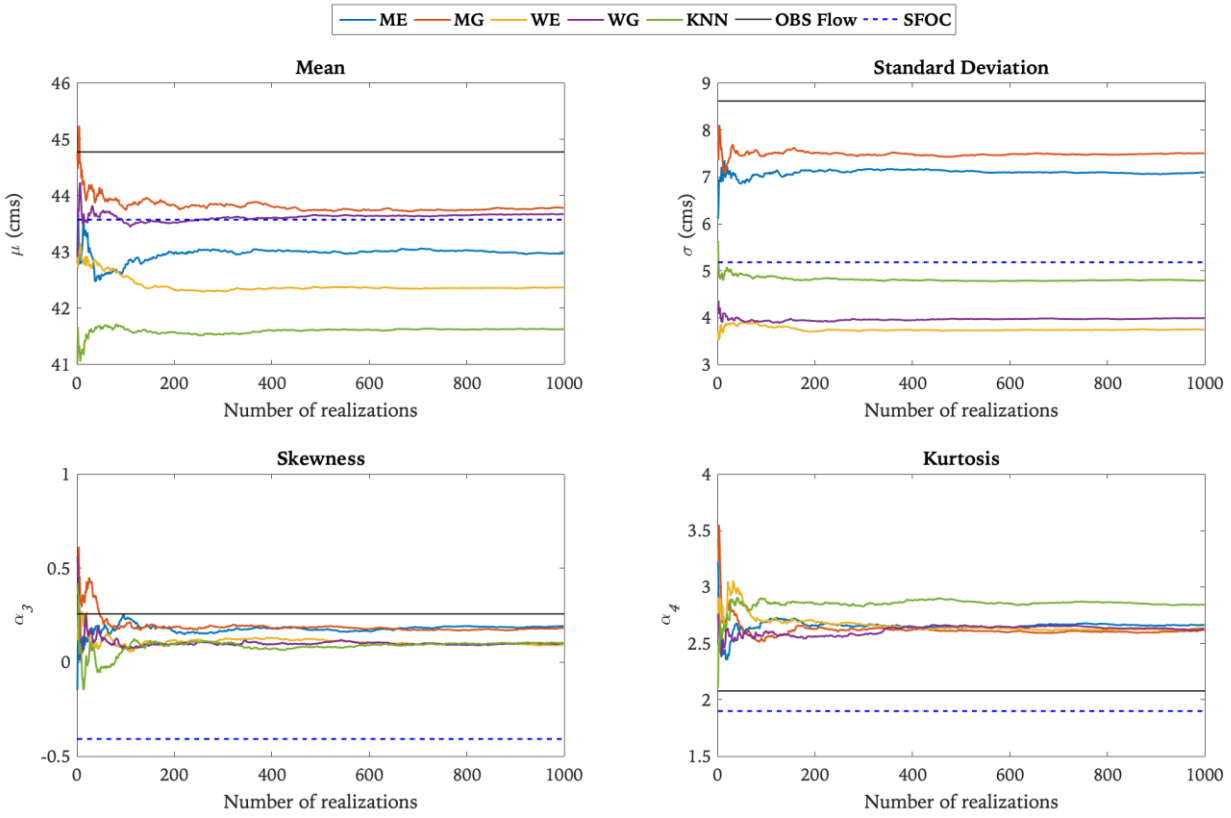

Figure 5.5 Running mean plots for the annual **streamflow** statistics generated by five SWGs in which the order of the realizations is random. The observed flow (SFOC) values are represented by the black (blue dashed) lines.

5.3.2 Variations in the spread, RMSEr's, and REs for key statistics as a function of the number of realizations

5.3.2.1 Climate space

As explained in the methodology section, the spread of the estimates was visualized using boxplots. As expected, the variability in each of the indicators decreases as the number of realizations increases (Figures 5.6, 5.7, and 5.8). The use of a single realization is obviously not recommended due to the high error expected, particularly for applications that depend heavily on higher moments, such as an assessment of extremes. For instance, the precision when estimating the α_3 of the annual precipitation using one realization can be off by more than 500%. Once the

number of realizations increases, the expected error decreases dramatically. This decrease in the expected error is particularly clear for higher moments at 25 realizations and higher. Moreover, the use of more than 100 realizations seems very unnecessary.

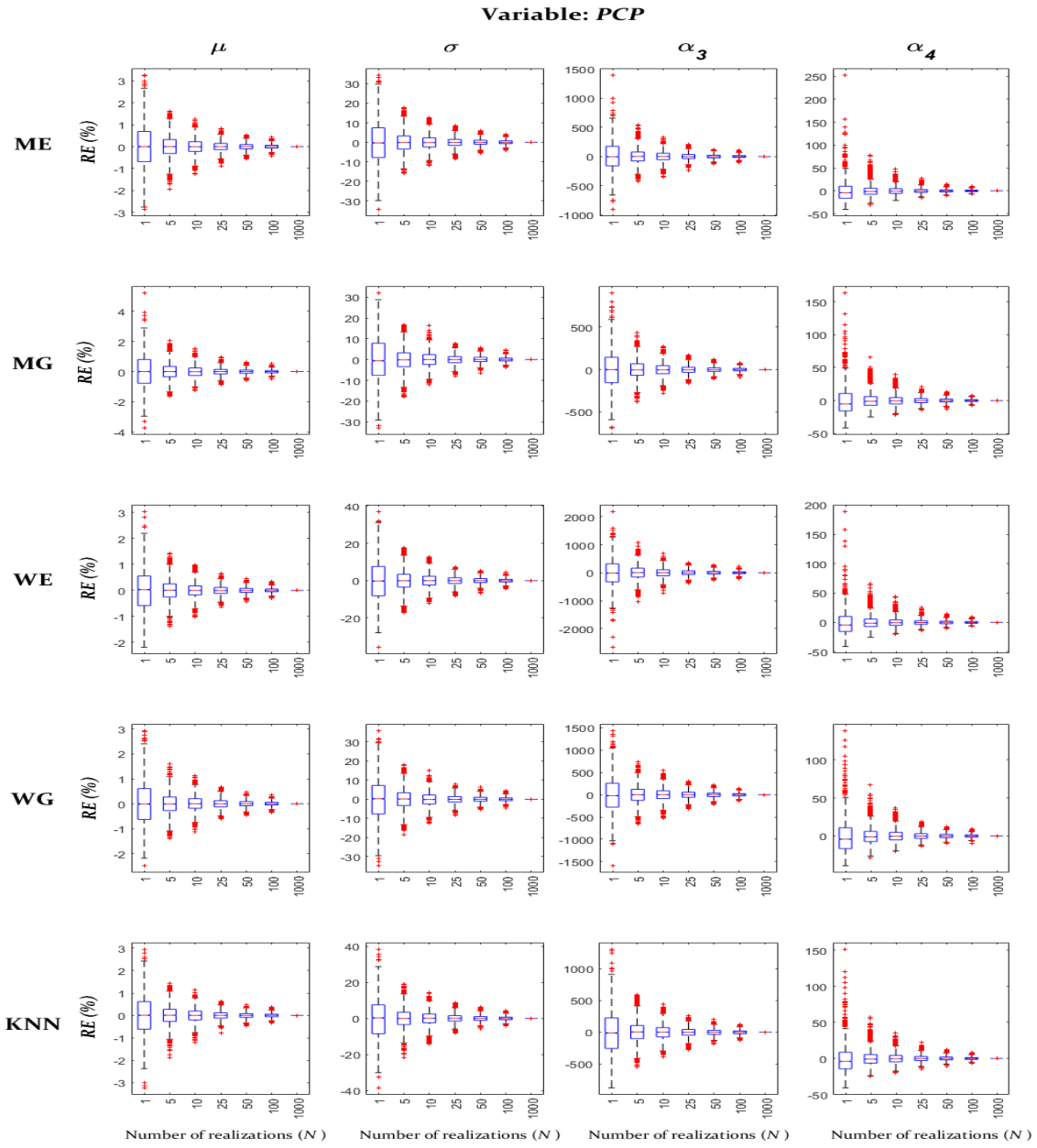

Figure 5.6 Boxplots of the relative errors (%) of the main *annual* precipitation statistics for the *N*-realization samples used to estimate these statistics from the cloud; an *N-realization* sample is derived from 10,000 different randomly selected sets, with the symbol "+" indicating outliers.

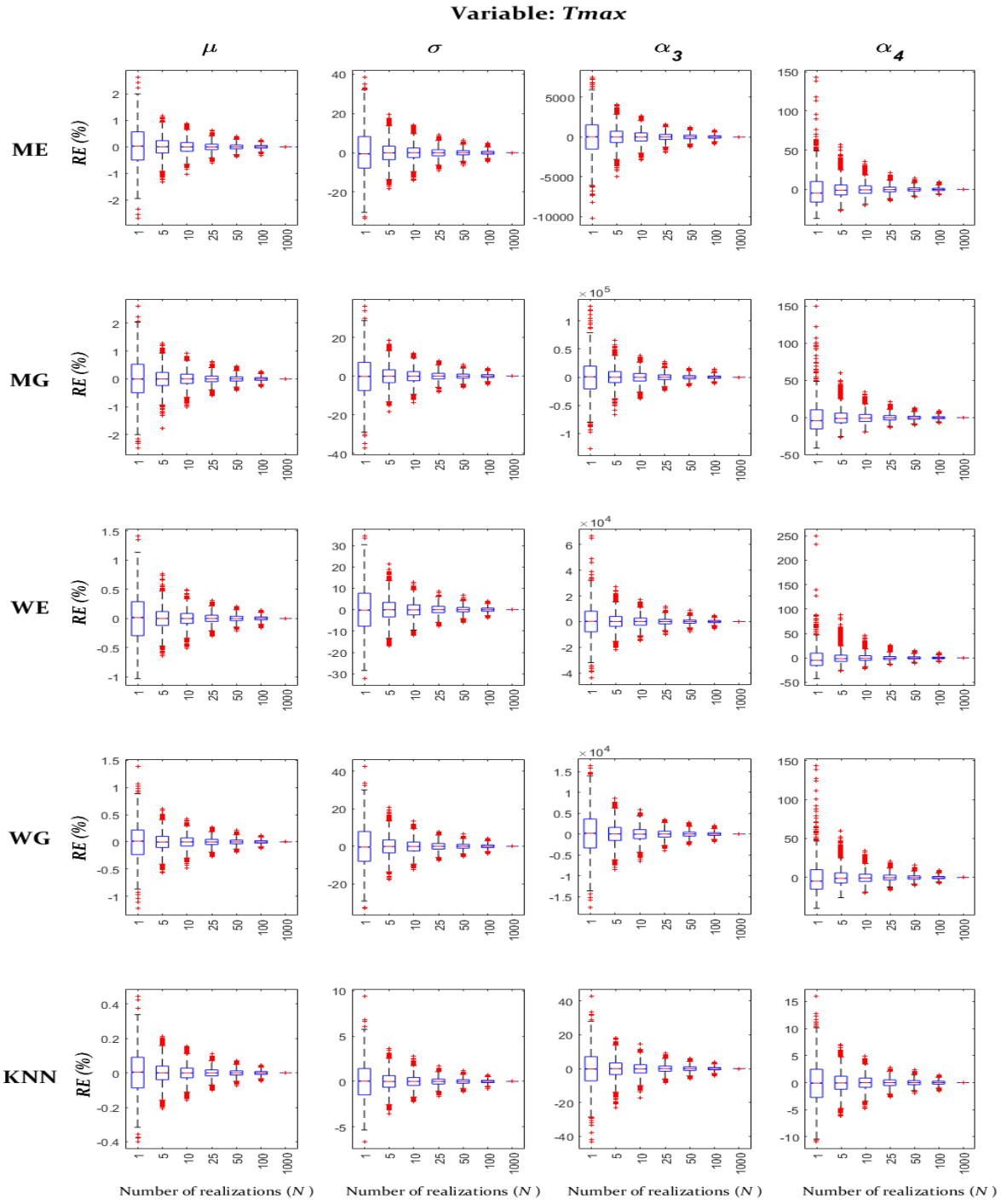

Figure 5.7 Boxplots of the relative errors (%) of the main *annual* maximum temperature statistics for the *N*-realization samples used to estimate these statistics from the cloud; an *N-realization* sample is derived from 10,000 different randomly selected sets, with the symbol "+" indicating outliers.

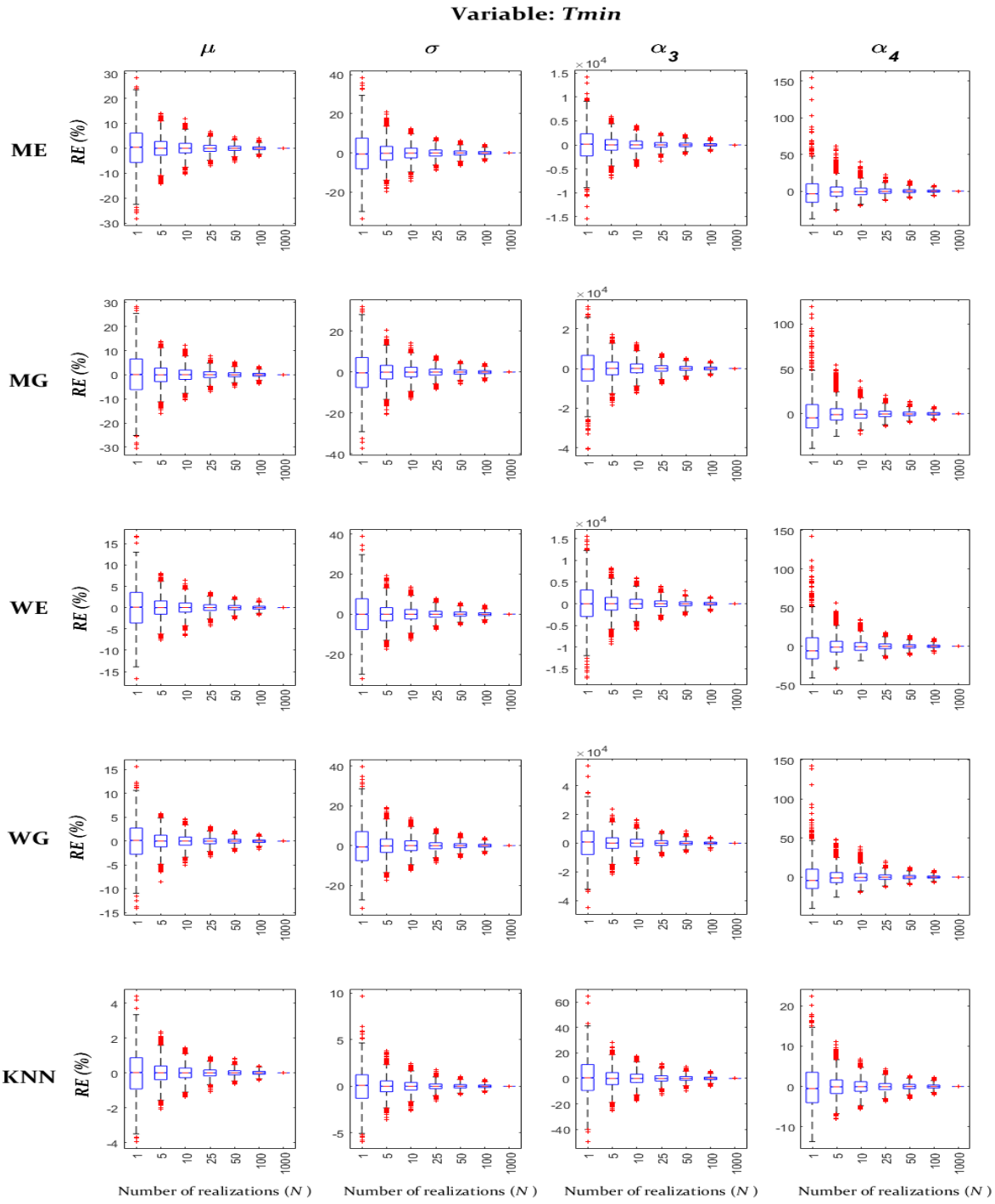

Figure 5.8 Boxplots of the relative errors (%) of the main *annual* minimum temperature statistics for the *N*-realization samples used to estimate these statistics from the cloud; an *N-realization* sample is derived from 10,000 different randomly selected sets, with the symbol "+" indicating outliers.

The marginal improvements in the RMSEr's of PCP, Tmax, and Tmin as the number of realizations increases are shown respectively in Figures 5.9, 5.10, and 5.11, where the synthetic climate using *N* realizations (relative to using *N-1* realizations) is compared to the two reference datasets: the climate cloud (synthetic climate) and the observed climate. Tables 5.2, 5.3, and 5.4 present a similar comparison for the three climate variables but relative to results of just a single realization. These results are consistent with the previous findings suggesting that after 100 realizations, the marginal improvement in the RMSEr becomes insignificant (e.g., less than a 0.21 (1.09)% improvement across SWGs in μ_{Tmax} (σ_{Tmax}) when adding 900 realizations). Also, 25 realizations appear to be reasonably adequate, particularly for the first two moments (e.g., less than a 0.46 (2.34)% improvement across SWGs in μ_{Tmax} (σ_{Tmax}) when adding 975 realizations). The results are very similar for the temperature variables, whereas precipitation indicators require even fewer realizations.

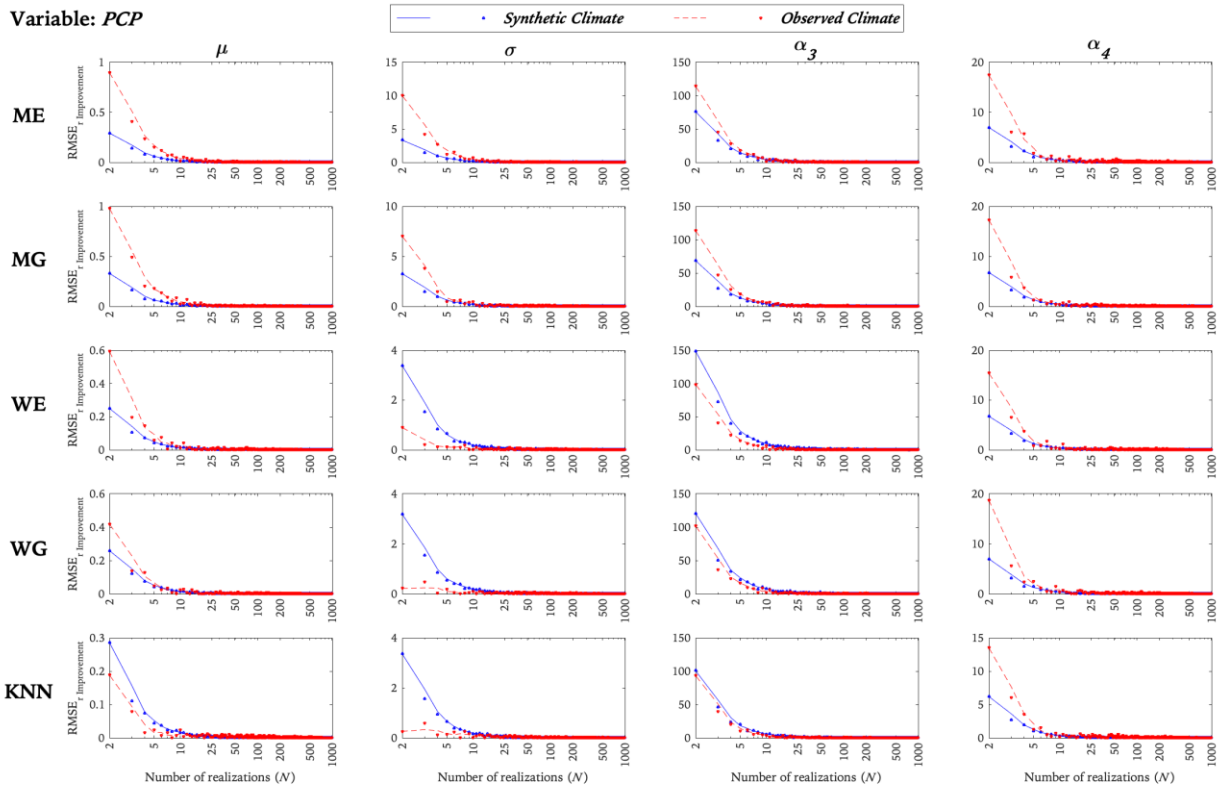

Figure 5.9 The improvement in the *RMSEr's* of the main annual precipitation statistics for the *N*-realization samples generated by the five SWGs versus the counterparts generated by two time series: the synthetic and observed climates. The *N*-realization samples are derived from 10,000 different randomly selected sets. Scattered markers represent actual results for which the lines are slightly smoothed by moving averages with spans of 3.

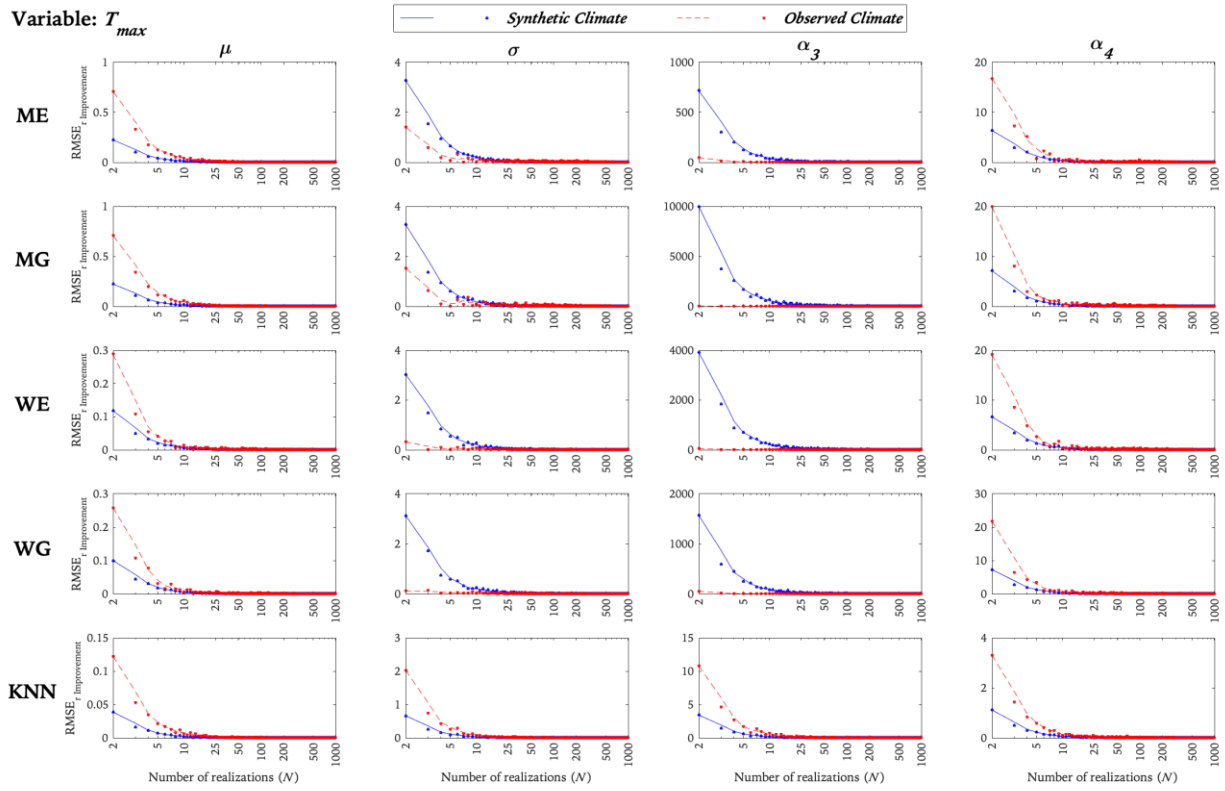

Figure 5.10 The improvement in the *RMSEr's* of the main annual maximum temperature statistics for the *N*-realization samples generated by the five SWGs versus the counterpart generated by two time series: the synthetic and observed climates. The *N*-realization samples are derived from 10,000 different randomly selected sets. Scattered markers represent actual results for which the lines are slightly smoothed by moving averages with spans of 3.

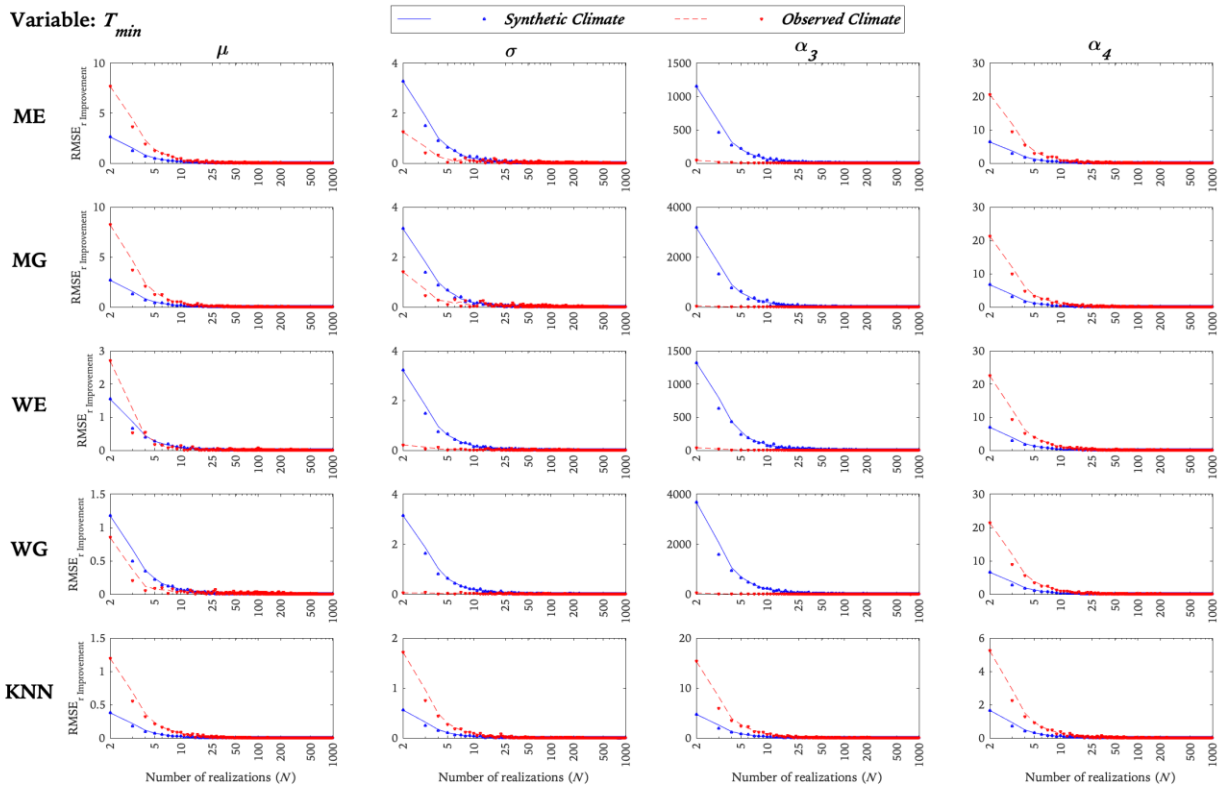

Figure 5.11 The improvement in the *RMSEr's* of the main annual minimum temperature statistics for the *N*-realization samples generated by five SWGs versus the counterparts generated by two time series: the synthetic and observed climates. The *N*-realization samples are derived from 10,000 different randomly selected sets. Scattered markers represent actual results for which lines are slightly smoothed by moving averages with spans of 3.

5.3.2.2 Hydrological space

For the streamflow data, Figure 5.12 presents the REs of the key annual streamflow statistics, including the mean, standard deviation, skewness, and kurtosis. The variability of each RE as a function of different numbers of realizations (1, 5, 10, 25, 50, 100, and 1000) is represented using boxplots, each of which is based on ten thousand *N*-realization samples randomly taken from the cloud containing all SFSC time series. Figure 5.12 clearly confirms that a sole realization is not

sufficient for representing SWGs in hydrological modeling. Similar to the situation for the climate variables, 100 realizations seem very adequate, with very low relative errors across different statistics.

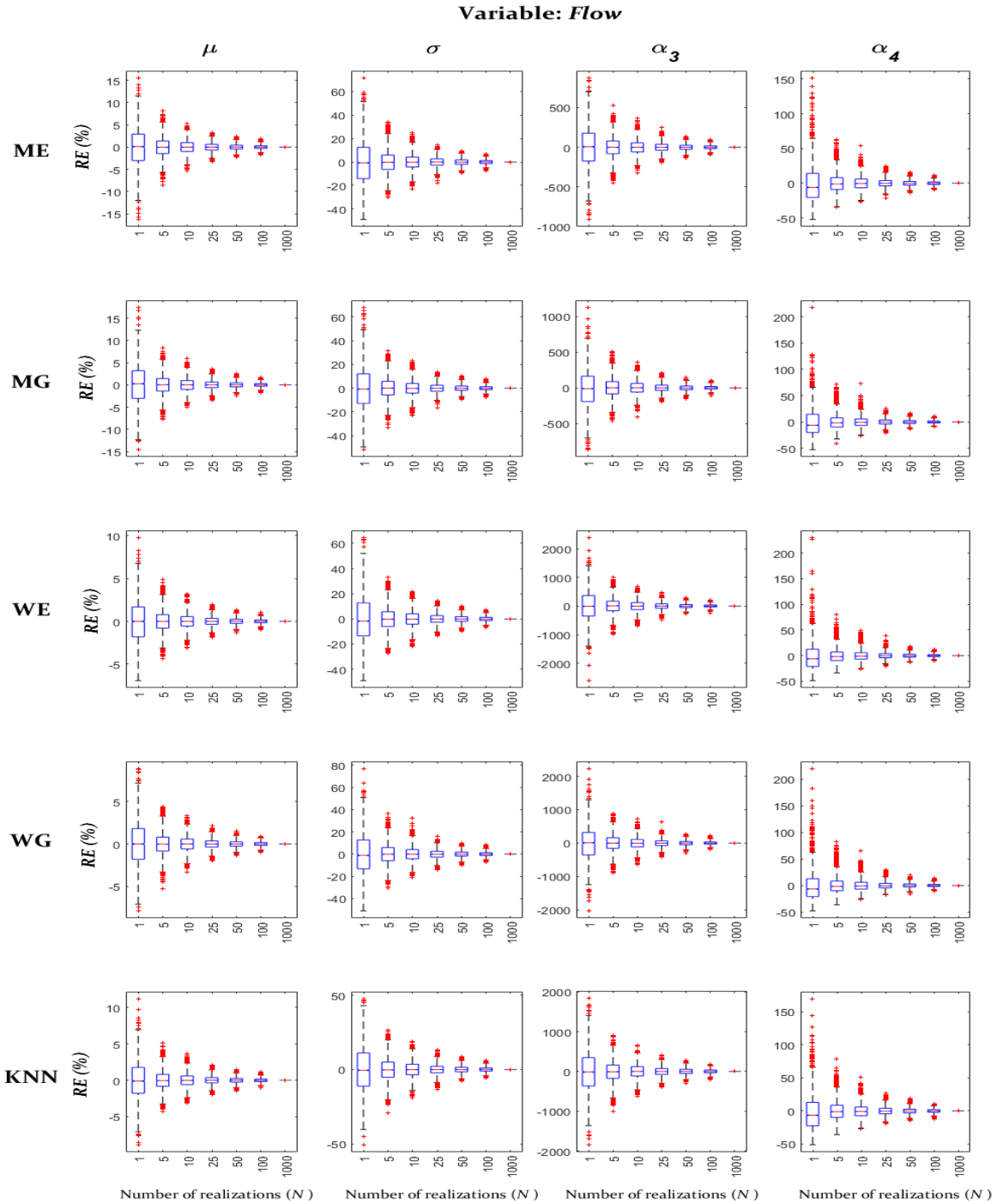

Figure 5.12 Boxplots of the relative errors (%) of the main *annual* streamflow statistics for the *N*-realization samples used to estimate these statistics from the cloud; an *N-realization* sample is derived from 10,000 different randomly selected SFSC sets, with the symbol "+" indicating outliers.

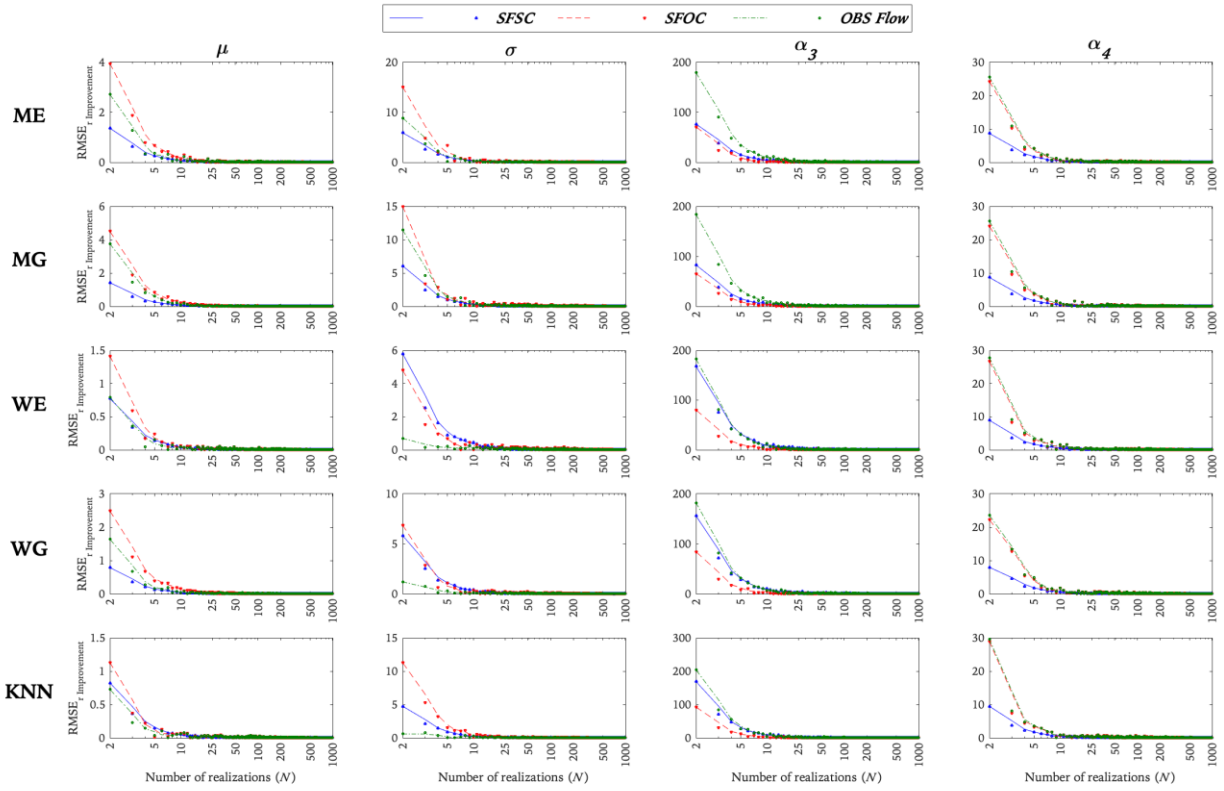

Figure 5.13 The improvement in the *RMSEr's* of the main annual streamflow statistics of the *N*-realization samples generated by five SWGs versus the counterparts generated by three datasets: the simulated flow using a synthetic climate (SFSC), simulated flow using the observed climate (SFSC), and observed flow (OBS Flow). The *N-realization* SFSC sample is derived from 10,000 different randomly selected SFSC sets. Scattered markers represent actual results for which lines are slightly smoothed by moving averages with spans of 3.

The marginal improvements in the RMSEr's of the streamflow statistics are plotted in Figure 5.13, and Table 5.5 lists these improvements as functions of the number of realizations. In Figure 5.13, the estimates are compared to the three reference values (SFSC, SFOC, and OBS Flow). In Table 5.5, the estimate is compared to the estimate obtained using a single realization. The results are consistent with the previous findings, which suggest that after 100 realizations, the marginal improvement in the RMSEr becomes insignificant (e.g., less than a 0.55% improvement for all three reference datasets and across all SWGs for μ when compared to the μ calculated from 1000 realizations). Also, 25 realizations appear to be reasonably adequate, particularly for the first two moments (e.g., less than a 1.78% improvement for all three reference datasets and across the SWGs for μ when compared to the μ calculated from 1000 realizations).

5.3.3 Discussion

The main finding of this work is that, while a larger number of realizations provides a better representation of climate variability, the use of a limited number of realizations can provide robust estimates of key risk statistics. In this particular application, the marginal improvements in the RMSEr's of all statistics (climatic and hydrological variables) are not substantial after 25 realizations, particularly for the first two moments (i.e., μ and σ) and to a lesser extent for higher moments (i.e., α_3 and α_4). The findings also demonstrate that going beyond 100 realizations is unnecessary, as the improvement afterward is very minimal even for higher moments.

An interesting finding is that there are systematic biases contained within the weather generators that lead to the SFSC and SFOC to be different from the OBS Flow. Additionally, increasing the number of realizations cannot reduce these biases. That is, repeated runs of a given SWG that tends to misestimate a particular variable will not be useful in obtaining a correct characterization of the observed variable. A few ways to decrease such biases include improving the SWGs, selecting an

SWG with minimal bias, and/or improving the rainfall-runoff model. Alternatively, one can consider generating a large dataset of realizations and then select a number of realizations that better represents the observed set, as suggested by Gitau *et al*. (2018). However, the latter approach still presents a challenge, as it can be a computationally expensive and time-consuming process. The simplest of these solutions is to use the methodology presented herein to select the number of realizations that leads to an acceptable RMSEr or RE for the problem at hand. Alternative methods for assessing SWGs include statistical tests of significance, such as the t-test and F-test (e.g., Min *et al*., 2011, Chen and Brissette, 2014); χ^2 goodness-of-fit test (e.g., Semenov *et al*., 1998); nonparametric tests, such as the Wilcoxon rank-sum test, the Kolmogorov–Smirnov (K–S) test, and Mann–Whitney test (e.g., Zhang and Garbrecht, 2003; Qian *et al*., 2004; Chen *et al*., 2010); the RMSEs of various statistics of interest (e.g., Mehrotra *et al*., 2006); measures of effect size, such as Cohen's *d* metric (e.g., Mehan *et al*., 2017); and employing distance techniques, such as the Mahalanobis distance between statistics derived from observations and simulations (e.g., Alodah and Seidou, 2019a).

One limitation of the present work is that the results are specific to a particular hydrological model on a particular watershed and to particular SWGs. However, the methodology can be applied to any case in which weather generators are screened and the number of realizations just enough for the variable of interest is selected, for saving time and computational resources. The current application required 5,000 runs (scenarios) of the SWAT model, and the computation time required to complete these scenarios was almost a month on a typical desktop computer workstation (Intel Core i7-4790 Processor @ 3.60GHz (8 CPUs), 16GB (2x8GB) RAM, 1TB disk), exclusive of the subsequent time spent in the post-processing of the output.rch files using a MATLAB code. The time involved could even be higher for larger watersheds or a longer simulation period. Thus, the

use of an adequately representative number of realizations, as determined herein, can minimize the computational challenge and reduce the simulation time significantly without losing much information (e.g., it would take less than a day for 25 realizations on a 3.60GHz Intel Core i7 CPU with a 16GB RAM machine). Furthermore, the methodology presented in this paper has the advantage of making a straightforward link between the number of realizations and common statistical indicators and is more likely to appeal to practitioners.

It can also be argued that other risk parameters, such as high quantiles of flow, and hydrological parameters, such as sediments, would perform differently. Therefore, the results of this work can be further extended to include such parameters. It is believed also that this domain can be further explored by incorporating more hydrological models since the results may vary when applying different algorithms to generate streamflow time series, perhaps in such a way as to be of use in different climate-sensitive decision contexts.

5.4 Conclusions

The required number of realizations of five SWGs, each coupled with a SWAT model, are used to generate multiple time series for four hydroclimatic variables at four climatic stations and one hydrometric station on the South Nation Watershed located in Ontario, Canada. The investigated variables are precipitation, maximum and minimum air temperature, and streamflow. Four risk and performance indicators, namely, the mean, standard deviation, skewness, and kurtosis of these variables were estimated using both synthetic time series and observations. The number of realizations required to reach a predefined Relative Root Mean Square Error is then investigated. Using the two error metrics, namely, *RE* and *RMSE*, it was shown that when the number of realizations is high, the considered five weather generators perform somewhat similarly in terms of reproducing the risk and performance indicators. Overall, the results indicate that there is no

very major benefit from generating more than 25 realizations in hydrological modeling. Applications requiring more precision (e.g., analysis of hydro-climatic extreme events) can use 100 realizations, as the results obtained from 100 realizations are not notably different from those obtained using 1000 realizations. Adopting a small, but carefully chosen, number of realizations can reduce the computational time and resources needed significantly and therefore benefit a larger audience, particularly when high-performance machines are not easily accessible.

5.5 References

Ailliot, P., Allard, D., Monbet, V., & Naveau, P. (2015). Stochastic weather generators: an overview of weather type models. *Journal de la Société Française de Statistique*, *156*(1), 101-113.

Al-Mukhtar M, Dunger V, Merkel B (2014) Evaluation of the climate generator model CLIGEN for rainfall data simulation in Bautzen catchment area, Germany. Hydrol Res 45(4–5):615–630

Alodah, A., & Seidou, O. (2019a). The adequacy of stochastically generated climate time series for water resources systems risk and performance assessment. *Stochastic environmental research and risk assessment*, *33*(1), 253-269.

Alodah, A., & Seidou, O. (2019b). Assessment of Climate Change Impacts on Extreme High and Low Flows: An Improved Bottom-Up Approach. *Water*, *11*(6), 1236.

Anyah, R. O., & Semazzi, F. H. M. (2006). Climate variability over the Greater Horn of Africa based on NCAR AGCM ensemble. *Theoretical and applied climatology*, *86*(1-4), 39-62.

Apipattanavis, S., Bert, F., Podestá, G., & Rajagopalan, B. (2010). Linking weather generators and crop models for assessment of climate forecast outcomes. *Agricultural and forest meteorology*, *150*(2), 166-174.

Baffault, C., Nearing, M.A., Nicks, A.D., 1996. Impact of CLIGEN parameters on WEPP-predicted average annual soil loss. Transactions of the ASAE 39 (2), 447–457.

Bastola, S., Murphy, C., & Fealy, R. (2012). Generating probabilistic estimates of hydrological response for Irish catchments using a weather generator and probabilistic climate change scenarios. *Hydrological processes*, *26*(15), 2307-2321.

Breinl, K., Di Baldassarre, G., Girons Lopez, M., Hagenlocher, M., Vico, G., & Rutgersson, A. (2017). Can weather generation capture precipitation patterns across different climates, spatial scales and under data scarcity? Sci Rep, 7(1), 5449.

Brown, C., Werick, W., Leger, W., & Fay, D. (2011). A Decision-Analytic Approach to Managing Climate Risks: Application to the Upper Great Lakes 1. *JAWRA Journal of the American Water Resources Association*, *47*(3), 524-534.

Candela, L., Tamoh, K., Olivares, G., & Gomez, M. (2012). Modelling impacts of climate change on water resources in ungauged and data-scarce watersheds. Application to the Siurana catchment (NE Spain). *Science of the total environment*, *440*, 253-260.

Caron A, Leconte R, Brissette F (2008) An improved stochastic weather generator for hydrological impact studies. Can Water Resour J 33:233–256

Chen J, Brissette FP, Leconte R, Caron A (2012) A versatile weather generator for daily precipitation and temperature. Trans ASABE 55(3):895–906

Chen JF, Brissette X, Zhang J (2014) A multi-site stochastic weather generator for daily precipitation and temperature. *Trans ASABE* 2014:1375–1391. https://doi.org/10.13031/trans.57.10685

Chen, J. and Brissette, F.P. (2014). Comparison of five stochastic weather generators in simulating daily precipitation and temperature for the loess plateau of China. *International Journal of Climatology*, *34*(10): 3089-3105

Chen, J., & Brissette, F. P. (2014). Comparison of five stochastic weather generators in simulating daily precipitation and temperature for the Loess Plateau of China. *International Journal of Climatology*, *34*(10), 3089-3105.

Chen, J., Brissette, F. P., & Leconte, R. (2010). A daily stochastic weather generator for preserving low-frequency of climate variability. *Journal of hydrology*, *388*(3-4), 480-490.

Deser, C., A. Phillips, V. Bourdette, and H. Teng (2012), Uncertainty in climate change projections: The role of internal variability, Clim. Dyn., 38(3), 527–546, doi:10.1007/s00382-010-0977-x.

Dubrovský, M., Buchtele, J., & Žalud, Z. (2004). High-frequency and low-frequency variability in stochastic daily weather generator and its effect on agricultural and hydrologic modelling. *Climatic Change*, *63*(1-2), 145-179.

Eames M, Kershaw T, Coley D (2012) A comparison of future weather created from morphed observed weather and created by a weather generator. *Build Environ* 56:252–264

Elliot W, Arnold C (2001) Validation of the weather generator CLIGEN with precipitation data from Uganda. Trans ASAE 44:53–58

Fatichi, S., V. Y. Ivanov, A. Paschalis, N. Peleg, P. Molnar, S. Rimkus, J. Kim, P. Burlando, and E. Caporali (2016), Uncertainty partition challenges the predictability of vital details of climate change, Earth's Future, 4(5), 240–251, doi:10.1002/2015EF000336.

Fodor, N., Dobi, I., Mika, J. and Szeidl, L. (2013). Applications of the MVWG multivariable stochastic weather generator. The Scientific World Journal, doi: 10.1155/2013/571367

Furrer, E. M., & Katz, R. W. (2008). Improving the simulation of extreme precipitation events by stochastic weather generators. *Water Resources Research*, *44*(12).

Gabriel, K.R.; Neumann, J. (1962) A Markov chain model for daily rainfall occurrence at Tel Aviv. *Q. J. R. Meteorol. Soc. 88*, 90–95.

Gitau, M. W., Chiang, L. C., Sayeed, M., & Chaubey, I. (2012). Watershed modeling using large-scale distributed computing in Condor and the Soil and Water Assessment Tool model. *Simulation*, *88*(3), 365-380.

Gitau, M. W., Mehan, S., & Guo, T. (2017). Weather generator utilization in climate impact studies: implications for water resources modeling. *Eur Water. Accepted*, *5*.

Gitau, M. W., Mehan, S., & Guo, T. (2018). Weather generator effectiveness in capturing climate extremes. *Environmental Processes*, *5*(1), 153-165.

Goyal MK, Burn DH, Ojha CSP (2013) Precipitation simulation based on k-nearest neighbor approach using gamma kernel. J Hydrol Eng 18:481–487

Guenni, L. (1994). Spatial interpolation of the parameters of stochastic weather models. *Climate Change, Uncertainty and Decision Making, Institute for Risk Research, University of Waterloo, Ontario and IGBP-BAHC, Berlin*, 61-79.

Guo, T., Mehan, S., Gitau, M. W., Wang, Q., Kuczek, T., & Flanagan, D. C. (2018). Impact of number of realizations on the suitability of simulated weather data for hydrologic and environmental applications. *Stochastic environmental research and risk assessment*, *32*(8), 2405-2421.

Hansen JW, Ines AV (2005) Stochastic disaggregation of monthly rainfall data for crop simulation studies. Agric For Meteorol 131:233–246

Ivanov, V. Y., Bras, R. L., & Curtis, D. C. (2007). A weather generator for hydrological, ecological, and agricultural applications. *Water resources research*, *43*(10).

Jeong, D. I., St-Hilaire, A., Ouarda, T. B., & Gachon, P. (2012). Multisite statistical downscaling model for daily precipitation combined by multivariate multiple linear regression and stochastic weather generator. Climatic Change, 114(3-4), 567-591.

Kilsby, C. G., Jones, P. D., Burton, A., Ford, A. C., Fowler, H. J., Harpham, C., ... & Wilby, R. L. (2007). A daily weather generator for use in climate change studies. *Environmental Modelling & Software*, *22*(12), 1705-1719.

Kim BS, Kim HS, Seoh BH, Kim NW (2007) Impact of climate change on water resources in Yongdam Dam Basin, Korea. Stoch Environ Res Risk Assess 21:355

Kim, J., Tanveer, M. E., & Bae, D. H. (2018). Quantifying climate internal variability using an hourly ensemble generator over South Korea. *Stochastic environmental research and risk assessment*, *32*(11), 3037-3051.

Kou, X., Ge, J., Wang, Y., & Zhang, C. (2007). Validation of the weather generator CLIGEN with daily precipitation data from the Loess Plateau, China. *Journal of hydrology*, *347*(3-4), 347-357.

Kwon, H. H., Sivakumar, B., Moon, Y. I., & Kim, B. S. (2011). Assessment of change in design flood frequency under climate change using a multivariate downscaling model and a precipitation-runoff model. *Stochastic Environmental Research and Risk Assessment*, *25*(4), 567-581.

Mehan, S., Guo, T., Gitau, M., & Flanagan, D. C. (2017). Comparative study of different stochastic weather generators for long-term climate data simulation. *Climate*, *5*(2), 26.

Mehrotra, R., Srikanthan, R., & Sharma, A. (2006). A comparison of three stochastic multi-site precipitation occurrence generators. *Journal of Hydrology*, *331*(1-2), 280-292.

Min, Y.M., Kryjov, V.N., An, K.H., Hameed, S.N., Sohn, S.J., Lee, W.J. and Oh, J.H. (2011). Evaluation of the weather generator CLIGEN with daily precipitation characteristics in Korea. Asia-Pacific Journal of Atmospheric Sciences 47(3): 255-263.

Minville, M., Brissette, F., Leconte, R., 2008. Uncertainty of the impact of climate change on the hydrology of a nordic watershed. Journal of Hydrology 358, 70–83.

Mithen S, Black E (2011) Water, life and civilisation: climate, environment and society in the Jordan Valley, vol Cambridge. University Press, Cambridge

Mukundan, R., Acharya, N., Gelda, R. K., Frei, A., & Owens, E. M. (2019). Modeling streamflow sensitivity to climate change in New York City water supply streams using a stochastic weather generator. *Journal of Hydrology: Regional Studies*, *21*, 147-158.

Neitsch, S. L., Arnold, J. G., Kiniry, J. R., & Williams, J. R. (2011). *Soil and water assessment tool theoretical documentation version 2009*. Texas Water Resources Institute.

Ott, R. L., and Longnecker, M. T. (2015). *An introduction to statistical methods and data analysis*. Thomson Learning, Inc. Duxbury, Pacific Grove, CA., Nelson Education.

Peleg, N., Fatichi, S., Paschalis, A., Molnar, P., & Burlando, P. (2017). An advanced stochastic weather generator for simulating 2-D high-resolution climate variables. *Journal of Advances in Modeling Earth Systems*, *9*(3), 1595-1627.

Qian, B., Gameda, S., Hayhoe, H., De Jong, R., & Bootsma, A. (2004). Comparison of LARS-WG and AAFC-WG stochastic weather generators for diverse Canadian climates. *Climate Research*, *26*(3), 175-191.

Räisänen, J., & Ruokolainen, L. (2006) Probabilistic forecasts of near-term climate change based on a resampling ensemble technique. *Tellus A: Dynamic Meteorology and Oceanography*, *58*(4), 461-472.

Santer, B. D., Thorne, P. W., Haimberger, L., Taylor, K. E., Wigley, T. M. L., Lanzante, J. R., ... & Karl, T. R. (2008). Consistency of modelled and observed temperature trends in the tropical troposphere. *International Journal of Climatology: A Journal of the Royal Meteorological Society*, *28*(13), 1703-1722.

Semenov MA, Barrow EM (1997) Use of a stochastic weather generator in the development of climate change scenarios. Clim Change 35:397–414

Semenov, M. A. (2008). Simulation of extreme weather events by a stochastic weather generator. *Climate Research*, *35*(3), 203-212.

Semenov, M. A., Brooks, R. J., Barrow, E. M., & Richardson, C. W. (1998). Comparison of the WGEN and LARS-WG stochastic weather generators for diverse climates. *Climate research*, *10*(2), 95-107.

Sharif M, Burn DH (2007) Improved K-nearest neighbor weather generating model. J Hydrol Eng 12(1):42–51

Smith, B. J. (2007). BOA: an R package for MCMC output convergence assessment and posterior inference. *Journal of Statistical Software*, *21*(11), 1-37.

Steinschneider, S., & Brown, C. (2013). A semiparametric multivariate, multisite weather generator with low-frequency variability for use in climate risk assessments. *Water resources research*, *49*(11), 7205-7220.

Stevens, T. & Madani, K. Future climate impacts on maize farming and food security in Malawi. *Scientific Reports* **6**, 36241 (2016).

Thompson, D. W. J., E. A. Barnes, C. Deser, W. E. Foust, and A. S. Phillips (2015), Quantifying the role of internal climate variability in future climate trends, J. Clim., 28(16), 6443–6456, doi:10.1175/JCLI-D-14-00830.1.

Todorovic, P.; Woolhiser, D.A. (1975) A stochastic model of n-day precipitation. *J. Appl. Meteorol. 14*, 17–24.

Vesely, F. M., Paleari, L., Movedi, E., Bellocchi, G., & Confalonieri, R. (2019). Quantifying Uncertainty Due to Stochastic Weather Generators in Climate Change Impact Studies. *Scientific Reports (Nature Publisher Group)*, *9*, 1-8.

Vu, T. M., Mishra, A. K., Konapala, G., & Liu, D. (2018). Evaluation of multiple stochastic rainfall generators in diverse climatic regions. *Stochastic environmental research and risk assessment*, *32*(5), 1337-1353.

Wheater, H. S., Chandler, R. E., Onof, C. J., Isham, V. S., Bellone, E., Yang, C., ... & Segond, M. L. (2005). Spatial-temporal rainfall modelling for flood risk estimation. *Stochastic Environmental Research and Risk Assessment*, *19*(6), 403-416.

Zhang X, Garbrecht JD (2003) Evaluation of CLIGEN precipitation parameters and their implication on WEPP runoff and erosion prediction. *Trans ASAE* 46:311

Zwiers F (1996) Interannual variability and predictability in an ensemble of AMIP climate simulations conducted with CCC GCM2. *Clim Dyn* 12: 825–847

Table 5.2 Marginal mprovements in *RMSEr* ($RMSE_{r,\ mar.\ improvement}$) of two precipitation reference datasets obtained by using *N* realizations relative to a single realization

		Synthetic Climate (PCP)				Observed Climate (PCP)			
SWG	***N***	μ	σ	α_3	α_4	μ	σ	α_3	α_4
ME	***5***	0.58	6.27	142.48	13.57	1.69	18.23	205.77	31.08
	10	0.71	7.83	176.22	16.87	2.02	22.43	244.79	34.62
	25	**0.84**	**9.12**	**206.82**	**19.84**	**2.31**	**25.01**	**274.30**	**37.75**
	50	0.90	9.79	222.73	21.36	2.41	25.98	286.04	38.50
	100	0.95	10.27	233.46	22.37	2.46	26.54	291.13	38.88
	1000	1.05	11.36	258.24	24.77	2.51	27.06	295.82	39.30
MG	***5***	0.63	6.28	126.99	13.11	1.86	12.79	205.97	28.18
	10	0.78	7.78	156.70	16.12	2.25	15.16	244.57	31.63
	25	**0.92**	**8.99**	**182.07**	**18.86**	**2.55**	**15.96**	**273.10**	**34.15**
	50	0.99	9.68	195.74	20.26	2.67	16.40	284.33	35.16
	100	1.04	10.16	205.83	21.24	2.74	16.61	290.43	35.34
	1000	1.15	11.20	226.93	23.47	2.80	16.75	294.98	35.72
WE	***5***	0.47	6.41	285.88	12.95	0.99	0.93	175.79	26.54
	10	0.58	7.79	356.21	15.78	1.14	0.93	207.24	29.59
	25	**0.68**	**9.11**	**417.09**	**18.59**	**1.25**	**1.08**	**226.50**	**32.37**
	50	0.73	9.80	448.82	19.97	1.29	1.10	232.03	33.13
	100	0.76	10.27	472.18	20.91	1.31	1.13	236.06	33.69
	1000	0.84	11.34	521.60	23.08	1.32	1.13	239.04	33.95
WG	***5***	0.49	6.13	226.69	13.12	0.73	0.93	177.44	29.27
	10	0.62	7.60	283.24	15.99	0.83	1.00	207.32	32.51
	25	**0.72**	**8.91**	**330.35**	**18.76**	**0.89**	**1.08**	**227.91**	**35.48**
	50	0.78	9.58	356.13	20.20	0.91	1.12	235.86	35.97
	100	0.82	10.05	373.48	21.16	0.93	1.11	240.65	36.19
	1000	0.90	11.11	412.88	23.38	0.94	1.14	243.46	36.65
KNN	***5***	0.52	6.51	191.85	11.95	0.31	0.84	163.73	24.35
	10	0.64	7.93	234.66	14.67	0.35	1.14	196.25	27.17
	25	**0.74**	**9.28**	**275.80**	**17.17**	**0.36**	**1.33**	**215.33**	**29.15**
	50	0.80	9.98	296.28	18.49	0.37	1.30	220.19	30.11
	100	0.84	10.47	311.13	19.43	0.37	1.30	223.98	30.65
	1000	0.92	11.56	343.50	21.46	0.37	1.33	227.40	30.77

Table 5.3 Marginal mprovements in *RMSEr* ($RMSE_{r,\ mar.\ improvement}$) of two maximum temperature reference datasets obtained by using *N* realizations relative to a single realization

		Synthetic Climate (Tmax)				Observed Climate (Tmax)			
SWG	***N***	μ	σ	α_3	α_4	μ	σ	α_3	α_4
ME	***5***	0.42	6.42	1351.87	12.17	1.34	2.11	74.70	29.94
	10	0.53	7.90	1657.07	15.19	1.67	2.46	83.22	35.15
	25	**0.62**	**9.23**	**1944.42**	**17.84**	**1.95**	**2.73**	**90.18**	**38.34**
	50	0.67	9.95	2089.46	19.21	2.09	2.85	92.18	39.41
	100	0.70	10.48	2190.06	20.17	2.18	2.94	92.34	40.07
	1000	0.77	11.57	2418.07	22.30	2.32	2.94	93.52	40.46
MG	***5***	0.43	6.20	18012.49	12.88	1.36	2.28	70.78	33.29
	10	0.54	7.56	22297.20	15.77	1.69	2.75	82.49	37.84
	25	**0.63**	**8.94**	**26099.98**	**18.56**	**1.98**	**3.02**	**87.79**	**41.25**
	50	0.67	9.59	27944.27	19.86	2.12	3.02	90.34	42.44
	100	0.70	10.05	29327.05	20.82	2.23	3.05	91.42	42.77
	1000	0.78	11.12	32349.77	22.96	2.44	3.08	92.27	43.36
WE	***5***	0.22	5.92	7365.25	13.16	0.49	0.43	72.32	35.22
	10	0.27	7.43	9071.86	16.28	0.57	0.51	85.17	40.58
	25	**0.32**	**8.67**	**10584.92**	**19.14**	**0.62**	**0.47**	**90.27**	**43.46**
	50	0.34	9.33	11364.65	20.67	0.64	0.48	92.55	45.00
	100	0.36	9.82	11947.48	21.70	0.65	0.49	93.55	45.71
	1000	0.40	10.87	13177.97	24.02	0.66	0.49	94.41	46.19
WG	***5***	0.19	6.19	2852.45	13.17	0.47	0.35	77.10	35.97
	10	0.24	7.72	3521.50	16.13	0.55	0.36	88.91	40.25
	25	**0.28**	**9.01**	**4121.78**	**18.84**	**0.61**	**0.44**	**94.49**	**43.68**
	50	0.30	9.67	4424.45	20.22	0.63	0.43	96.81	44.85
	100	0.31	10.16	4651.55	21.20	0.64	0.41	97.93	45.32
	1000	0.35	11.23	5136.53	23.36	0.65	0.43	99.02	45.86
KNN	***5***	0.07	1.18	6.41	2.15	0.23	3.45	19.76	6.16
	10	0.09	1.47	7.87	2.67	0.29	4.17	24.01	7.42
	25	**0.11**	**1.71**	**9.19**	**3.13**	**0.33**	**4.66**	**27.24**	**8.36**
	50	0.11	1.83	9.90	3.37	0.36	4.84	28.69	8.71
	100	0.12	1.93	10.39	3.54	0.38	4.95	29.54	8.89
	1000	0.13	2.12	11.48	3.92	0.41	5.04	30.36	9.08

Table 5.4 Marginal mprovements in *RMSEr* ($RMSE_{r,\ mar.\ improvement}$) of two minimum temperature reference datasets obtained by using *N* realizations relative a single realization

		Synthetic Climate (Tmin)				Observed Climate (Tmin)			
SWG	***N***	μ	σ	α_3	α_4	μ	σ	α_3	α_4
ME	***5***	5.03	6.31	2108.35	12.04	14.53	2.02	69.78	38.38
	10	6.26	7.76	2585.52	14.99	17.84	2.40	77.83	47.41
	25	**7.31**	**9.15**	**3034.60**	**17.70**	**20.25**	**2.65**	**84.66**	**54.45**
	50	7.84	9.85	3241.87	18.94	21.10	2.62	86.21	57.09
	100	8.23	10.35	3408.78	19.90	21.65	2.70	86.95	58.78
	1000	9.08	11.44	3762.85	21.99	22.12	2.70	88.16	60.46
MG	***5***	5.11	6.11	5881.90	12.33	15.25	2.03	67.72	39.32
	10	6.35	7.48	7281.93	15.14	18.78	2.54	77.99	47.48
	25	**7.41**	**8.85**	**8495.20**	**17.83**	**21.39**	**2.78**	**81.76**	**54.88**
	50	7.95	9.51	9083.50	19.09	22.41	2.81	83.99	57.90
	100	8.36	9.97	9537.18	20.04	23.06	2.84	85.11	59.57
	1000	9.24	11.03	10523.34	22.11	23.72	2.84	86.01	61.27
WE	***5***	2.87	6.10	2627.83	12.91	3.95	0.40	71.97	40.98
	10	3.54	7.54	3268.96	16.08	4.48	0.39	80.42	50.31
	25	**4.12**	**8.83**	**3840.86**	**18.87**	**4.71**	**0.43**	**86.16**	**57.61**
	50	4.45	9.46	4126.73	20.20	4.83	0.43	88.24	60.29
	100	4.66	9.96	4342.01	21.20	4.91	0.45	89.38	61.95
	1000	5.13	11.00	4799.23	23.46	4.92	0.44	90.39	63.59
WG	***5***	2.25	6.23	6879.67	12.30	1.20	0.16	70.64	39.40
	10	2.77	7.68	8491.17	15.24	1.38	0.20	80.76	48.17
	25	**3.25**	**8.99**	**9922.20**	**17.88**	**1.43**	**0.24**	**85.73**	**55.20**
	50	3.50	9.67	10678.55	19.16	1.45	0.23	88.08	57.95
	100	3.67	10.15	11216.60	20.11	1.47	0.21	89.14	59.54
	1000	4.06	11.22	12401.88	22.17	1.48	0.23	90.22	61.25
KNN	***5***	0.72	1.07	8.59	3.11	2.29	3.18	27.18	9.70
	10	0.90	1.32	10.71	3.87	2.85	3.86	33.68	11.96
	25	**1.05**	**1.54**	**12.51**	**4.52**	**3.31**	**4.40**	**38.80**	**13.80**
	50	1.12	1.67	13.42	4.86	3.55	4.61	41.10	14.55
	100	1.18	1.75	14.10	5.09	3.73	4.71	42.52	15.08
	1000	1.31	1.93	15.57	5.63	4.05	4.83	43.96	15.58

Table 5.5 Marginal mprovements in *RMSEr* ($RMSE_{r,\ mar.\ improvement}$) of three reference datasets obtained by adding *N* realizations relative to a single realization

		Streamflow (*SFOC*)				**Streamflow (*SFSC*)**				**Streamflow (*OBS Flow*)**			
SWG	***N***	μ	σ	α_3	α_4	μ	σ	α_3	α_4	μ	σ	α_3	α_4
ME	***5***	7.30	25.31	119.37	42.59	2.58	11.26	150.92	16.40	4.70	14.91	351.84	45.39
	10	8.75	27.55	134.23	49.14	3.18	13.90	185.64	20.42	5.38	17.73	430.93	52.83
	25	**9.96**	**29.1**	**146.16**	**52.81**	**3.75**	**16.2**	**217.89**	**23.73**	**5.94**	**19.40**	**498.71**	**57.12**
	50	10.35	30.31	149.08	53.81	4.01	17.49	233.76	25.55	6.07	19.58	529.46	58.41
	100	10.61	30.27	151.01	54.69	4.22	18.36	245.21	26.78	6.17	20.04	547.96	59.39
	1000	10.79	30.67	152.53	55.25	4.66	20.26	271.34	29.57	6.22	20.19	569.54	60.06
MG	***5***	8.25	22.32	114.69	42.13	2.63	10.90	157.65	16.49	6.62	19.32	344.81	45.42
	10	10.13	25.09	131.59	48.60	3.23	13.44	194.66	20.31	7.72	22.30	421.20	52.85
	25	**11.7**	**26.5**	**139.3**	**52.87**	**3.80**	**15.67**	**226.5**	**23.8**	**8.56**	**24.3**	**484.2**	**57.87**
	50	12.53	27.00	143.07	54.30	4.07	16.78	244.01	25.71	8.85	24.97	513.25	59.59
	100	13.01	27.43	144.61	55.02	4.27	17.59	255.97	26.95	8.99	25.21	529.91	60.44
	1000	13.56	27.65	146.05	55.63	4.72	19.42	282.57	29.77	9.13	25.55	547.54	61.19
WE	***5***	2.41	7.97	133.42	42.32	1.44	10.84	316.82	16.37	1.35	1.23	336.25	45.35
	10	2.78	9.13	153.59	49.63	1.79	13.54	391.76	20.56	1.54	1.43	403.62	53.63
	25	**2.96**	**9.93**	**166.7**	**54.0**	**2.09**	**15.78**	**457.2**	**24.0**	**1.61**	**1.63**	**451.17**	**58.76**
	50	3.03	9.98	171.59	55.88	2.25	16.99	492.42	25.89	1.65	1.57	470.14	60.79
	100	3.08	10.12	173.30	56.29	2.35	17.81	517.44	27.17	1.68	1.60	481.07	61.37
	1000	3.11	10.23	175.37	56.84	2.61	19.67	570.76	30.07	1.70	1.63	490.04	62.06
WG	***5***	4.66	11.46	139.17	44.84	1.48	10.82	295.18	16.53	2.73	2.12	337.98	47.66
	10	5.84	12.56	162.17	51.57	1.86	13.47	366.79	20.80	3.16	2.09	406.53	55.57
	25	**6.78**	**13.67**	**173.4**	**55.76**	**2.18**	**15.7**	**427.75**	**24.5**	**3.48**	**2.36**	**457.92**	**60.6**
	50	7.24	13.98	178.00	57.76	2.34	16.81	460.04	26.43	3.57	2.41	477.91	62.86
	100	7.54	14.08	180.45	58.16	2.45	17.67	483.34	27.69	3.61	2.40	488.35	63.44
	1000	7.92	14.18	182.23	59.04	2.72	19.53	533.48	30.73	3.65	2.41	498.54	64.46
KNN	***5***	1.73	21.30	152.63	43.95	1.56	9.19	314.20	17.24	1.06	1.72	371.78	46.04
	10	2.09	24.88	175.37	50.85	1.92	11.23	384.80	21.32	1.32	1.97	443.76	53.51
	25	**2.16**	**27.81**	**186.7**	**55.4**	**2.24**	**13.25**	**449.5**	**24.9**	**1.34**	**2.30**	**503.8**	**58.45**
	50	2.24	28.82	192.81	56.13	2.41	14.24	484.70	26.75	1.40	2.40	526.45	59.39
	100	2.24	29.25	196.46	56.78	2.53	14.96	508.68	28.11	1.39	2.39	536.67	60.13
	1000	2.27	29.69	198.02	57.60	2.79	16.53	560.89	31.08	1.41	2.42	548.85	61.02

CHAPTER 6. *Case Study*

The case study presented in this chapter aims to demonstrate the added value of the methodology developed by comparing the information that a decision-maker can get from a) the traditional top-down approach that has been used by the vast majority of climate change adaptation studies, b) the traditional bottom-up approach as proposed by Brown *et al.* (2012) and García *et al.* (2014), and c) the improved bottom-up approach proposed in this thesis. We will be using the outputs of 4 RCMs and 2 RCPs obtained from the CORDEX project and the SWAT model used in this thesis to generate that information. The outputs of the RCMs were downscaled using Quantile-Quantile mapping (QQ) and Change Factor method (CF).

6.1 Problem statement

Consider a hypothetic decision-maker who is overseeing the South Nation Watershed. Assume that there is a particularly flood-prone area that is flooded every 10 years under the current climate (1981-2010), which is estimated to be $AM10_{obs}$ = 763.86 *cms*; Assume that there is also a wastewater treatment plant designed for the 10 years 7 days low flows in the current climate, which is estimated to be $7Q10_{obs}$ = 8.8 *cms*. The decision-maker is aware that the hydrological regime will probably change because of global warming and is worried about two particular hydrologic extreme events in the future (2071-2100):

- *Event A* of having more extreme low flow events (i.e., $7Q10 \leq 8.8$ *cms*), and
- *Event B* of having more extreme high flow events (i.e., $AM10 \geq 763.86$ *cms*).

The decision-maker would like to know the likelihood of Event A, Event B, Events A and B occurring simultaneously in the same year, and Events A or B occurring in the same year, for the period between 2071 and 2100.

6.2 Traditional top-down approach

In the traditional top-down approach, the following steps are followed:

1. The outputs of the four climate models run under RCP4.5 and 8.5 are downscaled to obtain local information
2. *7Q10* and *AM10* are calculated for each of the eight time-series
3. The results of such exercise are presented in the table below (Table 6.1).

Table 6.1 Typical results of the traditional top-down approach

Climate Model GCM (RCM)	**RCP**	***7Q10* (*cms*)**		***AM10* (*cms*)**	
		CF	*QQ*	*CF*	*QQ*
CanESM2 (CanRCM4)	**RCP4.5**	12.58 (>$7Q10_{obs}$)	15.94 (>$7Q10_{obs}$)	412.63 (<$AM10_{obs}$)	357.43 (<$AM10_{obs}$)
	RCP8.5	12.37 (>$7Q10_{obs}$)	18.09 (>$7Q10_{obs}$)	348.26 (<$AM10_{obs}$)	415.48 (<$AM10_{obs}$)
CanESM2 (RCA4)	**RCP4.5**	14.85 (>$7Q10_{obs}$)	15.25 (>$7Q10_{obs}$)	638.41 (<$AM10_{obs}$)	385.18 (<$AM10_{obs}$)
	RCP8.5	16.81 (>$7Q10_{obs}$)	17.23 (>$7Q10_{obs}$)	530.90 (<$AM10_{obs}$)	403.96 (<$AM10_{obs}$)
ECEARTH (HIRHAM5)	**RCP4.5**	13.46 (>$7Q10_{obs}$)	15.13 (>$7Q10_{obs}$)	768.51 (>$AM10_{obs}$)	374.85 (<$AM10_{obs}$)
	RCP8.5	16.66 (>$7Q10_{obs}$)	18.32 (>$7Q10_{obs}$)	661.86 (<$AM10_{obs}$)	418.30 (<$AM10_{obs}$)
ECEARTH (RCA4)	**RCP4.5**	12.21 (>$7Q10_{obs}$)	14.70 (>$7Q10_{obs}$)	622.14 (<$AM10_{obs}$)	374.91 (<$AM10_{obs}$)
	RCP8.5	14.95 (>$7Q10_{obs}$)	16.76 (>$7Q10_{obs}$)	535.25 (<$AM10_{obs}$)	390.20 (<$AM10_{obs}$)

Looking at the data in Table 6.1, the decision-makers will conclude that 100% probability of seeing a decrease in *AM10* and 15/16 chance to see a decrease in *AM10*; however, given the limited number of points (16), the estimate is highly uncertain, and there may be up to 2/16 chance to see an increase in *AM10* (event A), and 1/16 chance to see a decrease in *7Q10* (event B); depending on the risk aversion of the manager and the values at risk, these numbers can be perceived as high, and a better precision in the estimation of the probabilities would have been appreciated. Furthermore, the estimates of P(A∩B) and P(AUB) are even more imprecise.

6.3 Traditional bottom-up approach

In the traditional bottom-up approach, the following steps are followed:

1. The observed temperature is gradually increased from 0.5 to 9 °C (16 ΔT), and the precipitation from –5% to 20% (25 ΔP), and both *7Q10* and *AM10* are calculated
2. A surface plot of the relationship between *7Q10* and *AM10* is generated
3. Points representing the 8 scenarios are added to the two graphs below (Figure 6.1).

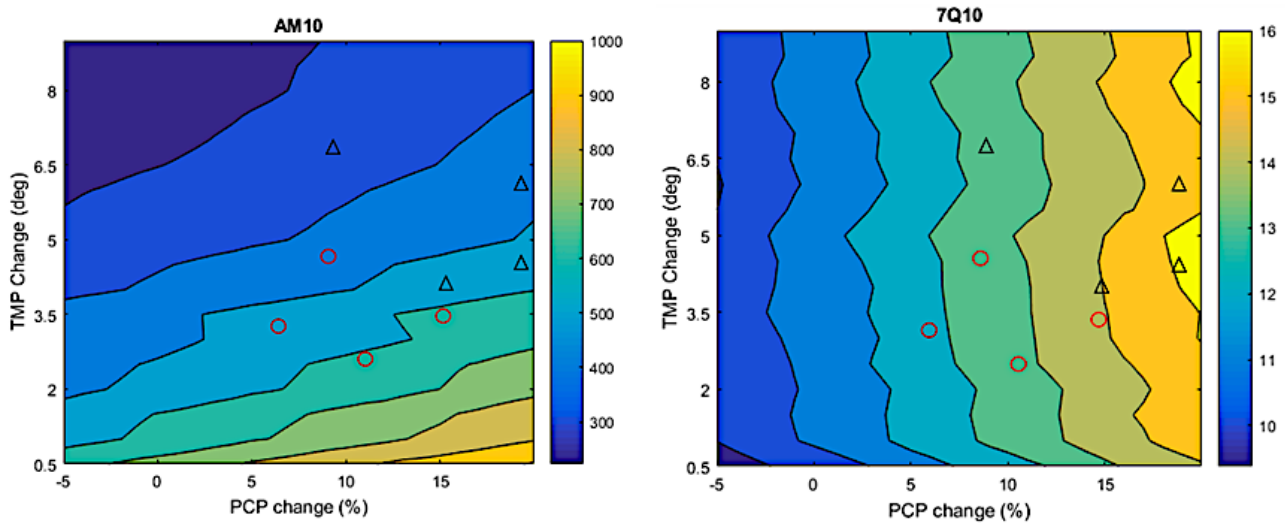

Figure 6.1 Typical results of the traditional bottom-up approach using two indices (*AM10* and *7Q10*).

Looking at Figure 6.1, the manager can have a sense of the order of magnitude and variability to expect for *7Q10* and *AM10*, but once again cannot associate them with a probability; hence, it lacks practical applicability. From the graph, one can infer that there is almost no chance for event A or event B to happen.

6.4 Improved bottom-up approach

In the improved bottom-up approach, 250 30-year climate time series were generated using MulGETS weather generator where precipitation amounts were generated by mixed Gamma distribution. The use of this particular model was based on its performance as demonstrated in Chapter 4. *7Q10* and *AM10* will be the two dimensions of the CSS. The methodology developed in Alodah and Seidou (2019) is used to generate the probability of any point in the CSS. P(A), P(B), P(A∪B) and P(A∩B) are represented by shaded areas in Figure 6.2.

a.

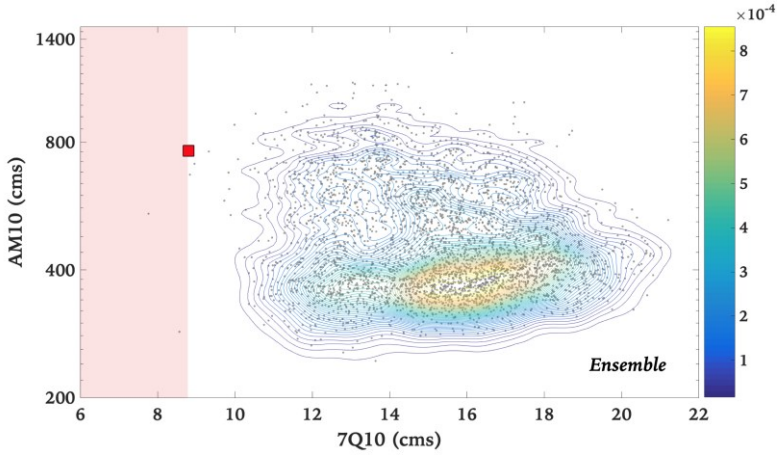

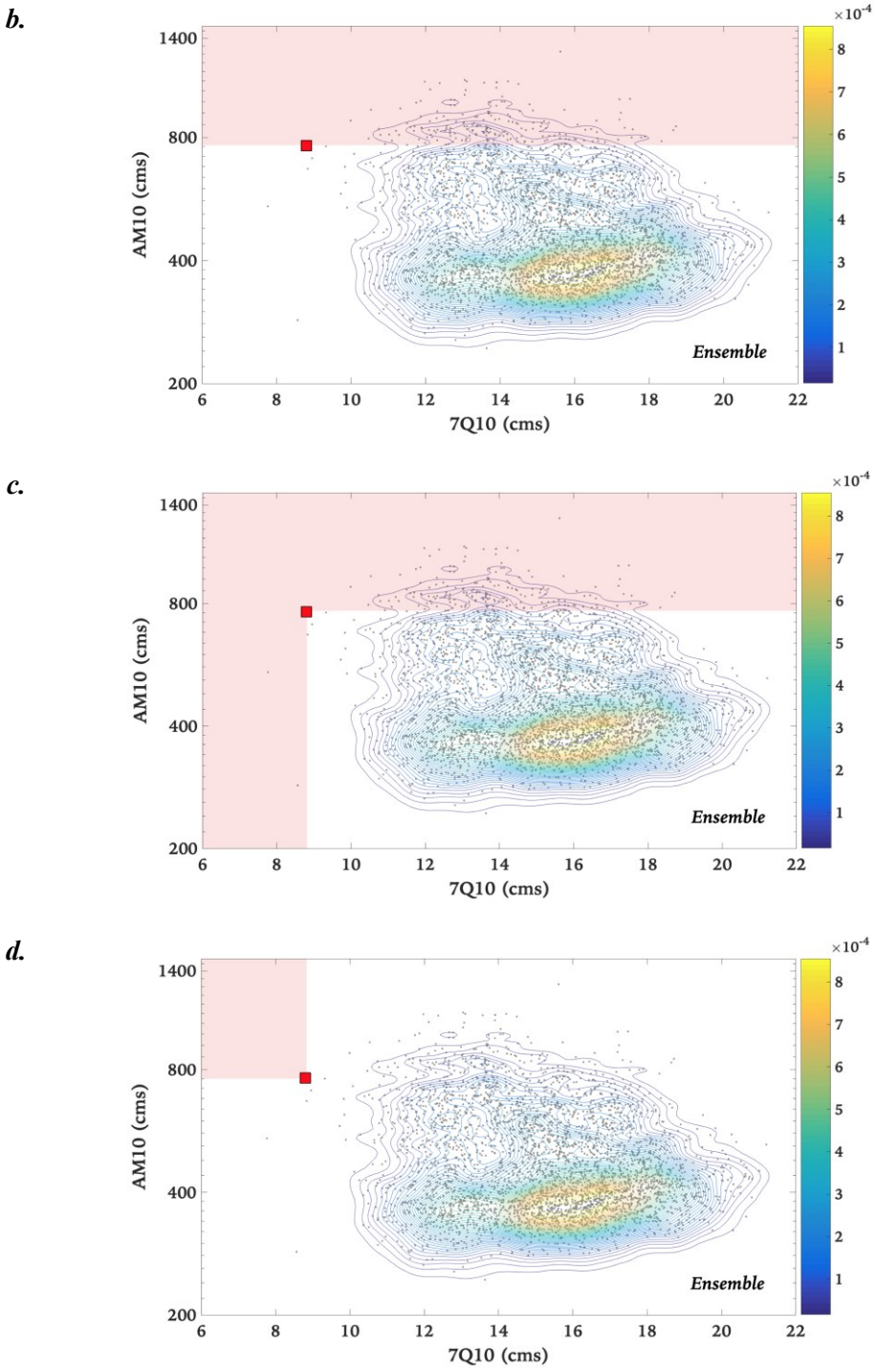

Figure 6.2 Examples of unwanted events applying the improved bottom-up approach, where shaded regions present the four extreme conditions: *a.* P(A), *b.* P(B), *c.* P(A∪B), and *d.* P(A∩B).

The estimated probabilities of the two independent events, *AM10* and *7Q10*, are obtained after integration of the probability under the shaded areas:

a. Event A alone: $P(A) = 6.614\ x10^{-4}$

b. Event B alone: $P(B) = 0.0534$

c. Events A or B: $P(A \cup B) = 0.0540$

d. Event A and B: $P(A \cap B) = 1.499\ x10^{-5}$

These results show that the possibility of event A is relatively small, but may of interest to the manager if the impacts of A are significant (e.g., loss of life). The probability of event B is rather significant (5%) and deserves the attention of the manager. This case study shows the benefits of the proposed approach versus the top-down approach:

- Better coverage of the RPIS unlike top-down where only a subset of all possible climate futures is considered, hence less probability of overlooking risky possibilities,
- Quantitative estimation of the probability of any event linked to the variables of the RPIS.

This case study also shows the benefits of the proposed approach compared to the traditional bottom-up:

- the proposed approach has the advantage of providing quantitative results that cannot be obtained by the traditional bottom-up,
- it is not based on simplistic Delta (Change Factors) method,
- it allows for multivariable analysis; the joint probability of unwanted events can be estimated, and
- less computational resources lost to calculate indices in low probability spaces (the cloud points are concentrated in areas that represent most likely events) by a better selection of the vulnerability range.

Yet, some limitations still need to be addressed. A limitation shared by the top-down, the traditional bottom-up, and the proposed approach is linked to uncertainty/bias in RCMs/GCMs even after downscaling raw climate change data and the addition of stochastically generated climate data. Impact models are well known for involving highly nonlinear rainfall-runoff transformation and a small bias could dramatically affect their results. These uncertainties have less impact on the traditional bottom-up approach as only the delta-change in precipitation and temperature are used, and the estimates of such changes from RCM outputs is relatively robust compared to the projection of other climate statistics. Despite these limitations, the proposed methodology is considered promising and may lead to better identification of risks associated with climate change, and better adaptation decision. A list of differences between the top-down, bottom-up, and improved bottom-up approaches are presented in Table 6.2.

Table 6.2 Summary of the differences between the top-down, bottom-up, and improved bottom-up approaches.

Criteria	Top-down approach	Bottom-up approach	Improved Bottom-up approach
Dependence on RCM outputs?	*Yes*	*Partial*	*Partial*
Coverage of the RPIS?	*No*	*Partial*	*Yes*
Quantitative estimation of the probability of any event?	*No*	*No*	*Yes*
Based on simplistic Delta method (ΔT and ΔP)?	*No*	*Yes*	*No*
Multivariable analysis?	*No*	*No*	*Yes*
Reasonable selection of the vulnerability range?	*N/A*	*No*	*Yes*
Ability to evaluate the credibility of a given projection scenario?	*No*	*Partial*	*Yes*

6.5 References

Brown, C., Ghile, Y., Laverty, M., & Li, K. (2012). Decision scaling: Linking bottom-up vulnerability analysis with climate projections in the water sector. *Water Resources Research*, *48*(9).

García, L. E., Matthews, J. H., Rodriguez, D. J., Wijnen, M., DiFrancesco, K. N., & Ray, P. (2014). Beyond downscaling: a bottom-up approach to climate adaptation for water resources management. AGWA Report 01. Washington, DC: World Bank Group.

CHAPTER 7. *Conclusions and Recommendations*

7.1 Summary and Conclusions

The main objective of the present study was to develop an improved version of the bottom-up framework for streamlining climate variability into water resources management decisions to cope with the present-day and future challenges induced mainly by climate. The proposed approach consists of a combination of three major components: the performance of stochastic weather generators assessment, the development of a new avenue to generate a wide range of climate scenarios, and the number of stochastic weather generators realizations component to minimize to computational time and cost. The feasibility of the suggested approach was tested on the South Nation Watershed in Eastern Ontario using different datasets including observed daily climate and streamflow data, synthetically generated climate and streamflow data, and climate change data extracted from RCM models. The main findings of the thesis include:

- It was demonstrated in this thesis that the performance of weather-generators varies according to the variable of interest. Their performance in the CSS does not necessarily translate in the RPIS. In the case of the South Nation Watershed, results demonstrated that MulGETS-models were often the better-performing weather generators for the South Nation area, followed by its counterpart the single site WeaGETS model, and the k-nearest neighbour approach. The statistics of simulated streamflow using observed climatic data were found to lie mostly outside a predefined set of normal behaviour for the WeaGETS and k-nn models. The MulGETS model, in its gamma and exponential configurations, thus considered the preferred choice candidates for risk analysis and discovery, mainly due to this model's ability to incorporate covariance for several stations
- A methodology was developed to generate a large number of climate projections using RCMs and stochastic weather generators. This large ensemble allowed the quantification of better coverage of the RPIS in the bottom-up approach, and the calculation of the probability of any point inside. The calculated likelihood measure provides a more

practical assessment of the plausibility of future risks to serve infrastructure design and allow more confidence in water-related management decisions. Ideally, the generation of such ensembles should contain - to a feasible extent - as many uncertainty elements as possible. Given that the choice of climate models, downscaling techniques, and weather generator affects the results, a super-ensemble of future climate series was used to derive flooding and drought indices, while bearing in mind the uncertainties inherent in the extreme value modeling under a changing climate at regional scales.

- The 10-year 7-day low flow on the South Nation River at Plantagenet will marginally increase in the future, whereas flood magnitude will noticeably weaken. A shorter and warmer winter is expected to result in an earlier disappearance of accumulated winter snow cover, early onset of snowmelt and consequently an earlier and less intensive peak spring flow.
- Using the two error-metrics (RE and RMSE), it was shown that when the number of realizations is high, the considered five weather generators perform somehow similarly in terms of reproducing the risk and performance indicators. Results generally indicate that there is no major benefit of generating more than 100 realizations as they are not notably different from results obtained using 1000 realizations. Adopting a small but carefully chosen number of realizations can significantly reduce the computational time and resources and therefore benefit a larger audience, particularly where high-performance machines are not easily accessible.

7.2 Recommendations for Future Work

Below are some recommendations for future research that could be of general interest to the water resources community:

- Develop a case study where the impact of adaptation policies on the likelihood in the RPIS is estimated, and propose a framework for policy selection. The effects of various watershed practices and the likelihood of unwanted events may be investigated by

following the same approach presented in Chapter 5. Their usefulness as adaptation strategies may be investigated.

- Considering RPIS of dimensions larger than 2. For practical reasons, the RPIS in this thesis were bidimensional, but the framework can apply to d-dimensional spaces. The challenge would be the number of points to estimate probabilities in these spaces.
- Apply the improved bottom-up approach to regions with different climate conditions (e.g., hot and dry) and other hydrological applications.
- Apply the improved bottom-up approach using more complete impact models, such as economic, ecological, or electricity demand models.
- While applications in this thesis were centered in one pilot watershed, the methodologies presented deliver new insights into hydrological processes under different climate conditions in general and will be of interest to Canada and beyond. The need is also manifest for examining a broader range of hydrologic indicators.
- Further improvement to the super-ensemble can be achieved by considering more stochastic weather generators, climate-change models, and downscaling methods to ensure a thorough evaluation and facilitate knowledge-driven decision.